TESIS DOCTORAL

CARACTERIZACIÓN HIDRODINÁMICA DE PRADERAS NATURALES DE MACRÓFITOS BENTÓNICOS EN FONDOS SOMEROS AFECTADOS POR MAREAS

HYDRODYNAMIC CHARACTERIZATION OF NATURAL BENTHIC MACROPHYTE MEADOWS INHABITING SHALLOW TIDAL ENVIRONMENTS

Francisco Miguel Lara Rallo

Universidad de Cádiz
Facultad de Ciencias del Mar y Ambientales
Departamento de Biología
Puerto Real, 2012.

Caracterización hidrodinámica de praderas naturales de macrófitos bentónicos en fondos someros afectados por mareas

Memoria presentada por D. Francisco Miguel Lara Rallo para optar al grado de Doctor por la Universidad de Cádiz.

Fdo. Francisco Miguel Lara Rallo

Los directores:

Prof. D. José Lucas Pérez-Lloréns
Catedrático de Ecología
Universidad de Cádiz

Dra. D. Gloria Peralta González
Profesora Titular de Ecología
Universidad de Cádiz

D. JOSÉ LUCAS PÉREZ-LLORÉNS, Catedrático de Ecología del Departamento de Biología de la Facultad de Ciencias del Mar y Ambientales de la Universidad de Cádiz, y Dª GLORIA PERALTA GONZÁLEZ, Profesora Titular de Ecología del Departamento de Biología de la Facultad de Ciencias del Mar y Ambientales de la Universidad de Cádiz:

HACEN CONSTAR:

Que el trabajo recogido en la presente memoria de Tesis Doctoral, titulada: "Caracterización hidrodinámica de praderas naturales de macrófitos bentónicos en fondos someros afectados por mareas", elaborada por el licenciado en Ciencias Ambientales D. Francisco Miguel Lara Rallo para optar al grado de Doctor en Ciencias del Mar, ha sido realizada bajo nuestra dirección y autorizamos su presentación y defensa.

Para que así conste a los efectos oportunos firmo la presente en Puerto Real a 21 de Septiembre de 2012.

Fdo. D. José Lucas Pérez-Lloréns Fdo. Dª Gloria Peralta González

Para la realización de esta Tesis Doctoral, el candidato Francisco Miguel Lara Rallo, ha disfrutado de una beca de Formación de Personal Investigador del Ministerio de Educación y Ciencia (BES) adscrita al proyecto del Plan Nacional de I+D+i "*Estudio integrado del efecto de las variables físico-químicas sobre la ecología de la praderas de macrófitos marinos del Parque Natural Bahía de Cádiz. Aplicaciones para la gestión*" (CTM2005-00395). Asimismo, parte del trabajo presentado en esta memoria ha sido parcialmente financiado por los proyectos: "*Interacciones entre la hidrodinámica y las praderas de macrófitos marinos: desde el organismo al ecosistema*" (CTM2008-00012/MAR) y "*Funciones de la diversidad de macrófitos marinos bentónicos: mecanismos de control en el ciclo de nutrientes de zonas costeras someras*" (P07-RNM-02516). Su actividad investigadora se ha realizado como miembro del grupo de investigación *Estructura y Dinámica de Ecosistemas Acuáticos* (PAIDI RNM-214).

Parte de la experimentación del presente trabajo se ha llevado a cabo durante estancias cortas de investigación en las siguientes instituciones: Centre for Estuarine and Marine Ecology, Netherlands Institute of Ecology (NIOO), Yerseke, Países Bajos; bajo la supervisión del Dr. Tjeerd Bouma; y Horn Point Laboratory, Centre for Environmental Science, University of Maryland, Cambridge, Maryland (USA); bajo la supervisión de la Dra. Evamaria Koch. Los resultados han sido parcialmente publicados o están bajo revisión en revistas internacionales indexadas como *Marine Pollution Bulletin* o *Marine Ecology Progress Series*, o divulgados en congresos internacionales (8th *International Seagrass Biology Workshop*, III *International Symposium in Marine Science*).

A mis dos hermanas Carmen y Beatriz, por saber aceptarme tal como soy

AGRADECIMIENTOS

En primer lugar, me gustaría agradecer enormemente a mis dos directores de tesis, el Prof. José Lucas Pérez-Llorens y la Dra. Gloria Peralta González, su esfuerzo y su paciencia durante todo el proceso de dirección. En el caso de Lucas, le debo sinceramente su confianza depositada al seleccionarme como investigador pre-doctoral, en un momento difícil para mí. Espero haber estado a la altura de las expectativas. En el caso de Gloria, le debo su pedagogía y su tesón por ordenar, simplificar y perfeccionar las ideas, y cuya práctica me será muy útil en el futuro.

El Dr. Tjeerd Bouma ha sido otra pieza clave en el proceso de elaboración de la tesis, con su instrucción y acogida en Yerseke. Sus valiosas enseñanzas destellan una pasión por la ciencia que te recuerda que, entre las manos llenas de fango y el tedioso procesado de datos del ADV, la Ecología es una bella pulsión experimental creadora de paradigmas.

No menos importante para la tesis resultó la supervisión en Maryland de la Dra. Evamaría Koch, que dispuso toda su logística y su prestigiosa experiencia al servicio de nuestras hipótesis de trabajo. Incluso en los peores momentos de inadaptación al *American way of life*, ella siempre insistía en la continuidad de mis objetivos. Junto con Dale Booth forman un equipo humano envidiable.

La aportación del Prof. Jose Juan Alonso ha sido fundamental en la fase final de la tesis. Rompiendo esa barrera comunicativa que parece existir entre físicos y ecólogos, corrigió y enriqueció totalmente mis planteamientos sobre la difusión turbulenta, hasta el punto de poder transformar un experimento colateral en una publicación indexada.

Mando también agradecimientos a los compañeros de área y de Departamento. Juanjo e Ignacio, por apoyar siempre en el plano organizativo; Fernando Brun, por brindarme esas pequeñas conversaciones y discusiones teóricas tan necesarias para reflexionar sobre lo que uno hace; Ed, por su receptividad y su espíritu crítico. Por supuesto, no se me pueden olvidar mis compañeros/as y amigos/as de la "sala PIF", que tantos almuerzos en cafetería han compartido conmigo: Carmen, una tía auténtica y cosmopolita con la que tantas experiencias he vivido (congreso de Canadá, muestreos de FAMAR, etc…, mil gracias!!); Bea, por saber escucharme desde su sitio; Irene, por sus consejos durante mi comienzo. Y cómo no: Cristian Tovilla, Ricardo (ese experto

ficólogo), Edu, María Morales, Juanlu, Sokratis, Nerea, Bárbara y Patri. Y las nuevas generaciones: Fran, Gonzalo y Rocío.

El CACYTMAR tampoco se queda corto. Allí reside el incansable Juanjo y su COT, con el que me une una gran amistad personal. También están Eli, esa vallecana de pura casta; Pablo y sus microalgas; Sergio, el futuro magnate de la potabilización a bajo coste… Con todos ellos coincido (o lo intento) en su quijotesco compromiso de lucha. No puedo olvidarme de Juan Vidal (maestro de los velocímetros de campo) y de Cristina Madrid (la escaladora). O de los geólogos Haris y Javito.

Durante mis estancias he conocido gente de una calidad humana extraordinaria. En Holanda, en 2008 como investigador y en 2010 como consorte, tengo gratos recuerdos de Tom, van Soelen, Tijs, Arnold, Achman, Mar, Yago, Diana, Yayu y Michelle. En USA (2009), de Chris y de los partidos de soccer organizados por Jeremy.

Agradezco especialmente a Vanessa todo su amor y su cariño hasta que nuestros caminos se separaron. Durante nuestro noviazgo me enseñó a valorarme a mí mismo (que no es poco) y también que el frikismo no es una enfermedad.

Estaré en deuda eterna con mis dos hermanas, Carmen y Beatriz, y con mis padres, por su cariño, comprensión y calor familiar, algo que no tiene precio.

Entre las gentes de Puerto Real y de Cádiz habría que hacer una lista que no cabría ni en una guía de teléfonos. Ahí están los miembros del club de Ajedrez ELECAM. Los alumnos y profesores del Centro de Adultos con el que colaboré me marcaron enormemente, especialmente Mamen y el campechano Manolo. Ahí estarán siempre, también, los compañeros libertarios del SOV y del 15-M, tanto de la plaza de Jesús como del Palillero (o de donde sean): Mi gran amiga Judit (jovial y rebelde), Antonio, Bali, Juanma, Carlos (el sevillano), Vane, Javi Lagarto, Aída, el colega roteño Juan Jesús, Tei, Becerra, Betanzos, Paco Delgado, Kranke, Leonor, Alfredo y los "amigachos" Paquito y Pepe.

En la última etapa de escritura recibí además el aliento cálido de Sandra Reyes, cantautora y maestra, la simpatía espontánea e infinita de Aixa y Antonela, la camaradería vegana de Lidia y toda la peña antitaurina, las llamadas de apoyo de mi viejo amigo Manu y la amabilidad de mi compañera de piso Flavia. Y las lentejas y la leche de soja que pude comprar gracias a mis alumnos de Física y sus problemas con los sistemas no inerciales. Finalmente, gracias a los mayas y su calendario podré defender la tesis antes del fin del mundo.

INDEX OF CONTENTS

“*Camina o revienta*”

Eleuterio Sánchez, alias “El Lute”

ABSTRACT

The inner water body of Cadiz bay is a shallow and tide-dominated lagoon, affected by episodic wind-storms and profusely inhabited by marine macrophytes (> 90% covering). These macrophytes are key to the functioning and productivity of this system and their interactions with hydrodynamics affects important ecological processes such as resources uptake and availability, bed stability and sedimentation. To understand the physical settings controlling such processes, the main objective of this PhD thesis was to study the effects of the marine macrophytes on the spatial patterns of current velocity and turbulence, and their potential consequences for sedimentary and nutrients dynamics. For this propose, hydrodynamic gradients along natural canopies, as well as the influence of some benthic landscape elements (i.e. microtopography, benthic transitions and patches fragmentation) were analysed with a combination of *in situ* measurements (e.g. acoustic Doppler velocimeter (ADV) and dye tracer measurements) and flume tank experiments. Main results revealed that (1) the flow accelerates over the canopies, being partially explained by submergence conditions, (2) fragmentation of intertidal patches augments horizontal turbulent diffusivity of solutes, whereas their retention time remains unaffected, and (3) the leading edge is the most active sedimentation zone on a seagrass meadow. Microtopography seems to promote the benthic macrophyte interactions only on cases affected by high flow events. Overall, diffusive limited- rather than mechanical stress- conditions dominate during no windy spring tide periods. Present study provides important keys to understand the role of marine macrophytes as ecosystem engineers from the inner Cadiz bay.

GENERAL INTRODUCTION

1. Hydrodynamics on seagrass habitat

Seagrasses are a small group of angiosperms monocots that succeeded colonizing marine habitats. This small group is characterized by a strongly developed aerenchyma, a root–rhizome system that allows the anchoring to the substrate and a biological activity fully adapted to the marine environment (Arber 1920, den Hartog 1970). Such adaptation includes the capacity to growth and to reproduce under marine water (with subsequent problems of pollination, Ackerman 1997a, 1997b), the resistance to hydraulic pressure (Beer and Waisel 1982) and the adaptation to hydrodynamic environment (Koch 2001).

The adaptation to hydrodynamic environments has been crucial for seagrasses to successfully colonize and survive on littoral habitats. Hydrodynamic forces on coastal waters can be basically classified as (1) unidirectional (e.g. tidal currents) and (2) orbital (e.g. swell or wind waves), and both types regulate biological processes in seagrass meadows by controlling momentum and mass transfer from the surrounding water (Koch and Gust 1999). The magnitude of these forces may determine habitat and development conditions affecting seagrass growth rate and plant morphological features (Schanz and Asmus 2003, Peralta et al. 2005, 2006, De los Santos et al. 2010), but also to nutrient uptake (Thomas et al. 2000, Thomas and Cornelissen 2003, Cornelissen and Thomas 2006, Morris et al. 2008) and light availability (Mc Kone 2009), with consequences for photosynthetic performance (Fonseca and Kenworthy 1987, Koch 1994, Enriquez and Rodriguez-Roman 2006). Furthermore, hydrodynamic conditions drive sediment dynamics, thus promoting risks of seagrass burial (Marbá and Duarte 1995, Cunha et al. 2005, Peralta el al. 2005) or erosion (Scoffin 1970, van Katwijk and Hermuss 2000). The direct and indirect control of hydrodynamics on these processes

may, consequently, shape the upper limit of seagrass distribution (Infantes et al. 2009) or their landscape patterns (Fonseca and Bell 1998).

Seagrass growth can be constrained or interrupted under extreme hydrodynamic conditions (i.e. very low or very high flow environments). At low flow conditions, the diffusive boundary layer (DBL), an unstirred layer of water generated around the leaf surface, restricts the mass-transport to the plant, limiting photosynthesis and uptake by reduced molecular diffusion of nutrients and gasses (e.g. CO_2, NO_3^- and NH_4^+, Koch 1994, Thomas et al. 2000). Recent evidences suggest that resource partitioning due to seagrass clonal integrity could play a key role against this impediment by distributing nutrients from active uptake zones of the meadow to those physically limited (Morris et al. 2008). Consequently, physiological responses to hydrodynamics are not expected to be spatially homogeneous, being necessary the analysis of spatial gradients within the meadow to integrate physical and biological studies on natural populations.

On the contrary, at high hydrodynamic conditions, mechanical stress imposed by high energy currents and waves could compromise seagrass survival by (1) increasing energetic costs to resist drag forces (Bouma et al. 2005, Peralta et al. 2008), (2) directly damaging aboveground biomass (Scoffin 1970, Pérez-Lloréns and Niell 1993; Schanz and Asmus 2003, Peralta et al. 2005) and (3) fostering substrate erosion and plant uprooting (Scoffin 1970, Pérez-Lloréns and Niell 1993, van Katwijk and Hermuss 2000, Paling et al. 2003, Schanz and Asmus 2003, Peralta et al. 2005). The corresponding seagrass acclimation and adaptation responses include (1) a strong anchoring system, as well as (2) thick leaves (Peralta et al. 2006), and (3) the capacity to reduce the frontal area exposed to the flow. This last strategy is usually accomplished by (a) development of small size morphotypes (Peralta et al. 2005), or simply by a high shoot flexibility allowing (b) the bending of the blades, which causes reduction of velocity due to

canopy compaction (Fonseca et al. 1982, Peralta et al. 2008, De los Santos 2011). Bending of blades is considered an "avoiding strategy" to hydrodynamic forces, and it is favoured by the biomechanical design of the leaves (i.e. flexibility and basal parts, De los Santos 2011). In summary, these large set of mechanisms reflect the importance of hydrodynamics as a forcing factor on seagrass habitat, by imposing energetic costs or adaptive constrains (De los Santos 2011).

For a seagrass meadow, the effects of water velocity (U, m s^{-1}) on diffusive boundary layer (DBL, µm) and drag forces are summarized in figure 1, pointing out that U values exceeding 0.30 m s^{-1} are high enough to avoid molecular diffusion restrictions to photosynthesis or nutrients uptake (Thomas et al. 2000, Morris et al. 2008). On the other hand, drag forces notably increase at U values larger than 0.25 m s^{-1}, promoting incipient sediment bed erosion (Bouma et al. 2009a). The optimal range of current speed to avoid problems associated to DBL and drag forces is very narrow, indicating that diffusive limitation vs. mechanical stress is a hydrodynamic trade-off for seagrasses (Fonseca and Kenworthy 1987). The thresholds for this trade-off are similar to the ones described for nutrient pool regeneration under contrasting hydrodynamic scenarios (ie. low versus high velocity). Nutrient regeneration within a submersed canopy has been attributed to the effect of vertical secondary flows from the sediment, enabling the transport (i.e. pore-water advection) to the canopy (Nepf and Koch 1999). At low flow, pore-water advection is small and nutrient regeneration limited. At high flow, a rapid pore-water advection occurs and canopy bending reduces the maximum height that nutrient transport reaches. Accordingly, submersed macrophyte optimum growth is usually observed at intermediate current velocities (Merrell 1996, Koch 1999 a), which implies maximum benefit from reduced mass transport problems, being decisive for

seagrass meadow development the attenuation of extreme hydrodynamic conditions or their effects.

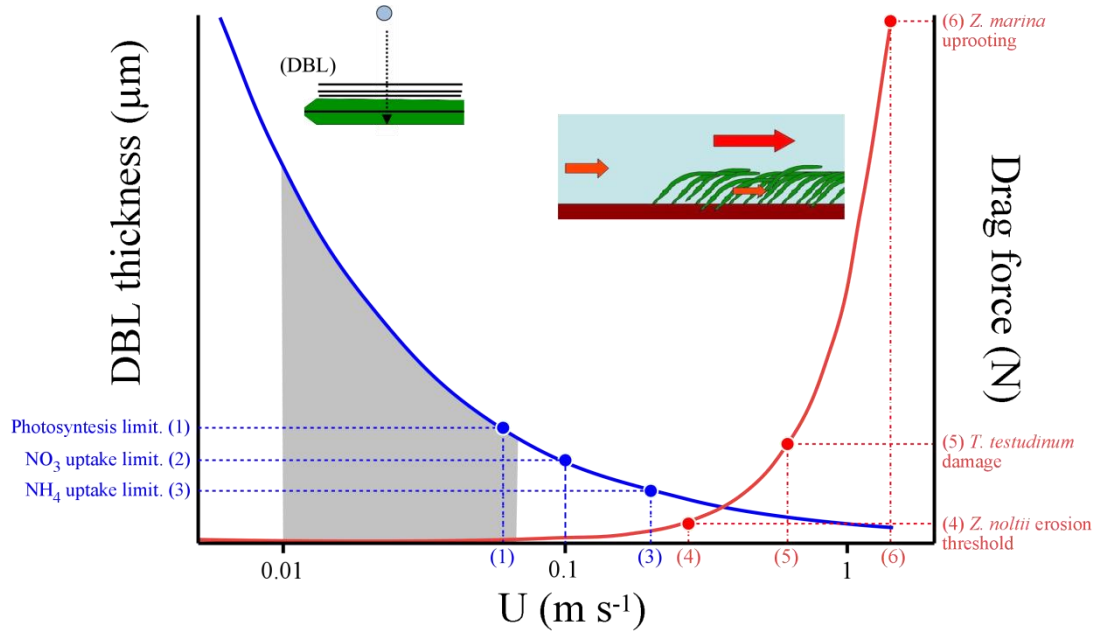

Figure 1. Diffusive boundary layer thickness (DBL, µm -in blue-) and drag force (N –in red-) as a function of current speed (U, m s^{-1}) on seagrasses (redrawn from Wheleer 1988 for macroalgae). Drag force was estimated as a quadratic law of the velocity, whereas DBL thickness was estimated assuming a constant friction coefficient and a power law of (-2/3) of the friction velocity (Koch 1994). Thresholds of representative biological processes (1-6) are included. Grey area indicates the range of current speed at Southwest corner of inner Cadiz bay during a typical spring tide cycle.

2. Seagrasses as ecosystem engineers

Further to seagrass adaptation to flow, seagrasses are able to modify their physical environment determining their survival and development (e.g. light availability, hydrodynamics and sedimentary environment, Bouma et al. 2005, Bos et al. 2007, van der Heide et al. 2007, Peralta et al. 2008). This capacity implies a set of feedback mechanisms between seagrasses and the surrounding habitat, affecting these changes to the entire community (i.e. from small bacterias to large organisms, including the seagrasses, Koch 2001, Bouma et al. 2009 b). For this reason, seagrasses are widely considered as ecosystem engineers (Jones et al. 1997). For example, seagrasses reduce

the nutrient levels in the water column (Moore 2004), but also attenuate waves and flow (Gambi et al. 1990, Fonseca and Cahalan 1992, Granata et al. 2001). Both mechanisms reduce turbidity by limiting phytoplankton and epiphytes or by decreasing suspended sediment concentrations (Ward et al. 1984, Twilley et al. 1985, Granata et al. 2001, Kemp et al. 2005). Reduction of turbidity implies increase in light availability, supporting a stable-state of high shoot density (van der Heide 2007), favoured by the positive feedbacks between velocity reduction and shoot density (Gambi et al. 1990, Peterson et al. 2004, Peralta et al. 2008).

Most of the seagrass-driven ecosystem engineer mechanisms are, directly or indirectly, related to hydrodynamics (Koch 2001). Thus, the physical interaction of seagrass with currents (1) affects solute or nutrient renewal within the canopy (Worcester 1995, Morris et al. 2008, Nepf and Ghisalberti 2008), (2) increases the stability of bottom substrate (Fonseca and Fischer 1986, Thompson et al. 2004) decreasing potential erosion (Thompson et al. 2004, Peralta et al. 2008, Bouma et al. 2009 a), (3) enhances sedimentation rates (Gacia et al. 1999, Hendriks et al. 2008, Hendriks et al. 2010) and (4) affects food availability for the associated fauna (Allen and Williams 2003, Brun et al. 2009). Hence, the knowledge on the interaction seagrass - fluid dynamics is crucial for a complete comprehension of the ecosystem engineering processes (e.g. Bouma et al. 2005), requiring the combination of several spatial scales (from µm to km, Koch et al. 2006) and being particularly relevant processes occurring at canopy and landscape scales.

2.1. Seagrass – hydrodynamic interactions at canopy scale

Current attenuation in submersed canopies is well documented in the literature (Koch et al. 2006 and references therein, Laccy and Willie-Echeverria 2011). Seagrass

beds reduce current velocity by extracting momentum from the moving water (Fig. 2A, Fonseca et al. 1982, Gambi et al. 1990). For *Zostera marina*, this reduction is effective even under very high velocity conditions (i.e. 1.5 m s^{-1}) due to the effects of bending and compaction of the canopy (Fonseca et al. 1982, 1983). However, this process is enhanced by increasing shoot density (Gambi et al. 1990, Peterson et al. 2004, Peralta et al. 2008), by tidal dominancy (low attenuation in wave-dominated areas, Koch and Gust 1999) and reduced by increasing depth (Fonseca et al. 1982). Furthermore, although velocity is reduced within most of seagrass canopies, species-specific differences of reduction magnitude can be also detected due to contrasting canopy features (van Keulen and Borowitzka 2002, Peterson et al. 2004, Morris et al. 2008).

Velocity attenuation within the canopy is normally accompanied by (1) flow re-direction and acceleration above the canopy (Fig. 2B, Fonseca et al. 1982, Gambi et al. 1990, Morris et al. 2008, Hendriks et al. 2010), and by (2) modification of the benthic boundary layer (BBL) velocity profile (see Fig. C1 *vs*. Fig. C2, Abdelrhman 2003, Nepf et al. 2007). Flow acceleration just on top of the canopy (h_c) is usually called "skimming flow" (Neumeier and Ciavola 2004). Although, a complete skimming flow is restricted to dense meadows where a layer of water can be trapped within the canopy (Koch et al. 2006, Peralta et al. 2008). Over bare areas, the BBL velocity profile has typically a logarithmic shape that can be modelling according to equation 1 (Denny 1988, see Fig. 2C1):

$$U(Z) = \frac{u_*}{\kappa} \ln\left(\frac{Z}{Z_0}\right) \qquad \text{(eq. 1)}$$

where u is the velocity (m s^{-1}), u_* is the friction velocity (m s^{-1}), z is the height above the bottom (m) and z_0 is the effective roughness height (m). In low-density canopies, the

effects of submersed vegetation on this vertical profile are negligible (Koch et al. 2006). Emergent canopies (i.e. when water column height, H is <1.5 h_c) are a special case, since the logarithmic layer cannot be developed on top and the velocity profile becomes upright (Nepf et al. 2007). In contrast, within medium to high-density canopies, the logarithmic layer usually is shifted above the vegetation (eq. 2, Fig. 2C2), being the profile within the canopy exponential (Abdelrhman 2003) or vertical (Maltese et al. 2007, Peralta et al. 2008):

$$u(z) = \frac{u_*}{\kappa} \ln\left(\frac{z-d}{z_0}\right) \qquad \text{(eq. 2)}$$

where d is a displacement term (m) which is proportional to the canopy height (h_c) and represents a measure of the height that momentum from the overlaying flow penetrates into the canopy (Nepf and Vivoni 2000).

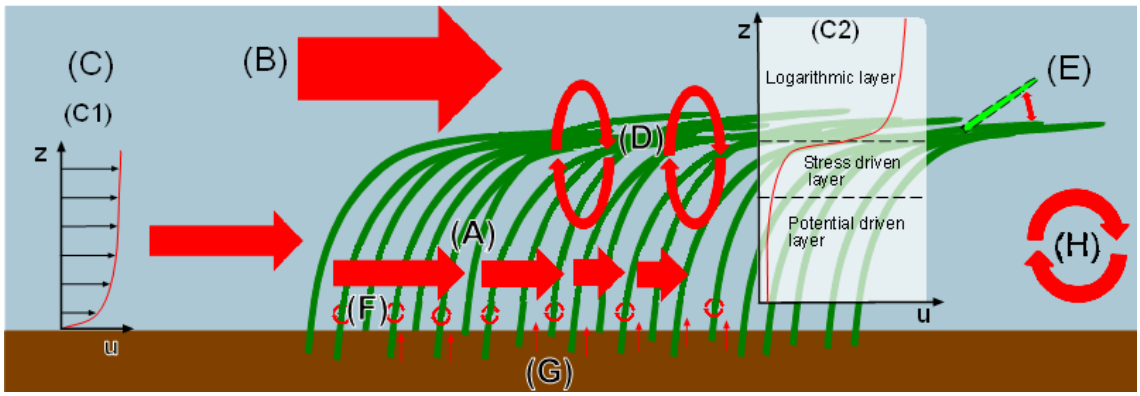

Figure 2. Conceptual model of the hydrodynamic effects associated to the seagrass canopy-flow interactions. (A) Current velocity reduction within the canopy, (B) Flow acceleration and re-direction above the canopy, (C) Typical velocity profiles on a benthic boundary layer without vegetation (C1) or forming a mixing layer due to the presence of a submersed canopy (C2), (D) shear scale turbulence at the canopy-water column interface, (E) "monami" effect, (F) stem-scale turbulence, (G) vertical secondary flow, (H) recirculation cell.

Seagrass canopies also affect turbulence patterns (e.g. Ackerman and Okubo 1993, Ackerman 2002, Maltese et al. 2007, Peralta et al. 2008). In the water column, the

vertical distribution of seagrass biomass generates a shear layer across the canopy-water interface very similar to a mixing layer (Fig. 2D, Ghisalberti and Nepf 2002). This effect is usually accompanied by a leaf synchronous waving movement -called "monami"- which contributes to the vertical mixing (Grizzle et al. 1996, Ackerman 2002, Fig. 2E). The strength of the shear layer usually delimits two vertical regions with different scales of turbulence; (1) the upper canopy, with high turbulence generated by coherent Kelvin-Helmholtz-type vortex structures determining canopy-water exchange (Maltese et al. 2007, Nepf and Ghisalberti 2008), and (2) the lower canopy, where turbulence is generated by interactions at the stem-scale (Nepf and Vivoni 2000, Ghisalberti and Nepf 2008, Fig. 2F) and the erosive stress is reduced (Hendriks et al. 2008, Peralta et al. 2008). Close to the bottom, drag pressure gradients around shoots dominate the turbulent environment (Huettel and Gust 1992). These drag pressure gradients generate vertical secondary flows, promoting nutrient exchange with the sediment (Fig. 2G, Nepf and Koch 1999).

Finally, gaps or bare spaces among seagrass patches can also generate vortices at the downstream end (Fig. 2H, Folkard 2005, Maltese et al. 2007). In such cases, the bottom shear flow increases within the gaps, limiting sedimentary events and even favouring erosive ones (Folkard 2005). The existence of gaps or patchiness is a widely spread situation along seagrass habitats (Bell et al. 1999, Brun et al. 2003, Sleeman 2005). Therefore, the hydrodynamic consequences of this spatial patchiness should be taken into account when studying processes at landscape scale.

2.2. Seagrass – hydrodynamic interactions at landscape scale

As abovementioned, seagrass landscapes are commonly patchy (Brun et al. 2003, Sleeman 2005). In a gradient from low to high hydrodynamic conditions,

seagrasses tend to develop spatial patterns from continuous to sparse or discrete patches (Fonseca and Bell 1998). Presumably, patchy, or even banded, patterns may arise from physical disturbances and feedback processes that chronically confine seagrass bed development (Marbá and Duarte 1995, Fonseca 1996, van der Heide 2010). However, a complete hydrodynamic characterization over a landscape area requires synchronous measurements at several points (e.g. Fonseca and Bell 1998), and such experimental set up is hardly feasible. For this reason, a whole seagrass landscape approach is rarely performed, and flume tank experiments comparing different seagrass patches patterns are used instead, revealing that spaces between consecutive patches promote a sweep flow that enhances turbulent mixing (Folkard 2005, Maltese et al. 2007).

Alternatively to a whole seagrass landscape approach, the hydrodynamic consequences of seagrass patchiness have been inferred by analyzing horizontal gradients that are established from the meadow leading edge (Peterson et al. 2004, Folkard 2005, Morris et al. 2008, Hansen and Reidenbach 2012). For instance, Morris et al. (2008) measured the highest nutrient uptake rates at the leading edge of *Zostera noltii* and *Cymodocea nodosa* meadows, and deduced that a patchy or fragmented landscape (with high proportion of edge zones or perimeter) should be able to incorporate more nutrients than a homogeneous one. Flow patterns associated to meadow edges are usually called “edge effects” (Folkard 2005), affecting important processes such as the replenishment of nutrients, the sediment erosion or the resources availability (Koch et al. 2006, Macreadie et al. 2010). For seagrass landscapes, edge effects mainly imply (1) lower (or absent) vertical vortex dissipation (Ghisalberti and Nepf 2002), and (2) higher flow penetration (Peterson et al. 2004) compared to downstream positions. The magnitude and the extension of these effects depend on the seagrass patch features (Peterson et al. 2004), so the distance that current penetrates

inside the meadow ranges between 1 m (Fonseca and Fisher, 1986) and 50-fold the height of the canopy (Nowell and Jumars 1984, Granata et al. 2001). This distance can be modelled as a function of the seagrass patch drag (Abdelrhman 2003, Peterson et al. 2004). However, too few times have been tested in the field (Granata et al. 2001, Peterson et al. 2004) whereas the validity of flume tank tests can be inconvenient for small patch models that are affected by flume wall effects (Fonseca and Koehl 2006). In this sense, further research of *in situ* edge effects is needed to corroborate the existence of gradients similar to the ones observed in flume tank experiments.

3. The inner basin of Cadiz bay as environmental framework

Bay of Cadiz is located in the west of the Gulf of Cadiz, SW Spain, between 36° 23' to 36° 37'N and 6° 8' to 6° 15'W. The bay is divided in two basins, a deeper outer bay (mean depth of 12 m mean low water, MLW) and a shallower inner one (mean depth of 3 m, MLW), both connected by the Puntales channel (Alvarez et al. 1999, Freitas et al. 2008). The characteristics of the inner bay (shallowness, tide-dominated environment with dense macrophytobenthos coverage) are excellent to be used as a natural laboratory for the study of the seagrass-hydrodynamic interactions. Next section depicts in detail the special features of this system (i.e. hydrodynamics, sediment dynamics and benthic macrophytes).

3.1. Hydrodynamics

The hydrodynamic conditions of inner bay of Cadiz are mainly related to (1) tides, which generate flood or ebb unidirectional flow, and (2) wind, which generate orbital flow. This bay is affected by semidiurnal co-oscillating tides with meso-tidal range (2-4 m). Principal lunar component (M_2) contributes with amplitudes of ~1 m and the principal solar (S_2) with ~0.4 m (Alvarez et al. 1999). Tidal currents also oscillate

according to these semi-diurnal periodicities, with minimum velocities during low and high tide and maximum ones during the intermediate periods. During spring tides, the tidal velocity modulus ranged between 0.01 and 0.08 m s^{-1} (Fig. 3A), being flooding currents faster than the ebbing ones and detecting the maximum values 3 h after low tide. Furthermore, flow direction varied from NW component (flooding phase) to W component (ebb phase) (Fig. 3B), being the main flooding surge re-conducted as a long-shore current by the friction of surrounding coast (Achab and Gutierrez Mas 2005, Benavente et al. 2011). The inner bay velocity range (0.01-0.08 m s^{-1}) is considered low when compared to other seagrass habitats (e.g. Fonseca et al. 1983, Koch 1999), even when compared to adjacent areas (ie. 0.05-0.3 m s^{-1} at outer bay, Brun et al. 2009). Accordingly, diffusive limited processes (i.e. physical control of nutrient uptake and photosynthesis, see previous sections above) could constrain seagrass development in the inner bay of Cadiz. Consequently, this environment can be used to study seagrass hydrodynamic interactions on a physical restriction scenario.

A)

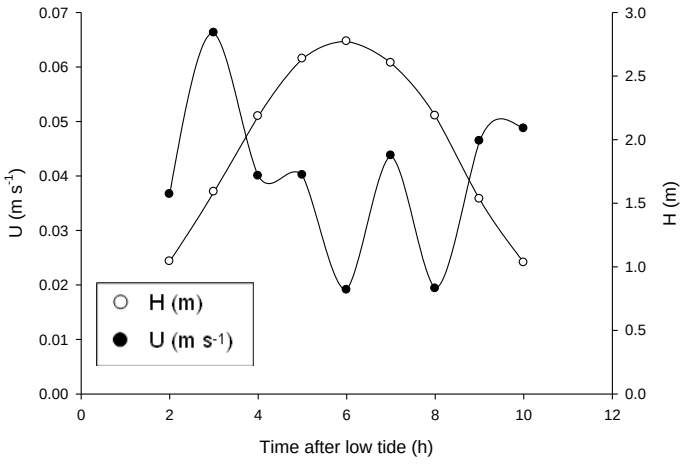

B)

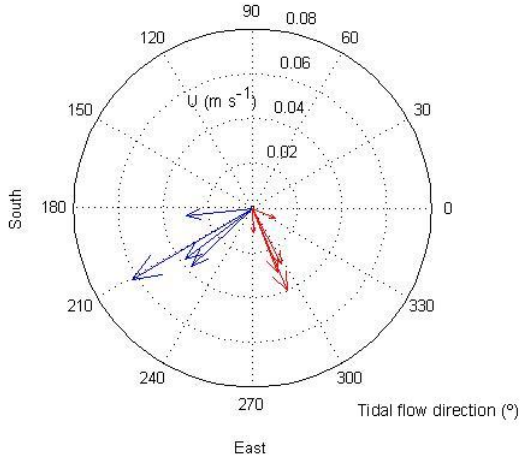

C)

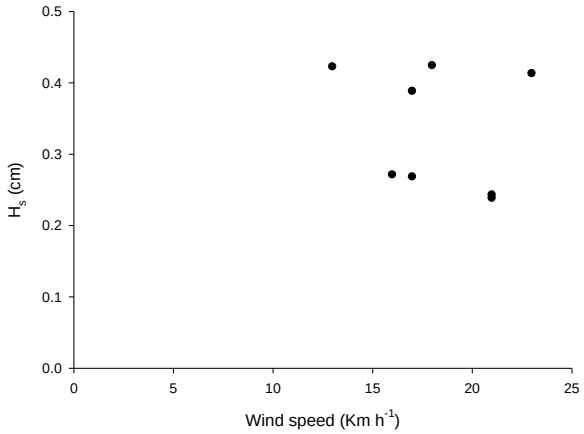

Figure 3: Preliminary hydrodynamic characterization at a bare area of the SW corner of the inner bay of Cadiz (0.32 m above bed). (A) Modulus of tidal current velocity (U, m s^{-1}) and water column height (H, m) during the spring cycle (tidal range = 2.43 m), (B) Main direction of tidal current during flooding (blue arrows) and ebbing phase (red arrows), and (C) Significant wave height (H_s, cm) as a function of wind speed (km h^{-1}) recorded during sampling day.

Geomorphology of the bay of Cadiz prevents the inner bay from the effects of oceanic waves (Alvarez O., personal communication), so the generation of orbital flow is completely due to windstorms. Wind-waves have different frequency and persistence depending on the dominant wind component. Main wind components affecting the bay of Cadiz are E and W. Westerlies (13.6 % frequency, 30 km h^{-1} average) are strong, but squally and inconsistent, whereas easterlies (12.3% frequency, 50 km h^{-1} average) are strong and constant (blowing during seven consecutive days, Lobo et al. 2000, Achab and Gutierrez-Mas 2005). Typical wind waves have short period (i.e. below 7 s) with 0.5 m amplitude in summer and 1 m in winter (Kagan et al. 2003). However, at the

inner bay, wave height is highly variable depending on wind intensity, direction and location. Preliminary measurements of the significant wave height (H_s) during a period of westerlies suggest that even velocities higher than 20 km h^{-1} did not promote an appreciable orbital flow at the SW corner of the inner bay (Fig. 3C). At the same location, easterlies (16.6 km h^{-1}) generated H_s > 20 cm, whereas the sea breeze (15 km h^{-1}, South wind) generated H_s < 5 cm (Garcia-San Miguel 2010).

3.2. Sediment characteristics and dynamics

Although tidal flow is able to drive sediment resuspension by itself (Alvarez et al. 1999), sedimentary dynamics is controlled by waves due to windstorms. Sediment resuspension within the inner bay is originated by the orbital flow driven by easterlies, whereas West and North winds have no influence (Gutierrez Mas et al. 2000). Resuspended sediment is then transported by tidal and wind-induced currents to the outer bay as a turbidity blob, or relocated along the inner bay by West component currents (Gutierrez Mas et al. 2000). The turbidity blobs attenuates considerable the light available to the phytobenthos (Garcia-San Miguel 2010). Size and composition of sediment resuspended or deposited at the inner bay may vary from siliciclastic clay to sand with biogenic carbonated component, although the most representative sediment fraction is the siliciclastic silt (i.e. illite of grain size ranging 8-62 μm, Gutierrez Mas et al. 1997, Achab and Gutierrez Mas 2005).

3.3. Benthic macrophytes in the inner Cadiz bay

The bay of Cadiz has three out of the four European seagrass species: *Zostera noltii* Hornem. *Cymodocea nodosa* Ucria (Ascherson), which both thrive around the shoreline perimeter of the inner bay, and *Zostera marina* Linnaeus (located in a very small area at the SW corner). Moreover, the green rhizophytic macroalgae *Caulerpa*

prolifera Forsskaal (Lamouroux) is widely distributed across the outer and the inner bay (Morris et al. 2009) and it constitutes the most extensive habitat to benthic fauna (Rueda and Salas 2003).

The fieldwork of this PhD Thesis has been developed in the SW corner of the inner bay, in a shallow and protected muddy area called Santibañez (36º28'N, 6º14'W). Benthic macrophyte distribution on this area shows a clear zonation pattern. From the intertidal to the subtidal locations (Fig. 4), distribution areas of *Zostera noltii* (intertidal), *Cymodocea nodosa* (from 0.40 to -0.50 m relative to the lowest astronomical tide, LAT) and *Caulerpa prolifera* (subtidal -0.08 to - 2 m LAT) are found. In the area between -0.08 and -0.50 m LAT, *C. nodosa* and *C. prolifera* cohabit forming a patchy landscape (Fig. 4D).

Zostera noltii belongs to Zosteraceae family and it is characterized by an aboveground biomass composed by flexible and thin tape-like leaves (0.5-2 mm width and 0.04-0.35 m long, Fig. 4A) including a basal meristem (Brun et al. 2006). In the inner bay of Cadiz, the shoot density of this species is quite variable and follows a seasonal trend, ranging between 100 (winter) and 18000 shoots m^{-2} (early summer, Brun et al. 2006). Moreover, the distribution area of this species is highly affected by physical anthropogenic disturbances (i.e. shellfishing, boat anchoring scars), generating a highly fragmented landscape with numerous gaps or un-vegetated (bare) zones (e.g. Brun et al. 2003).

Cymodocea nodosa belongs to Cymodoceae family (Fig. 4B) and its leaves are more elastic, wider (2-8.7 mm) and longer (0.05-0.98 m) than that of *Z. noltii* (Brun et al. 2006, De los Santos 2011). However, shoot density usually is 2 - 10 times lower than *Z. noltii* one (Brun et al. 2006). Flume tank experiments revealed that *C. nodosa*

canopies were 2-fold more permeable to flow than *Z. noltii* ones (Morris et al. 2008). However, *in situ* studies are still needed to corroborate these results on nature.

Caulerpa prolifera is a green macroalgae belonging to the family of Caulerpaceae (Fig. 4C). Its aboveground biomass is constituted by erect oval assimilators (7-50 mm size), which may be detached directly from a creeping stolon (primary assimilator) or from the main frond (Malta et al. 2005, Vergara et al. in press). When exposed to flow, frontal area of canopy only represents a thin friction layer for near bed currents. However, frond density is usually 2- to 20-fold higher than those of seagrass canopies. As a result, the velocity reduction in *C. prolifera* beds is very high (i.e. volumetric flow is 65-75% lower than those of bare bed) and it enhances relevant ecological processes such as sediment particle trapping (Hendriks et al. 2010).

At the band between -0.08 and -0.50 m LAT, the distributions of *C. nodosa* and *C. prolifera* exhibit alternate patchy spatial patterns (Fig. 4D). This spatial structure must behave, in terms of ecological functioning, differently than homogeneous landscapes (Robbins and Bell 2000). Across this patchy landscape, a microtopographic pattern makes the *C. prolifera* beds to be 5-10 cm above the *C. nodosa* ones (Benavente et al. 2008). Therefore, in the inner bay of Cadiz there are three spatial types of benthic macrophyte discontinuities (i.e. patchiness, microtopography and fragmentation), making the interaction hydrodynamics - benthic vegetation more complex than expected for monospecific canopies (Folkard 2005, Fonseca and Koehl 2006).

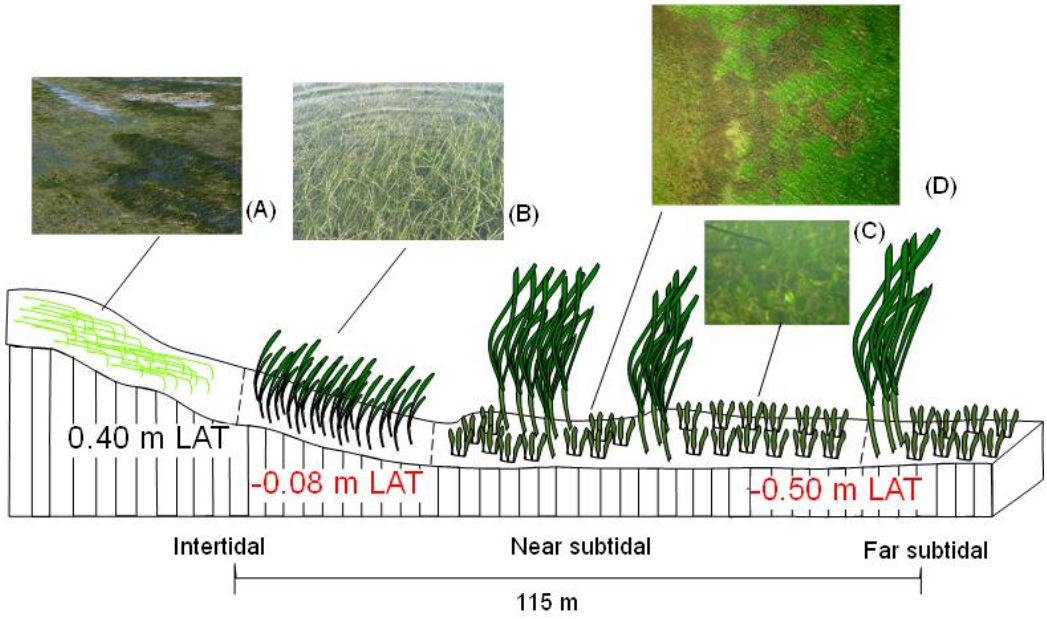

Figure 4: Marine benthic macrophyte zonation pattern at Santibañez (SW inner bay of Cadiz). Distribution depth is referred to the low astronomical tide (LAT) (positive values are above LAT, negative values are below LAT). Photographs show (A) intertidal *Zostera noltii* meadow, (B) intertidal *Cymodocea nodosa* stand, (C) subtidal *Caulerpa prolifera* bed. Photograph D shows an aerial view of the patchy landscape formed by subtidal *C. nodosa* and *C. prolifera* populations.

4. Thesis outline and specific objectives

The current PhD Thesis is embodied in the outlines of the Spanish National Research Projects EVAMARIA (CTM 2005-00395), IMACHYDRO (CTM 2008-0012) and in the Andalusian Excellence Research Project FUNDIV (P07-RNM-02516). These projects focus on the study of the effect of key environmental variables, including hydrodynamics, on the primary productivity, structure and function of marine macrophytes from Cadiz Bay Natural Park (CBNP) at several spatial scales. Such approach requires the understanding of how marine macrophytes are able to modify their physical environment. Considering seagrasses as ecosystem engineers is generally based on their capacity to increase bed stability and sedimentation and to modify resources availability (i.e. nutrients and food particles) when compared to un-vegetated areas, which is mainly hydrodynamic-mediated (i.e. controlled by velocity levels and by

key turbulent variables). In achieving this general goal, two specific objectives need to be addressed: (1) the effects of marine macrophytes populations on spatial patterns of current velocity and turbulence, and (2) the potential consequences of such effects for nutrients and sedimentary dynamics. Since spatial homogeneity cannot be assumed along natural seagrass landscapes (e.g. the inner bay of Cadiz), it is needed to understand (3) how spatial discontinuities (i.e. patchiness, fragmentation or microtopography) would alter the macrophyte – hydrodynamic interactions. To cope with the overall objective, it will be examined the hydrodynamic effects of natural and/or simulated canopies for the three representative marine macrophyte species from the inner bay of Cadiz (i.e. *Zostera noltii*, *Cymodocea nodosa* and *Caulerpa prolifera*). The influence of spatial discontinuities is tackled by comparing the current flow environment in homogeneous versus sloped or fragmented bed, or by analyzing horizontal gradients from the edge of the meadows.

On this basis, the PhD thesis is divided into four sections corresponding to the specific objectives. In the first part (chapter 1), the hydrodynamic effects of the transition between patchy areas of *C. nodosa* and *C. prolifera* beds are studied. In this context, chapter 1 focuses on the spatial patterns on velocity and turbulence for *in situ* horizontal gradients under tidally dominated conditions. The interpretation of "proxy" variables helps to infer the implications of this singular benthic transition for nutrients limitation at canopy scale. Second section of chapter 1 focuses on the effects of the microtopography using a patchy landscape *C. nodosa – C. prolifera* model. To do so, a small-scale transition zone *C. prolifera – C. nodosa* was simulated in a flume tank. This experiment tested the influence of (1) realistic free stream velocity levels (i.e. 0.065 and 0.14 m s^{-1}), and (2) the microtopography (5-10 cm) on bed shear stress, turbulent

mixing and volumetric flow rate, being considered as the set of key hydrodynamic variables that control sediment deposition and bed stability.

In the second part of the thesis (chapter 2), spatial sedimentation rates patterns within a single *C. nodosa* patch are studied using a flume tank with artificial plants and simulating three contrasting velocity levels. This study responds whether or not seagrass patches may act as sediment sinks even under the low flow environment (i.e. limited sediment transport) frequently described at CBNP, also helping to determine the critical thresholds of seagrass patch size for sedimentation success. The real role of seagrass as ecosystem engineers when limited depositional and sediment transport occurs is an aspect poorly understood of their ecology.

Finally, the third part (chapter 3) studies the consequences of seagrass landscape fragmentation to the local solute transport. Advection and turbulent diffusion processes were achieved within natural (fragmented versus homogeneous) *Z. noltii* patches by employing dye tracer techniques and *in situ* velocity records. This study is also a pioneer approximation to the measurement of water renewal rate within seagrass patches, which is a key hydrodynamic variable determining nutrient availability due to the solute dispersion.

CHAPTER 1:

Flow along benthic macrophytes transitions: Ecological implications

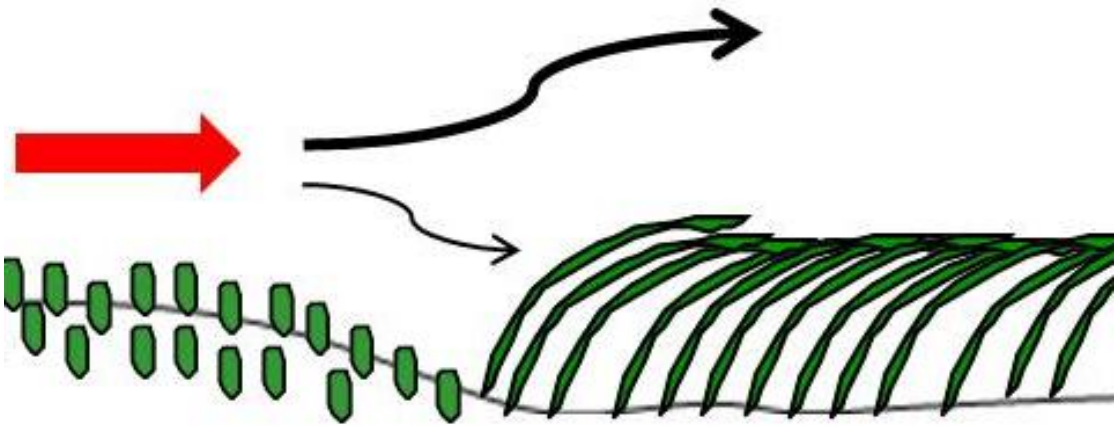

Hydrodynamics along seagrass patch edges: a field study

M. Lara[1*], G. Peralta[1], I. E. Hendriks[2], J. Benavente[3], F. G. Brun[1], E. P. Morris[1], T. Van Engeland[4], T. J. Bouma[4], J. L. Pérez-Lloréns[1]

[1]Department of Biology, Faculty of Marine and Environmental Sciences, University of Cadiz, 11510 Puerto Real (Cadiz), Spain

[2]IMEDEA (CSIC) C/ Miquel Marques, 21 07190 Esporles, (Mallorca) Islas Baleares, Spain

[3]Department of Earth Sciences, Faculty of Marine and Environmental Sciences, University of Cadiz, 11510 Puerto Real (Cadiz), Spain

[4]Netherlands Institute of Ecology (NIOO-KNAW), Centre for Estuarine and Marine Ecology, PO Box 140, 4400 AC Yerseke, The Netherlands

This article was submitted to Marine Ecology Progress Series. Comments and suggestions from anonymous reviewers were considered on the final version.

ABSTRACT

Within Cadiz Bay Natural Park, a mosaic of neighbouring *Cymodocea nodosa* (seagrass) and *Caulerpa prolifera* (macroalgae) patches comprises a zone with many edges that define the transition between each species. Previous flume studies demonstrated that these transitions generated spatially explicit hydrodynamic gradients affecting in both flow velocity and turbulence, which determine the transport of nutrients. Edge effects were investigated *in situ* within a natural patchy landscape of *C. nodosa* and *C. prolifera* occurring in a shallow and low-flow tidal-environment. During a flood tide, vertical profiles of velocity components (u and w), turbulent kinetic energy (TKE) and vertical Reynolds stress (τ_R) over a 2.2. m long transect perpendicular to the boundary between the two species were measured. Vertical Reynolds stress was negatively related with u above the *C. nodosa* canopy, which may limit the response of turbulent vertical exchange to tidal current changes. A TKE peak was observed at 0.69 m from the leading edge within the *C. nodosa* patch, suggesting a spatial limit to the edge effect. Recorded low velocities above canopies and the evidence of restrictions to turbulent exchange indicate the system as physically constrained. Gradients in turbulent energy and velocity resulting from seagrass patchiness are likely to have consequences for the functioning of shallow benthic habitats.

INTRODUCTION

Seagrass meadows are considered one of the most productive and valuable ecosystems of the biosphere (Constanza et al. 1997, Duarte and Chiscano 1999, Mann 2000). They provide habitat and food resources for a broad range of organisms (Mc Roy and Helfferich 1977), enhance particle retention (Koch 2001) and increase bed stability (Granata et al. 2001). This ecological functionality is directly or indirectly due to modification of physical environment by the seagrass canopy.

Seagrass meadows interact with tidal currents modifying velocity profiles, turbulence and vertical advection (Gambi et al. 1990, Widdows et al. 2008). In general, flow velocities inside the seagrass canopy are reduced by the frictional effects of the vegetation (Fonseca et al. 1982, Koch and Gust 1999, Abdelrhman 2003) causing enhanced velocities above the canopy due to the redirection of the current (i.e. skimming flow). This effect contributes to the production of new regions of turbulence at the top of the canopy (Ghisalberti and Nepf 2002) and to the instability (reduction) of current velocity along a horizontal gradient (Peterson et al. 2004). Understanding these interactions between seagrass and hydrodynamics is important, as they control several essential diffusion-limited processes such as nutrients uptake (Thomas et al. 2000, Morris et al. 2008) and photosynthesis (Koch 1994).

Although seagrasses tend to form continuous meadows, it is also frequent to find them as a patchy landscape (e.g. Salita et al. 2003, Brun et al. 2003). This patchy distribution can be a result of both natural and anthropogenic causes. For example, boat propellers (Zieman 1976), storm events (Preen et al. 1995) or algal mats (Cowper 1978) can generate gaps within the meadow, thereby producing a mosaic of un-vegetated and vegetated areas (Bell et al. 1999). Banded patch formation may, however, also be

originated from environmental gradients in growing conditions (van der Heide et al. 2010). Coexisting patches of several macrophytes species is another frequent type of landscape (Robbins and Bell 2000). In these patchy landscapes, meadow edges are very important features, since at the transition zones (boundaries between neighbouring patches), the hydrodynamic patterns diverge from that observed within homogeneous beds (Folkard 2005, Morris et al. 2008).

Understanding the downstream hydrodynamics associated with edge effects is a first step towards discerning biological consequences of patchy macrophyte landscapes. Previous works in flume tanks have described hydrodynamic as function of distance from the vegetation leading edge (e.g. Fonseca et al. 1982, Gambi et al. 1990, Morris et al. 2008) or in relation to adjacent patches (Folkard 2005, Maltese et al. 2007). These studies showed that (1) inside the canopy water velocity decelerated, (2) once skimming flow was established, it was maintained along the canopy (Gambi et al. 1990), and (3) in between two nearby patches, the turbulent wake of the first patch was dissipated by the presence of a second one (Folkard 2005). Furthermore, these small-scale variations in hydrodynamics where shown to generate spatial-explicit physiological responses by the individual components of the macrophyte communities (Morris et al. 2008).

Unfortunately, conclusions obtained from flume tank experiments are limited because of the restricted physical conditions (Nowell and Jumars 1987). Laboratory conditions may generate artefacts in skimming flow and turbulence intensity (Gambi et al. 1990, Fonseca and Koehl 2006). Moreover, downstream wakes due to skimming flow may be modified in comparison to field conditions, where there are no lateral restrictions to the flow (Hendriks et al. 2006, Morris et al. 2008). Until now, very few edge effect studies have been carried out in natural seagrass meadows (Fonseca et al. 1983, Granata et al. 2001, Peterson et al. 2004).

The present fieldwork focuses on the velocity and turbulence patterns caused by edge effects within a seagrass-macroalgae patchy landscape (*Cymodocea nodosa* and *Caulerpa prolifera*, respectively) in a shallow, protected tidal bay. We hypothesize that edge effects do generate horizontal hydrodynamic gradients, as described in flume tank experiments, but due to the absence of lateral restrictions to the flow, with a different magnitude and spatial scaling. We compare the trends recorded in previous flume tank literature with our field observations to asses (1) whether the phenomenon of vertical flow re-direction (skimming flow) occurs in the field and (2) whether the magnitude and spatial scale of effects on turbulence are similar. Finally, the potential consequences of these hydrodynamic effects in ecological processes are considered.

MATERIAL AND METHODS

Study site

The study was conducted in Cadiz Bay Natural Park (SW Spain, 36º 29'N-6º15'W). The bay is an Atlantic system dominated by tidal currents of medium range during spring (ie. average tidal range of spring tides between 2-4 m, Davies 1964). It is divided into 2 basins: a shallow inner bay (3 m mean depth at low water, MLW, Freitas et al. 2008) and a deeper outer bay (12 m mean depth MLW). Measurements were carried out in the South-West corner of the inner Cadiz Bay (Fig.1) which is covered for more than 90 % by benthic macrophyte communities (Morris et al. 2009). Among dominant species, the seagrass *Cymodocea nodosa* Ucria (Ascherson) and the benthic macroalgae *Caulerpa prolifera* Forsskaal (Lamouroux) are distributed according to a general depth zonation, in shallow-subtidal and deep-subtidal areas, respectively. However, particularly within the low intertidal as well as the shallow subtidal zones

mixed or patchy populations of *C. nodosa* and *C. prolifera* are common. Furthermore, a smooth slope of about 10% and a gradient on height of *C. nodosa* canopy was achieved within this area.

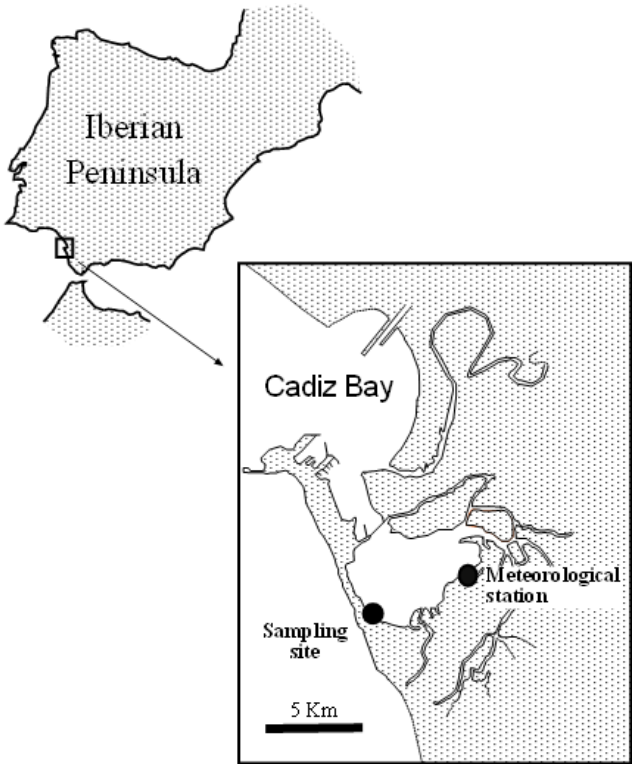

Figure 1. Map of location of the sampling site and meteorological station.

Gradient characteristics: canopies and microtopography

In situ horizontal gradient was investigated in one representative transect across adjacent patches of *Caulerpa prolifera* and *Cymodocea nodosa*. Measurements were carried out using four 3D acoustic Doppler velocimeters (ADV, see description below) mounted into a PVC frame. Individual velocimeters were placed at 0.77 m before the *C. nodosa* leading edge (i.e. on the *C. prolifera* bed, -0.77 m), at 0 m (on the edge

between the patches) and two additional positions within the *C. nodosa* canopy (0.69 m and 1.46 m from the leading edge, Fig. 2). The position space (0.75 m) was designed to provide a handy PVC frame that would be able to cover the maximum horizontal variability.

The measuring cell of every velocimeter was fixed to read at the same distance from the water surface. The microtopography of the measuring transect was determined by divergences of measuring cell - bottom floor distances among the velocimeters (Fig. 2). As a 0.2 m difference in the depth of the sediment surface was found between the *C. prolifera* and *C. nodosa* beds, zero depth was set as the sediment surface at 1.46 m within *C. nodosa* bed. The canopy height (above the sediment surface) was between 0.3 and 0.5 m and shoot density of *C. nodosa*, estimated with a 0.2x0.2 m^2 minimum sampling area, 356 ± 60 (standard error) shoots m^{-2} (n = 4 sampling areas). *C. prolifera* canopy height was measured *in situ* and resulted 0.1 m, whereas fronds density was recorded independently with a 0.3x0.3 m^2 minimum sample area. When estimated, the secondary proliferations from the original fronds were not considered (ie. only 'primary assimilators' were counted, Malta et al. 2005) and a total of n=10 stolons were subsampled, yielding 8700 ± 146 (standard error) primary assimilators m^{-2}.

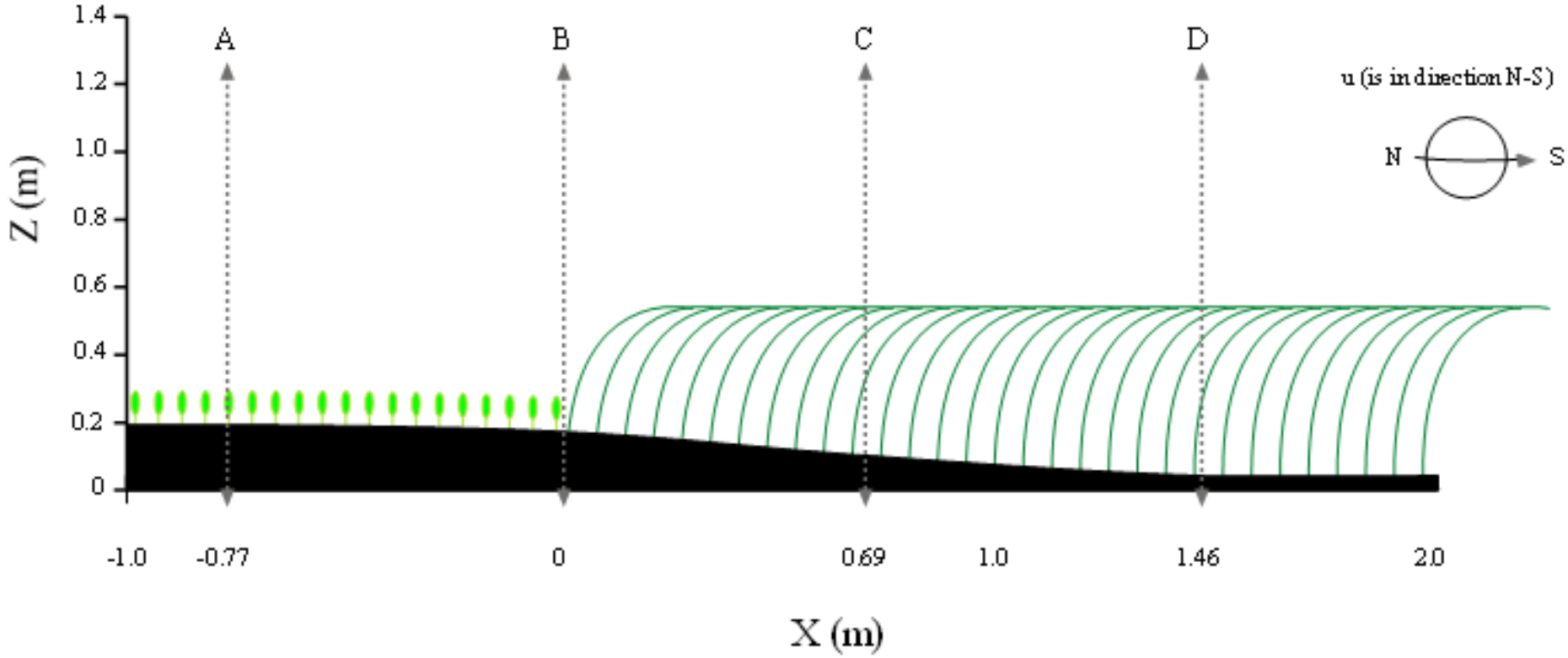

Figure 2. Position of 3D Doppler velocimeters along the sampled gradient *Caulerpa prolifera – Cymodocea nodosa*. X (m) is the horizontal distance from the leading edge of *Cymdocea nodosa* bed and Z (m) is the vertical distance from the sediment level reference.

Hydrodynamics measurements in the field

Four 3D acoustic Doppler velocimeters were used for data acquisition: 2 Vectors (x=-0.77 and 0 m), 1 Vectrino (x=1.46 m) and 1 Nortek Doppler Velocimeter (NDV, x=0.69 m), all of them from Nortek AS. The velocimeters provided detailed measurement of the three velocity components (u, v and w) allowing calculation of turbulence terms. Sampling rates were selected at the maximum possible for each device (64 Hz for Vectors and Vectrino, and 25 Hz for NDV).

Every 4 minutes the height of the frame was set to a different vertical position so as to collect profiles of the velocity components (i.e. 2000-5000 data for each measuring point). Two vertical profiles separated in the beginning by 30 min (ie. 1.5 and 2 hours after low tide, profile 1 and profile 2 respectively) were collected for every velocimeter position. Measurements were carried out at 0.53, 0.73, 0.93, 1.03, 1.13 and 1.18 m (or 1.33 m for the second profile) above the reference sediment surface (ie. reference surface set at the sediment level located at 1.46 m downstream, Fig. 2). Water column height difference due to the delay of both profiles was just 0.2 m.

Tides and meteorological conditions

The hydrodynamic measurements were performed during the flood tide (2.9 m tidal range), once the canopies were submerged. Wind direction and velocity were obtained from Andalusian Department of Environment (Subsystem of Environmental Climatic Information, CLIMA). The location of the meteorological station is indicated (Fig. 1). Wind velocity (between 7 and 8 Km h^{-1} or 4 Knots) and the direction (230º South-West direction) remained constant during the measurements. These values represented very small wavelets according to Beafourt wind scale and particular calm conditions for Cadiz Bay. Previous wave height records at the area during conditions of

higher wind speed than present work (16 Km h^{-1}, 270º West direction) yielded a negligible average wave height (0.27 cm).

Data processing

Prior to processing, the hydrodynamic database was filtered and the reference system rotated to fix the x-axis as the main velocity direction (in our case, the main velocity direction was N-S), which was approximately perpendicular to the edge of the *C. nodosa* canopy. Data with a beam correlation below 70% were rejected (Folkard 2005, Bouma et al. 2007). Rotation was carried out using the angle formed clockwise in between the N direction and the velocimeter x-direction (α), according to Kundu (1990):

$$u = u_0 \cos(\alpha) + v_0 \sin(\alpha) \qquad \text{(eq. 1)}$$

$$v = v_0 \cos(\alpha) - u_0 \sin(\alpha) \qquad \text{(eq. 2)}$$

where u_0 and v_0 are the original (measured) velocity components, u and v are the rotated velocity components and α is the rotation angle. The u component represented the main current direction (N-S), v component was perpendicular to N-S and w was the vertical component.

Data analysis

To describe the effects of benthic macrophytes on the local hydrodynamics and to understand the associated feedback effects, the following variables were considered: (1) u profiles; (2) turbulent kinetic energy (TKE), as an indicator of turbulence dissipation along the gradient (Denny 1988); (3) vertical Reynolds stress (τ_R) as indicator of vertical transport and mixing (i.e. exchange processes between canopy and overlaying water column; Velasco et al. 2003, Peralta et al. 2008, Hendriks et al. 2010), and (4) Stanton number (St) as an indicator of mass transfer efficiency towards the canopy,

which controls processes such as nutrient uptake (Thomas et al. 2000). Furthermore, the relationship between τ_R and u was studied as a proxy for vertical mixing processes, as well as w was plotted against u to evaluate vertical current re-direction.

The 3D Doppler velocimeters provide detailed information on the three velocity components (u, v, w):

$$u = \bar{u} + u' \quad \text{(eq. 3)}$$

$$v = \bar{v} + v' \quad \text{(eq. 4)}$$

$$w = \bar{w} + w' \quad \text{(eq. 5)}$$

where $\bar{u}$, $\bar{v}$, $\bar{w}$ are the time-averaged values and u', v', w' the fluctuations from the averaged velocity components, respectively. These components allow the estimation of TKE (eq. 6) and τ_R (eq. 7).

$$TKE = \frac{1}{2}\left(\overline{u'^2 + v'^2 + w'^2}\right) \quad \text{(eq. 6)}$$

$$\tau_R = -\overline{u'w'} \quad \text{(eq. 7)}$$

Finally, the Stanton Number (St, eq. 8) is a non-dimensional ratio between mass flux to a surface and its advection past the surface (e.g. leaves surface), and according to Thomas et al. (2000) the efficiency of nutrient transfer in seagrass communities scales with the (-0.6) power of bulk velocity (u_b).

$$St \propto u_b^{-0.6} \quad \text{(eq. 8)}$$

where u_b was estimated as the z-averaged local velocity u (z).

Statistical differences in hydrodynamic variables (u, w, TKE and St) were tested by non-overlapping of the 95 % confidence intervals (95% CI). Standard error of St was computed from transformed variance of u ($\sigma^2 u_b$) using Taylor's theorem (eq.9):

$$\sigma_{St}^2 = \left(-0.6\left(\overline{u_b}\right)^{-1.6}\right)^2 \sigma^2 u_b \qquad \text{(eq. 9)}$$

Significant correlations between combinations of hydrodynamic variables were assessed using the product-moment correlation coefficient. Data from different depths or x-positions were crossed in these correlations. The significant level was set at 0.05.

RESULTS

Velocity profiles

Distance from the leading edge (x) significantly affected the u profiles (Fig. 3 A-D). A clear acceleration of flow was observed at the top of the *C. nodosa* canopy (z = 0.53-0.73 m) at x = 0.69 m and x = 1.46 m, with values ranging between 0.025 and 0.035 m s^{-1} (Fig. 4). Contrastingly, values were lower than 0.01 m s^{-1} at the same canopy height when measured at the edge of *C. nodosa* patch (x = 0) or above the *C. prolifera* vegetation (x = -0.77 m). However, close to water surface ($z \geq 1.13$ m), u effectively decreased a 50% behind the leading edge (i.e. 0.035 m s^{-1} at x = 0 m, and 0.02 m s^{-1} at x = 0.69 and 1.46 m).

Short term increase of tidal flow did not change the u profile (Fig. 3 A-D). Profile 2 exhibited a quite similar pattern than profile 1 (i.e. around 0.030 m s^{-1} at x = 0.69 m and around u = 0.035 m s^{-1} at x = 1.46 m from the leading edge). Most measurements showed differences lower than 17 % between the two profiles, except for those depths

closest to the water surface (i.e. for $z \geq 1.13$), where u increased by 25% from profile 1 to profile 2.

When comparing horizontal (u) and vertical (w) components (Fig. 4), w was one order of magnitude lower than the u component, ranging between -0.002 and 0.007 m s^{-1} and the lowest values recorded at x = 1.46 m. In most cases, there was a low ascending movement of water (i.e. $w > 0$), suggesting that the flow was mostly directed upwards from the leading edge. On a horizontal plane, flow direction was generally constant at all depths and x-positions (i.e. North-South), with deviations during the measuring period of less than 10º except at the top of the canopy (graphs not shown). On this position, the angle of deviation reached maximum values of 22º, meaning that edge effects on the v component were negligible.

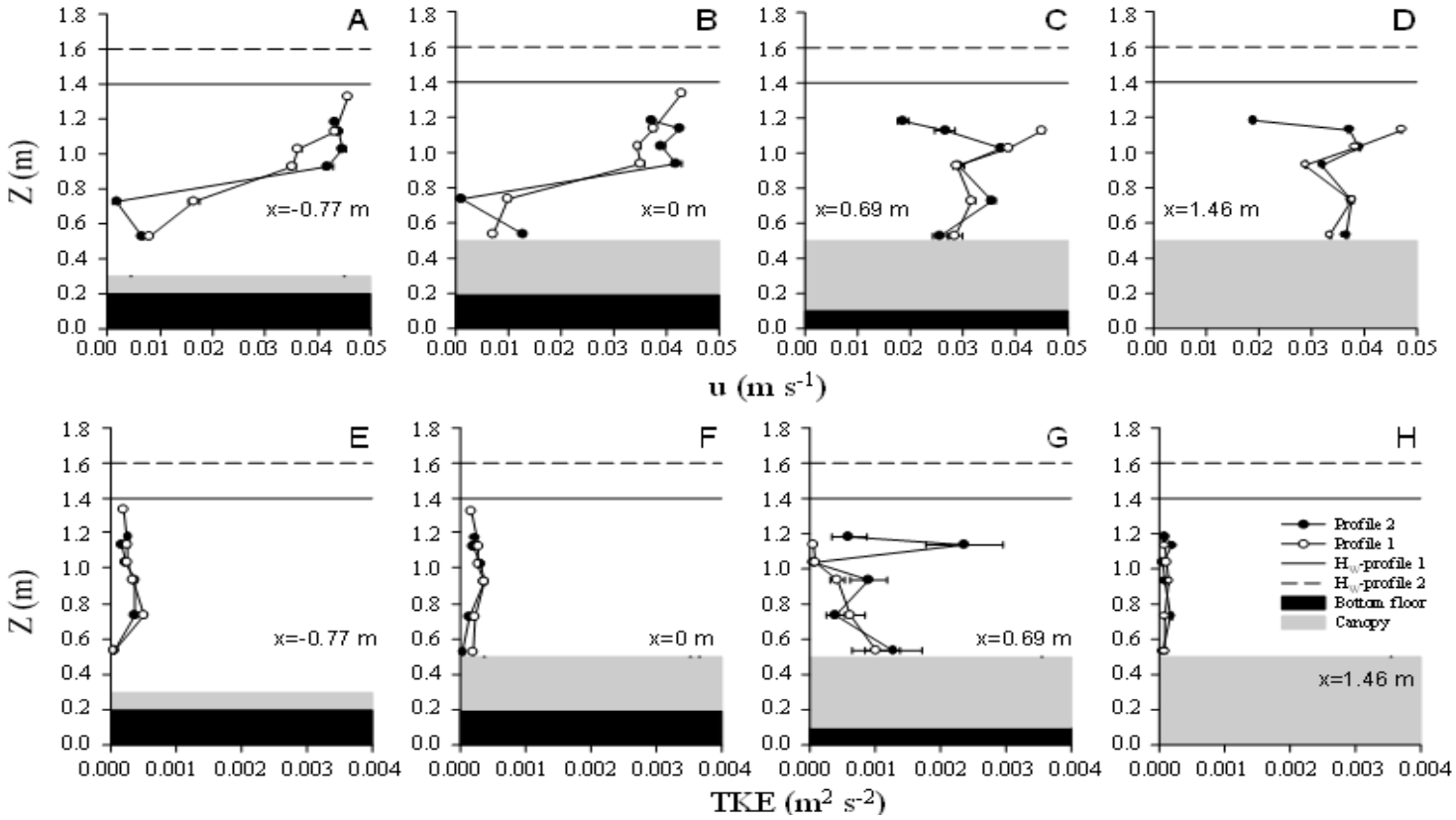

Figure 3. Vertical profiles of u velocity (m s^{-1}) on positions x = -0.77(A), 0 (B), 0.69 (C) and 1.46 (D) m from the leading edge after 1.5 h (black circles) and 2 h (white circles) of low tide. Vertical profiles of Turbulent Kinetic Energy (TKE, m^2 s^{-2}) on positions x = -0.77(E), 0 (F), 0.69 (G) and 1.46 (H) m from the leading edge after 1.5 h (black circles) and 2 h (white circles) of low tide. Dashed line symbolizes canopy height and dotted lines water column height. Error bars are 95% confidence intervals.

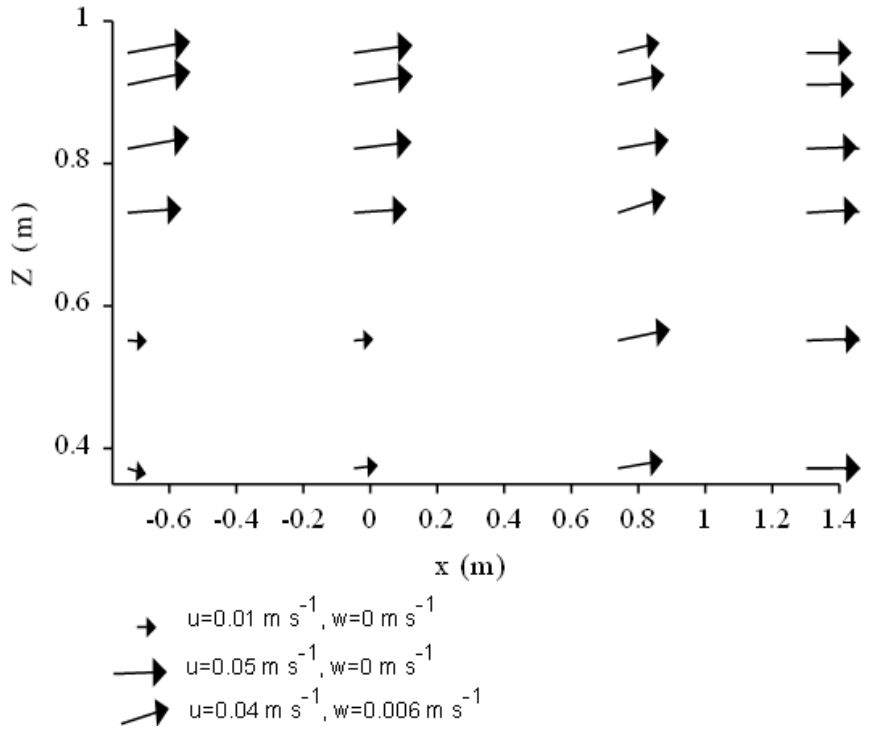

Figure 4. Spatial orientation of the water movement on the vertical plane Z-X at the studied system. Vertical component of arrows represents w component of velocity.

TKE profiles and vertical Reynolds stress

TKE profile showed spatial variation with distance to the leading edge (Fig. 3 E-H). At Profile 1, the highest turbulence (1.3 x 10^{-3} m^2 s^{-2} and 2.5 x 10^{-3} m^2 s^{-2}) was detected at x = 0.69 m (Fig. 3G), with two peaks, one on top of the canopy (z = 0.53 m) and another at z = 1.13 m above the seabed, respectively. This layer of high turbulence indicates the existence of a region of fluctuating velocity (i.e. wake or vortices), which is dissipated downstream. Profile 2 showed that tide evolution also affected the TKE pattern at x = 0.69 m (Fig. 3G). At this distance, the second profile showed a much smoother TKE trend than the first one, with a disappearing of the peak near the water surface (z = 1.13 m) and, therefore, exhibiting a maximum value on top of canopy (z = 0.53 m).

The vertical Reynolds stress (τ_R) at the top of the canopy also showed spatial variations (Fig. 5). At x = 0.69 m behind the leading edge, τ_R was 100 times higher than that at x = -0.77 m (before the leading edge) and 10 times higher than that at x = 0 m. In spite of the high τ_R error at x = 0.69 m, τ_R means were significantly different to the values at the other x-positions. Positive τ_R values at x = 0.69 m indicates the existence of a transfer of turbulent moment from the water column towards the canopy, whereas the slightly negative τ_R values at the other positions would indicate the opposite.

There was a significant negative correlation between τ_R and u above the *C. nodosa* canopy (ie. at x = 0.69 m and x = 1.46 m from the leading edge), whereas above *C. prolifera* (x = -0.77 m) and at the leading edge (x = 0 m) there was no correlation (Fig. 6). In the *C. nodosa* canopy a negative correlation means that turbulent transfer due to changes in velocity is opposite to the expected one (i.e. a positive correlation between τR and u). Thus, at high current velocity the vertical mixing processes at the top of canopy could be physically limited because τ_R did not increase due to tidal variation.

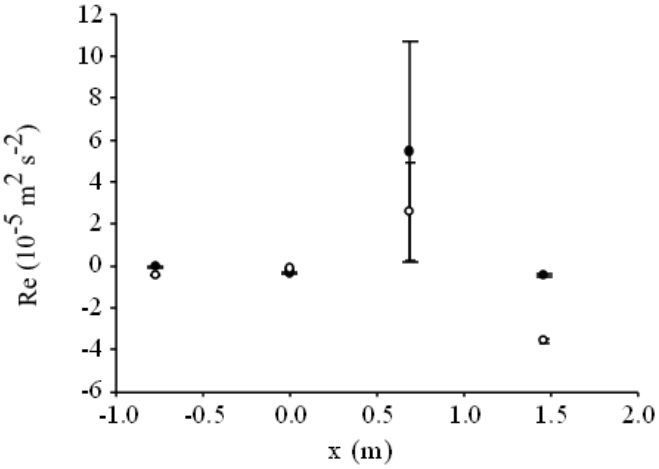

Figure 5. Vertical Reynolds stress (Re) (x10^{-5} m^2 s^{-2}) at the top of the canopy along a gradient from *Caulerpa prolifera* to *Cymodocea nodosa* (x = 0 indicates the leading edge of the *C. nodosa* patch). Error bars represent 95% confidence intervals.

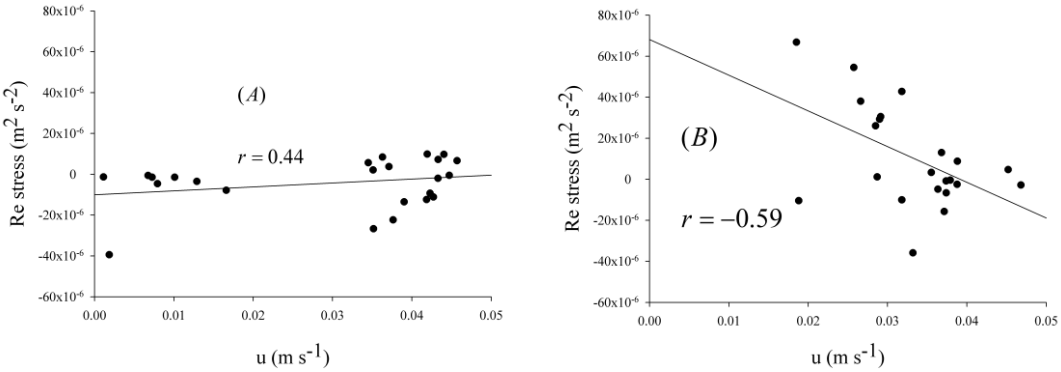

Figure 6. Correlation between the main velocity component (u) and vertical Reynolds stress values (Re stress) before and at the edge of the *Cymodocea nodosa* patch (A) and above it (B).

Stanton number (St) above Cymodocea nodosa canopy

Error bars of St were lower than the range of mean, but high enough to overlap the values of St at the different horizontal positions (Fig. 7). The St above *C. nodosa* canopy was mostly the same downstream from x = 0 m (St = 8.12) to 1.46 m (St = 7.7)

(Fig. 7) suggesting a constant physical transport limitation downstream. The constant St found would indicate that the positive effects on mass transfer due to local hydrodynamics are not maxima at the edge of the patch neither at the sampled gradient.

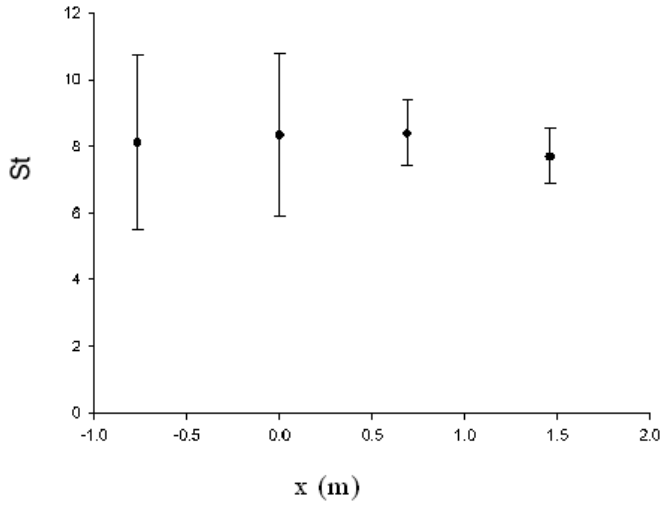

Figure 7. Values of St, a hydrodynamic indicator of nutrient transfer efficiency, along a gradient from *Caulerpa prolifera* to *Cymodocea nodosa* (x = 0 indicates the leading edge of the *C. nodosa* patch). Error bars represent 95% confidence intervals.

DISCUSSION

Fieldwork is a central issue needed to contrast the validity of the submersed vegetation–hydrodynamic models developed under non-natural conditions (ie. flume tank or in situ flume work, see Fonseca et al. 1982 vs. Fonseca et al. 1983). Given that previous studies about edge effects developed under natural conditions (ie. direct measurements) are limited (e.g. Fonseca et al. 1983, Peterson et al. 2004), our field study has shed light on how particular conditions promoted by canopy transition interacts with hydrodynamics. The existence of vegetated edges or the transition to different canopy morphologies (1) influenced on establishing current redirection and (2)

generated spatial gradients on turbulence dissipation. Such effects likely affect hydrodynamic-mediated processes like resources availability to the seagrass meadow and associated community (ie. nutrients and food supply, Thomas et al. 2000, Brun et al 2009).

Current speed and flow redirection

The main component of velocity (u) was within the range of previous estimations in the inner Cadiz Bay (0.001 – 0.05 m s^{-1}; Kagan et al. 2003). These values are lower than those frequently assayed within flume tanks, but common in tidal systems (e.g. Bouma et al. 2005). As previously observed in flume tanks for similar velocity levels (Morris et al. 2008, data not shown), the low flow did not produce a strong plant deflection on natural *Cymodocea nodosa* stands, implying that natural populations do not behave as a solid obstacle as described by Fonseca et al. (1982) for *Zostera marina*.

Even without the lateral restrictions from flume tank experiments, there was an increase in velocity on the top of the canopy. This effect differed along *C. nodosa* transect, with u increasing a 100 % at x = 0.69 m and a 200 % at x = 1.46 m with respect to the values observed at the same height above the *Caulerpa prolifera* bed (x = -0.77 m; z = 0.53 m). The observed pattern could be explained by the establishment of an incipient skimming flow (Gambi et al. 1990, Fonseca and Koehl 2006), showing that this effect is also present in natural patches from shallow environments. However, the low w recorded (Fig. 4) suggests that the magnitude of the flow redirection was smaller *in situ* than under flume tank conditions (Morris et al. 2008). Such reduction could be attributed to lateral flow around patches (Nowell and Jumars 1987), but also to the poor shoot deflection and canopy compaction due to the low natural free stream velocity. Besides the needs for more fieldwork to understand the implications of patchy seagrass

arrangement, it seems clear that such landscape topology must strongly affect qualitatively and quantitatively to current redirection (Granata et al. 2001, Luhar et al. 2008).

Turbulence levels

Maximum τ_R values had been previously reported before or at the leading edges, and explained comparing the canopy with a consistent physical obstruction causing drag (Granata et al. 2001, Thompson et al. 2004). In our case, data exhibited a significant downstream increase on τ_R, implying that (1) the canopy is not acting like a physical obstruction (ie. low shoot density and high permeability to flow), and (2) drag forces are reduced and do not cause high stresses at the leading edge. Hence, under conditions of reduced drag the edge of natural canopies could not be considered as the most active zones of vertical turbulent exchange. This idea is consistent with results reported on a flume tank experiment with *Z. marina* (Fonseca et al. 2007). In such study, drag forces were minimized by canopy orientation so the turbulent mixing increased downstream (ie. it was not maximum at the leading edge).

A significant negative correlation between u and τ_R was found above the *Cymodocea nodosa* patch, which was not observed neither before nor at the patch edge (Fig. 6). Consequently, velocity changes due to the tidal current must have limited the effect on τ_R above the canopy, and therefore in the canopy-water column exchange rate, with reduced nutrient turnover rates in the canopy as a result. Nutrient limitation has been previously related to low turnover rates due to low volumetric canopy flow rates (Morris et al. 2008, Peralta et al. 2008). In addition, *C. nodosa* meadows thriving at Cadiz Inner Bay could be considered as a physically limited system because of (1) the low free stream velocity and (2) the low turbulent vertical exchange that is not

effectively increased by tides. In fact, tides are less effective in mixing the water column in seagrass meadows than waves (Koch and Gust, 1999).

Our data exhibited a TKE peak at x = 0.69 m that decreased downstream. The dissipation of the turbulent peak implies that turbulent structures generated by the meadow have a horizontal limit. Morris et al. (2008) reported a maximum TKE value (0.0008 m^2 s^{-2}) at 0.2 m from the *C. nodosa* leading edge (at 0.30 m s^{-1} free stream velocity). Despite a considerable difference on free stream velocities (0.30 vs 0.05 m s^{-1}), maximum TKE values in flume tanks were similar to values observed in this work (0.001 m^2 s^{-2}). For 0.05 m s^{-1} free stream velocity, flume tank experiments also showed a gradual TKE increase downstream from the leading edge (Morris et al. 2008). However, maximum values were clearly lower (0.00001 to 0.00025 m^2 s^{-2}). Observed TKE differences in magnitude and scale (i.e. distance) with respect to flume tank studies imply that scaling edge effects to natural systems needs to be done carefully.

Ecological consequences

Edge effects associated with patchy seagrass landscapes generate further spatial gradients on biological responses concerning to mass transfer process, like photosynthesis, nutrient uptake or food supply (Fonseca and Kenworthy 1987, Thomas et al. 2000, Brun et al 2009). For instance, water-column ammonium is a key nitrogen source for seagrasses (Tourchette and Boulkholder 2000) and foliar uptake within a seagrass bed is spatially explicit affected by hydrodynamics (Morris et al. 2008). *In situ* observations in seagrass plants pointed out that ammonium transfer was physically limited at velocities lower than 0.3 m s^{-1} (Thomas et al. 2000). In the present work, horizontal gradients of mass transfer were evaluated using an estimation of the Stanton Number (St) instead of Reynolds stress because this last variable did not correlate with

C. nodosa ammonium assimilation rates (Morris et al. 2008). The results showed St did not change from outside to inside the *C. nodosa* patch (Fig. 7), suggesting than spatial patterns on mass transfer, and therefore in nutrient uptake, are not expected to be found in the field for assay conditions. Constancy in St has agreed with *in situ* measured uptake rates, which revealed that the highest N uptake did not occur close to the edge of *C. nodosa* patches (Morris et al. in prep.) but not with a previous flume tank experiment, which obtained a maximum uptake at the leading edge (Morris et al. 2008). Conclusions of that study involved that, given the same aboveground biomass, patchy seagrass landscapes should be able to uptake more nutrients than homogeneous landscapes. However, prediction power of St should be taken carefully before excluding any physiological consequences deduced from edge effects because, as defined by Thomas et al. 2000: (1) u_b (z-averaged velocity) could not be accurately reflecting the small scale variations on velocity that involves spatial patterns on physiological responses, and (2) the empirical relationship between u_b and St was deduced from declining frictional effects because of plant deflection, whereas deflection was absent in our canopy.

CONCLUSIONS

In conclusion, patchy landscapes of *Cymodocea nodosa* spatially affect to *in situ* flow velocity, flow direction and patterns of turbulence. Our data pointed out that *C. nodosa* edge effects displayed differences and analogies with flume tank studies, especially regarding the establishment of a skimming flow and the position of maximum turbulence. Whereas a turbulence gradient existed along our horizontal transect, the Stanton Number exhibited no differences, hence suggesting spatially

homogeneous transfer of resources. Vertical Reynolds stress was negatively correlated with u above the canopy, limiting the response of turbulent vertical exchange to tidal flow. Considering low flow environments as physically limited by resources supply (C, N) seems reasonable from a hydrodynamic point of view. Therefore, this type of systems is excellent to study ecological and physiological consequences of hydrodynamic effects on seagrass landscapes.

ACKNOWLEDGEMENTS

This work was supported by the Spanish National Research Projects EVAMARIA (CTM2005-00395/MAR), IMACHYDRO (CTM2008-0012/MAR) and by the Andalusian Excellence Research Project FUNDIV P07-RNM-2516. First author is supported by a FPI grant of the Spanish Ministry of Science and Technology. I.E. Hendriks was supported by grant number JCI-2007-123-844 of the Spanish Government. We would like to thank J. Vidal, C. Martinez and D. Rubio for their valuable help.

REFERENCES

Abdelrhman (2003). Effect of eelgrass *Zostera marina* canopies on flow and transport. Mar Ecol Prog Ser 248:67-83.

Bell SS, Robbins BD and Jensen SL (1999). Gap dynamics in a seagrass landscape. Ecosystems 2(6):493-504.

Bouma TJ, De Vries MB, Low E, Kusters L, Herman PMJ, Tanczos IC, Temmerman S, Hesselink A, Meire P and van Regenmortel S (2005). Flow hydrodynamics on a mudflat and in salt marsh vegetation: identifying general relationships for habitat characterizations. Hydrobiologia 540:259-274.

Bouma TJ, van Duren LA, Temmerman S, Claverie T, Blanco-Garcia A, Ysebaert T and Herman PMJ (2007). Spatial flow and sedimentation patterns within patches of epibenthic structures: Combining field, flume and modelling experiments. Cont Shelf Res 27:1020-1045.

Brun FG, Pérez-Lloréns JL, Hernandez I and Vergara JJ (2003). Patch distribution and within-patch dynamics of the seagrass *Zostera noltii* Hornem in Los Toruños Salt-Marsh, Cádiz Bay, Natural Park, Spain. Bot Mar 46:513-524.

Brun FG, van Zetten E, Cacabelos E and Bouma TJ (2009). Role of two contrasting ecosystem engineers (*Zostera noltii* and *Cymodocea nodosa*) on the food intake rate of Cerastoderma edule. Helgoland Mar Res 63 (1): 19-25.

Costanza R, D'Arge R, De Groot R, Farber S, Grasso M, Hannon B, Limburg K, Naeem S, O'Neill RV, Paruelo J, Raskin RG, Sutton P and Van Den Belt M (1997). The value of the world's ecosystem services and natural capital. Nature 387: 253-260.

Cowper SW (1978). The drift algal community of seagrass beds in Redfish Bay, Texas. Contrib Mar Sci 31:125–32.

Davies JL (1964). A morphogenic approach to world shorelines. Z Geomorphol 8:27-42.

Duarte CM, and Chiscano CL (1999). Seagrass biomass and production: A reassessment. Aquat Bot 65: 159-174.

Denny MW (1988). Biology and the Mechanics of the Wave-Swept Environment. Princeton University Press. 319 pp.

Folkard AM (2005). Hydrodynamics of model *Posidonia oceanica* patches in shallow water. Limnol Oceanogr 50(5):1592-1600.

Fonseca MS, Fisher JS, Zieman JC and Thayer GW (1982). Influence of the seagrass, *Zostera marina* L., on current flow. Est Coast Shelf Sci 15: 351-364.

Fonseca MS, Zieman JC, Thayer GW and Fisher JS (1983). The Role of Current Velocity in Structuring Eelgrass (*Zostera marina* L.) Meadows. Est Coast Shelf Sci 17:367-380.

Fonseca MS and Kenworthy WJ (1987). Effects of current on photosynthesis and distribution of seagrasses. Aquat Bot 27: 59-78.

Fonseca MS and Koehl MAR (2006). Flow in seagrass canopies: the influence of patch width. Est Coast Shelf Sci 67: 1-9.

Fonseca MS, Koehl MAR and Koop BS (2007). Biomechanical factors contributing to self-organization in seagrass landscapes. J Exp Mar Biol Ecol 340:227-246.

Freitas R, Rodrigues AM, Morris EP, Perez-Llorens JL and Quintino V (2008). Single-beam acoustic ground discrimination of shallow water habitats: 50 kHz or 200 kHz frequency survey? Est Coast Shelf Sci 78(4): 613-622.

Gambi MC, Novell ARM and Jumars PA (1990). Flume observations on flow dynamics in *Zostera marina* (eelgrass) beds. Mar Ecol Prog Ser 61:159-169.

Ghisalberti M and Nepf H (2002). Mixing layers and coherent structures in vegetated aquatic flow. J Geophys Res C 107 (C2):1-11.

Granata TC, Serra T, Colomer J, Casamitjana X, Duarte CM and Gacia E (2001). Flow and particle distribution in a nearshore seagrass meadow before and after a storm. Mar Ecol Prog Ser 218:95-106.

Hendriks IE, van Duren LA and Herman PMJ (2006). Turbulence levels in a flume compared to the field: Implications for larval settlement studies. J Sea Res 55(1):15-29.

Hendriks IE, Bouma TJ, Morris EP and Duarte CM (2010). Effects of seagrass and algae of the *Caulerpa* family on hydrodynamics and particle trapping rates. Mar Biol 157(3):473-481.

Kagan BA, Alvarez O, Izquierdo A, Mañanes R, Tejedor B and Tejedor L (2003). Weak wind-wave/tide interaction over a moveable bottom: results of numerical experiments in Cadiz Bay. Cont Shelf Res 23(5):435-456.

Koch EW (1994). Hydrodynamics, diffusion-boundary layers and photosynthesis of the seagrasses *Thalassia testudinum* and *Cymodocea nodosa*. Mar Biol 118: 767-776.

Koch EW and Gust G (1999). Water flow in tide- and wave-dominated beds of the seagrass *Thalasia testudinum*. Mar Ecol Prog Ser 184:63-72.

Koch EW (2001). Beyond light: physical, geological and geochemical parameters as possible submersed aquatic vegetation habitat requirements. Estuaries 24: 1-17.

Kundu PK (1990). Fluid Mechanics. Academic Press, p 26-27, 450.

Luhar M, Rominger J and Nepf H (2008). Interaction between flow, transport and vegetation spatial structure. Environ Fluid Mec 8:423-439.

Malta E, Ferreira DG, Vergara JJ and Perez Llorens JL (2005). Nitrogen load and irradiance affect morphology, photosynthesis and growth of *Caulerpa prolifera* (Bryopsidales: Chlorophyta). Mar Ecol Prog Ser, 298:101-124

Maltese A, Cox E, Folkard A, Ciraolo G, La Loggia G and Lombardo G (2007). Laboratory measurements of flow and turbulence in discontinuous distributions of ligulate seagrass. J Hydraul Eng 133(7):750-760.

Mann KH (2000). Ecology of coastal waters with implications for management. Blackwell Science, p 64-79.

McRoy CP and Helfferich, C (1977). Seagrass ecosystems: a scientific perspective. Mareel Dekker, Inc., New York. 314 pp.

Morris EP, Peralta G, Brun FG, van Duren L, Bouma TJ and Perez-Llorens JL (2008). Interaction between hydrodynamics and seagrass canopy structure: spatially explicit effects on ammonium uptake rates. Limnol Oceanogr 53:1531–1539.

Morris E. P., Peralta G, Benavente J, Freitas R, Rodrigues AM, Quintino V, Alvarez O, Valcárcel-Pérez N, Vergara JJ, Hernández I and Pérez-Lloréns JL (2009). *Caulerpa prolifera* stable isotope ratios reveal anthropogenic nutrients within a tidal lagoon. Mar Ecol Prog Ser, 390: 117–128.

Nowell ARM and Jumars PA (1987). Flumes: theoretical and experimental considerations for simulation of benthic environments. Oceanogr Mar Biol 25:91-112.

Peralta G, van Duren LA, Morris EP and Bouma TJ (2008). Consequences of shoot density and stiffness for ecosystem engineering by benthic macrophytes in flow dominated areas: a hydrodynamic flume study. Mar Ecol Prog Ser 368: 103 – 115.

Peterson CH, Luettich RA Jr, Micheli F and Skilleter GA (2004). Attenuation of water flow inside seagrass canopies of differing structure. Mar Ecol Prog Ser 268:81-92.

Preen AR, Lee Long WJ and Coles RG (1995). Flood and cyclone related loss and partial recovery of more than 1000 km^2 of seagrass in Hervey Bay, Queensland, Australia. Aquat Bot 52:3–17.

Robbins and Bell SS (2000) Dynamics of a subtidal seagrass landscape: Seasonal and annual change in relation to water depth. Ecology 81:1193-1205.

Salita JT, Ekau W and Saint-Paul U (2003). Field evidence on the influence of seagrass landscapes on fish abundances in Bolinao, Northern Philippines. Mar Ecol Prog Ser 247:183–195.

Thomas FIM, Cornelisen CD and Zande JM (2000). Effects of water velocity and canopy morphology on ammonium uptake by seagrass communities. Ecology 81(10):2704-2713.

Thompson CEL, Amos CL and Umgiesser G (2004). A comparison between fluid shear stress reduction by halophytic plants in Venice Lagoon, Italy and Rustico Bay, Canada—analyses of in situ measurements. J Mar Syst 51: 293-308.

Touchete BW and Burkholder JM (2000). Review of nitrogen and phosphorus metabolism in seagrasses. J Exp Mar Biol Ecol 250:133-167.

van der Heide T, Bouma TJ, van Nes EH, van de Koppel J, Scheffer M, Roelofs JGM, van Katwijk MM and Smolders AJP (2010). Spatial self-organized patterning in seagrasses along a depth gradient of an intertidal ecosystem. Ecology 91(2):362-369.

Velasco D, Bateman A, Redondo JM and De Medina V (2003). An open channel flow experimental and theoretical study of resistance and turbulent characterization over flexible vegetated linings. Flow Turbul and Combust 70:69-88.

Widdows J, Pope ND, Brinsley MD, Asmus H and Asmus RM (2008). Effects of seagrass beds (*Zostera noltii and Z. marina*) on near-bed hydrodynamics and sediment resuspension. Mar Ecol Prog Ser 358:125–136.

Zieman JC (1976). The ecological effects of physical damage from motor boats on turtle grass beds in southern Florida. Aquat Bot 2:127–139.

Hydrodynamic effects of macrophyte bed microtopography: Spatial consequences of benthic transitions

M. Lara[1*], T. J. Bouma[2], G. Peralta[1], J. van Soelen[2], and J. L. Pérez-Lloréns[1]

[1]Department of Biology, Faculty of Marine and Environmental Sciences, University of Cadiz, 11510 Puerto Real (Cadiz), Spain.

[2]Netherlands Institute of Ecology (NIOO-KNAW), Centre for Estuarine and Marine Ecology, PO Box 140, 4400 AC Yerseke, The Netherlands.

ABSTRACT

The green rhizophytic algae *Caulerpa* spp. is a classic space competitor for seagrass habitats and its spread is usually attributed to a rapid clonal growth combined with a high capacity to modify sedimentary dynamics. At the Cadiz Bay Natural Park (CBNP), *Caulerpa prolifera* and *Cymodocea nodosa* (seagrass) usually occur in overlapping patches called transition zones (TZs) and a sloped microtography causes that *C. prolifera* beds are located 5-10 cm above the *C. nodosa* ones. We tested the hypothesis that hydrodynamic effects of the sloped microtopography promote sedimentary conditions at *C. nodosa* bed boundaries, therefore facilitating *C. prolifera* spread. To evaluate such effects, a TZ between *C. prolifera* and *C. nodosa* patches was simulated in a flume tank to test the influence of (1) free stream velocity (LV=0.065 and HV=0.14 m s^{-1}) and (2) microtopography (flat and sloped) on bed shear stress (τ), turbulence above canopies (TKE) and volumetric flow rates through the canopies (Q_c). The comparison of τ values with theoretical thresholds revealed that, under these experimental settings, (1) there were no conditions for erosion, (2) hydrodynamics was favorable to sedimentation within *C. nodosa* beds regardless velocity treatment, and (3) there was a low sedimentation probability in *C. prolifera* beds under HV conditions. Sloped microtopography did not significantly affected τ, but caused a large velocity reduction and halved Q_c when compared to flat beds. Overall, results suggest (1) more favorable sedimentation conditions in *C. nodosa* than in *C. prolifera* beds, and (2) sloped microtopography may only facilitate this contrasting effect during HV conditions (i.e. with gentle sediment availability). Results also highlight that an accurate analysis of TZs requires hydrodynamic studies dealing with patchiness.

INTRODUCTION

Seagrass meadows are suffering a severe decline worldwide (Orth et al. 2006), offering chances to opportunistic species, exotic or/and local, to invade these habitats (Meinesz et al. 2001, Piazzi et al. 2001, Occhipinti-Ambrogi and Savini 2003, Stafford and Bell 2006, Tweedley et al. 2008). The green rhizophytic algae *Caulerpa* spp. is a classic competitor for seagrass habitats. There are numerous reports on *Caulerpa* spp. expansions, such as *C. racemosa* (Piazzi et al. 2001), and *C. taxifolia* at the Mediterranean Sea (Meinesz et al. 2001), or *C. prolifera* at Lassing Park, Florida (Stafford and Bell 2006). The genus *Caulerpa* exhibits an array of spreading strategies that benefit their spatial competition capability against seagrasses, including both, random dispersion mechanisms, such as fragmentation (Smith and Walters 1999) or sexual reproduction, and direct space preemption strategy by clonal growth (e.g. Stafford and Bell 2006, Wright and Davis 2006). For *C. prolifera* the clonal expansion throughout stolon growth seems more effective than by thallus fragmentation (Stafford and Bell 2006). Under high sedimentation rates scenarios, such rapid reproduction mechanism likely favor the space colonization chance when compared to seagrasses. The burial scenarios also imply enrichment in organic matter, enhanced sulfide pools and decreases in redox potential, and all of these factors provide comparative advantage to *Caulerpa* spp. (Piazzi et al. 2005, 2007, Holmer et al. 2009).

Species-specific differences in sedimentation rates among macrophyte sharing the same habitat have been previously observed (Gacia et al. 2003, Hendriks et al. 2010), and this fact may create sedimentary gradients along overlapping distribution areas (i.e. transition zones, TZs). At TZs, the conjunction of (1) sedimentary gradients, and (2) their contrasting outcomes to macrophytes spreading, evidence that physical studies are needed to a fully comprehension of spatial interaction processes. In this way, Hendriks

et al. (2010) reported that *Caulerpa prolifera* canopies have a sediment trapping capacity 2.5 fold higher than that of seagrass canopies such as *Posidonia oceanica* or *Cymodocea nodosa*. This large trapping capacity was attributed to the increased transport of particles resulting from a reduced shear force (Reynolds stress) in the near-bottom regions and a high turbulent mixing above the canopy (Hendriks et al. 2010). On the other hand, seagrass meadows capacity to stabilize and retain sediments is generally related to a reduction of water velocity within the canopy (Fonseca and Fischer 1986, Almasi et al. 1987, Gacia et al. 1999, Hendriks et al. 2010). In spite of the distinct nature and magnitude of their interaction with flow (Hendriks et al. 2010), there are no previous reports addressing the effects of TZs between adjacent *Caulerpa prolifera* and *Cymodocea nodosa* patches.

The most abundant macrophytes thriving at Cadiz Bay Natural Park (CBNP, Spain) are the chlorophyte alga *Caulerpa prolifera* Forsskaal (Lamouroux) and the seagrass *Cymodocea nodosa* Ucria (Ascherson), occurring in a wide belt around the bay where the patch edges on both species tend to overlap (Morris et al. 2009). Such overlapping area is what we have called the transition zone (TZ). Differences in bottom microtopography have been observed in previous studies, with *C. prolifera* beds usually occurring at 5-10 cm above the *C. nodosa* ones (Benavente et al. 2008). Carpenter and Williams (1993) demonstrated that differences in microtopography modify the macrophyte-hydrodynamic interactions in turf algae. Microtopography would add resistance to the flow and intensify benthic shear stress at elevated areas (Walter 1971), but also would favor sedimentation in depressed environments (Carpenter and Williams 1993). The interaction between microtopography and sedimentation processes may also affect the abundance of macrophytobenthos (e.g. Irving and Connell 2002). Hence, understanding the interactions among hydrodynamic-driven sediment dynamics,

microtopography and vegetation types is especially important at the TZs where macrophytes coexist and compete.

We hypothesize that the presence of microtopography at the TZs between *Cymodocea nodosa* and *Caulerpa prolifera* patches, as observed at Cadiz bay, will affect hydrodynamic variables controlling the sedimentation processes. In more detail, we hypothesize that these outcomes enhance sediment transport and deposition at the TZ, what probably will promote the spreading of *C. prolifera*. For this purpose, we evaluated in a flume experiment the hydrodynamic effects of microtopography at the TZ between *Cymodocea nodosa* and *Caulerpa prolifera* patches. The hydrodynamic variables evaluated were velocity patterns, bottom turbulence and volumetric flow rate through the canopy. The effects in these variables were tested for two free stream velocities within the natural velocity range observed in Cadiz bay. Spatial gradients on bed shear stress were also analysed in comparison with sedimentation/erosion thresholds.

MATERIAL AND METHODS

Plant collection and spatial arrangements

Specimens of *Caulerpa prolifera* and *Cymodocea nodosa* were collected from Cadiz Bay Natural Park (CBNP, SW Spain, 36º28´12.79´´N, 06º15´7.07´´W) in May 2008. The collecting area is a shelter and tide-dominated coastal lagoon profusely vegetated (Morris et al. 2009). Collected plants were cleaned, wrapped in moist tissue paper and sent to the NIOO-CEME laboratory (Yerseke, The Netherlands), 12 days before beginning the experiment. Upon arrival, plants were kept in a filtered natural seawater tank with aeration (salinity 31, temperature 18ºC) under a 14 h photoperiod at 160 µmol photons m^{-2} s^{-1}. During the experiment, plants were kept illuminated with

mercury lamps at night. Special care was taken to prevent any release of *C. prolifera* to the local environment, and flume water was disposed onto the freshwater sewage system.

A 2 m long bed was constructed within the flume tank test section by planting *Caulerpa prolifera* and *Cymodocea nodosa* specimens into ten siliceous sediment boxes (details in the next section). Stolons of *C. prolifera* and rhizomes of *C. nodosa* were buried, ensuring that fronds and shoots remained emerged. Plant density, leaf length and leaf area index were similar to those observed in summer at CBNP (table I, Hernandez et al. 2010, Vergara et al. 2012). Regardless of the microtopography treatment, the upstream end of the test section was planted with *C. prolifera* (0.8 m x 0.6 m), whereas the downstream end of the test section was shared by *Cymodocea nodosa* (1.2 x 0.3 m, left side, CN in Fig. 1, table I) and *Caulerpa prolifera* (1.2 x 0.3 m, right side, CP in Fig. 1). The downstream area occupied by both species (1.2 x 0.6 m) is considered the transition zone (TZ in Fig.1).

Flume tank and hydrodynamic measurements

The flume tank used for this work was a 10 m^3 unidirectional flow 'race track' with a 0.6 x 2 m test section (for further details, see Jonsson et al. 2006). The test section was entirely occupied by ten stain steel boxes (0.390 x 0.285 x 0.150 m each). Each box was planted with either *Cymodocea nodosa* or *Caulerpa prolifera* specimens. The small gaps between the boxes were avoided by filling with sediment.

Table I. Plant density, leaf length and leaf area index of *Caulerpa prolifera* and *Cymodocea nodosa* canopies used during flume tank experiment.

Variables / Species	***C. prolifera* (± SE)**	***C. nodosa* (±SE)**
Plant density (fronds or shoots m^{-2})	6890	443
Leaf length (cm)	4.7(±0.59)	20.35(±2.88)
Leaf area index (m^2 leaves m^{-2} surface projected area)	3.66	0.59

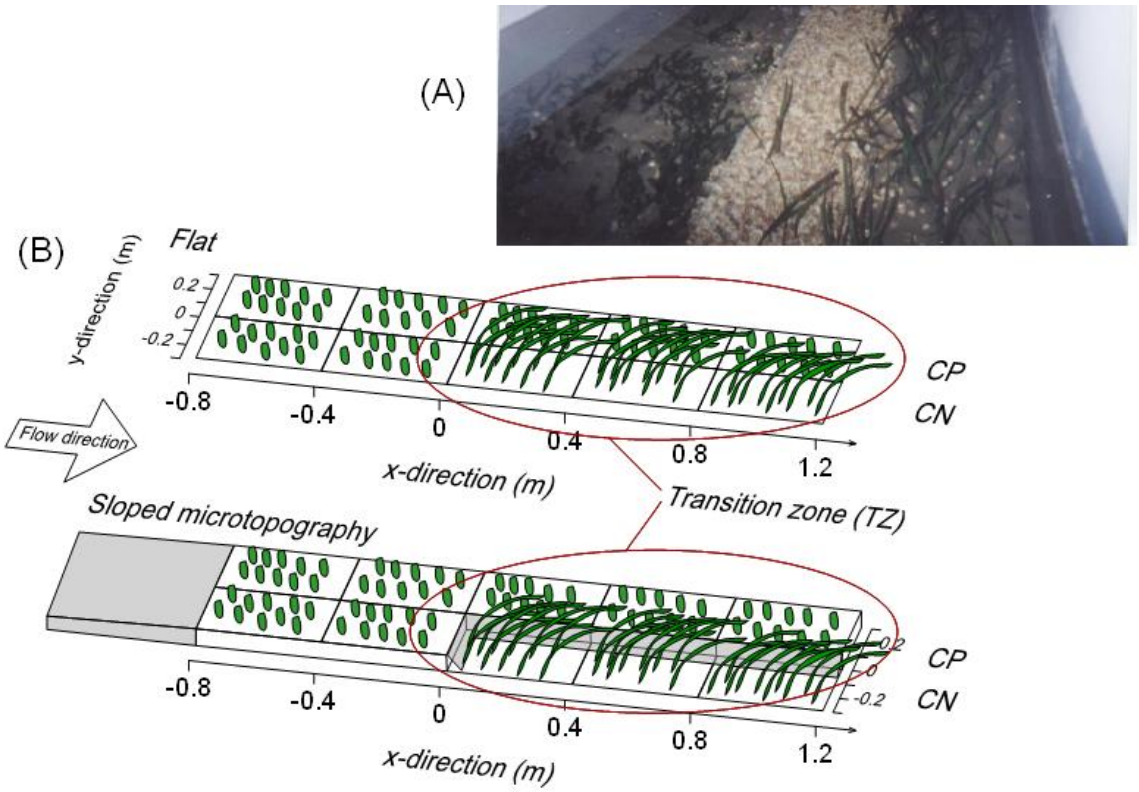

Figure 1. (A) Photography of experimental set-up with *Caulerpa prolifera* bed (left), gravel microtopography and *Cymodocea nodosa* bed (right). (B) Scheme of plant configurations before and along transition zone (TZ), for flat (up) and sloped (down) microtopography.

The microtopography treatment had two levels: flat and sloped. The latter one was achieved by raising the *Caulerpa prolifera* boxes 0.1 m with respect to the *Cymodocea nodosa* ones (Fig 1B). Undesired effects due to sharp vertical edges were avoided by making a smooth 3 m slope (3%) upstream of the test section. Since *C. nodosa* bed was depressed compared to *C. prolifera* one, the steps between boxes were smoothed by adding fine-gravel slopes (see details in Fig. 1A). The water column height on the flume tank varied between 0.32 - 0.42 m depending on the microtopographic level.

The free stream velocity treatment had also two levels, low velocity (LV, 0.065 m s^{-1}) and high velocity (HV, 0.14 m s^{-1}). Sedimentary dynamics at CBNP is mainly controlled by East wind induced events of sediment re-suspension associated with high current velocities, and subsequent tidal transport along the inner part of the bay (Alvarez et al. 2000, Gutierrez-Mas et al. 2000). Given that such dynamics occurs along the natural transition zones, experimental design represented events of high current velocity by including a treatment of peak velocity (HV, maximum values predicted for windy conditions by Kagan et al. 2003).

The 3 velocity components (u, v and w) were measured at 10 Hz with an acoustic Doppler velocimeter (ADV, Nortek field version), during 270 seconds following a 3D grid with 280 points. The points were distributed as 7 x-locations (at -0.15, -0.05, 0.1, 0.15, 0.30, 0.60 and 0.90 m from the *C. nodosa* leading edge), 4 y-positions (at -0.20, -0.10, 0.10 and 0.20 m from the flume tank cross section center) and 10 z-locations (at 0.01, 0.02, 0.03, 0.04, 0.06, 0.08, 0.10, 0.15,0. 20 and 0.24 m above the bottom of *C. prolifera* bed and at 0.03, 0.04, 0.06, 0.08, 0.10, 0.12, 0.15, 0.18, 0.20 and 0.24 m above the bottom of *C. nodosa* bed, Fig 1B). For the sloped treatment, the 3D grid z-locations were elevated 0.10 m above the *C. prolifera* bed. Height and shape of the *C. nodosa*

canopy were measured at every x-position by drawing the projected area on the test section window.

Hydrodynamic variables

Data with beam correlations below 70% were filtered (Bouma et al. 2007, Morris et al. 2008), remaining at least 2000 data per 3D grid point. The velocity components were estimated as the time-averaged values of the filtered data, and analyzed according to equations 1, 2 and 3:

$$\mathrm{u} = \bar{u} + u' \qquad \text{(eq. 1)}$$

$$\mathrm{v} = \bar{v} + v' \qquad \text{(eq. 2)}$$

$$\mathrm{w} = \bar{w} + w' \qquad \text{(eq. 3)}$$

where u, v and w are the instantaneous velocity components, $\bar{u}$, $\bar{v}$ and $\bar{w}$ are the averaged components, and *u*', *v*' and *w*'are the fluctuation terms.

The fluctuation terms were used to estimate turbulent variables such as turbulent kinetic energy (TKE, $mm^2\ s^{-2}$, eq. 4):

$$TKE = 0.5 * (\overline{u'^2} + \overline{v'^2} + \overline{w'^2}) \qquad \text{(eq. 4)}$$

The TKE values were measured close to the top surface of both *Cymodocea nodosa* and *Caulerpa prolifera* canopies. This position allows estimate the magnitude of the turbulent mixing above the canopy, what can be used as a proxy for the magnitude of sediment transport from the overlaying flow into the canopy (Hendriks 2010). The effects of microtopography and free stream velocity treatments on TKE above the canopy were tested with a two-way ANOVA of log-transformed values (n=8, significance level was set at 0.05) separately for each species. The contribution of each

factor to the total variance was estimated from the sum of squares (SS) between treatments.

The bottom shear stress (τ, Pa, eq. 5) is a turbulence variable used as a proxy for bed stability and sedimentation probability (e.g. Fonseca and Fischer 1986, Zong and Nepf 2010). In our case, it was used as a proxy to compare the spatial patterns on sedimentation probability for *C. prolifera* and *C. nodosa* beds. Values of τ were estimated at 0.03 m from the bottom floor using the TKE method. This method is specially recommended for estimating τ in complex bed forms like this one (Biron et al. 2004):

$$\tau = C_1 \rho TKE \qquad \text{(eq. 5)}$$

where τ is bottom shear stress (Pa), C_1 is a constant (C_1=0.19, Soulsby 1983), ρ is water density (1025 Kg m^{-3}) and TKE the turbulent kinetic energy (m^2 s^{-2}). A three-way ANOVA with log-transformed values (n = 8, significance level = 0.05) was used to test the occurrence of significant effects of current velocity, microtopography and species bed composition on the bottom shear stress. Species composition was considered a nested factor on microtopography. The corresponding SS between treatments was used to calculate the contribution (percentage) of each factor to the total variance. Values of τ contour maps (software Surfer 8.05) were also performed for both flat and sloped levels following the Kriging method. Sloped microtopography maps were depicted as separated interpolations for *C. prolifera* and *C. nodosa* beds.

Analysis of bed stability and sedimentation probability due to the different macrophyte species were performed along cross-stream (y) and downstream (x) gradients of τ. For this purpose, theoretical thresholds for erosion (τ_{cr}) and sedimentation (τ_{sed}) were calculated assuming representative values of particle size (d,

μm) and composition of field recent sediments: clay (illite, d≈4 μm, ρ=2800 kg m^{-3}), silt (illite, d≈44 μm; ρ=2800 kg m^{-3}) and fine-sand (quarz, d≈280 μm, ρ=2600 kg m^{-3}) fractions (Gutierrez-Mas et al. 1997, Achab and Gutierrez-Mas 2005). The τ_{cr} predictions were achieved by two standardized curves modified from Shield's diagrams (eq. 6 and 7), which depend on a dimension particle size (D*, eq. 8) (van Rijn 2007):

$$\tau_{cr} = 0.115(D^*)^{-0.5} \text{ ; for } D^* < 4 \qquad \text{(eq. 6)}$$

$$\tau_{cr} = 0.14(D^*)^{-0.64} \text{; for } 4 \leq D^* < 10 \qquad \text{(eq. 7)}$$

$$D^* = d\left(\left(\frac{\rho_s}{\rho_w} - 1\right)\frac{g}{v^2}\right)^{\frac{1}{3}} \qquad \text{(eq. 8)}$$

where ρ_s (kg m^{-3}) is the particle density, ρ_w is the seawater density (1025 kg m^{-3}) and *v* ($1.15*10^{-6}$ m^2 s^{-1}) is the kinematic viscosity of the water at 15ºC. Values of τ_{sed} were predicted with the empirical relationship reported by Self et al. (1989) (eq. 9):

$$Log_{10}(\tau_{sed}) = 0.76 * Log_{10}(d) - 2.76 \qquad \text{(eq. 9)}$$

Finally, the volumetric flow rate crossing the canopy in the TZ (Q_c, m^3 s^{-1}) was used as a proxy for the suspended sediment supply rate to the canopies. To estimate Q_c the procedure followed was: (1) the TZ (i.e. 1.2 m on the test section) was laterally divided in 4 proportional sections (i.e. 0.15 m width each by 1.2 m length, each section is indicated as $y_{w1/4}$ in eq. 11). This division leaves two sections with *Caulerpa prolifera* on one flume tank side and two sections with *Cymodocea nodosa* on the other side; (2) on each section, the velocity profiles were vertically and transversally integrated rendering the Q_i values (equation 11); (3) Q_c was finally estimated as the addition of the different Q_i values (eq. 10). The values of Q above the canopy were calculated following a similar procedure (eq. 11).

$$Q_c = \sum_{0}^{h_C} Q_i \quad \text{(eq. 10)}$$

$$Q_{above} = \sum_{h_c}^{h_w} Q_i \quad \text{(eq. 11)}$$

$$Q_i = \sum_{j=1}^{j=2} y_{\frac{1}{4}W} * (z_i - z_{i-1}) * u_{z_i y_j} \quad \text{(eq. 12)}$$

where h_c is the canopy height (m), h_w is the water column height (m), $y_{\frac{1}{4}W}$ is the quarter part of flume tank width and $u_{z_i y_j}$ is the u (m s^{-1}) at height z_i on the corresponding $y_{\frac{1}{4}W}$ and cross-stream positions y_1 and y_2, respectively. The flow rate through the flume tank side corresponding to each species (Q_{side}) was also estimated according to equation 13.

$$Q_{side} = \sum_{i=0}^{i = h_w} Q_i \quad \text{(eq. 13)}$$

To facilitate the comparison between treatments, the three variables (Q_c, Q_{above} and Q_{side}) were normalized by the total flow rate through the entire flume tank section (Q, eq. 14), and the resulting value was expressed as percentage ($\%Q_c$, eq. 15, $\%Q_{above}$, eq. 16 and $\%Q_{side}$, eq. 17, respectively).

$$Q = Q_{side\_Cn} + Q_{side\_Cp} \quad \text{(eq. 14)}$$

$$\%Q_c = \frac{Q_c}{Q} * 100 \quad \text{(eq. 15)}$$

$$\%Q_{above} = \frac{Q_{above}}{Q} * 100 \quad \text{(eq. 16)}$$

$$\%Q_{side} = \frac{Q_{side}}{Q} * 100 \quad \text{(eq. 17)}$$

RESULTS

Velocity profiles

The u-profiles revealed species-specific vertical flow patterns, regardless the free stream velocity and microtopography treatments (Fig. 2). Velocities near the bottom were lower within the long *Cymodocea nodosa* canopy ($u < 3$ mm s^{-1}) than within the short *Caulerpa prolifera* one ($u > 5$ mm s^{-1}). The difference on canopy architecture (i.e. canopy height and morphology) between species also affected to the shape of the vertical u-profiles. Vertical u-profiles above the *C. prolifera* canopy were closer to the typical boundary layer logarithmic profile than those observed above the *C. nodosa* canopy. Together with the velocity reduction within the canopy, it was expected an increase on velocity above it (i.e. skimming flow). However, skimming flow was only notable above *C. nodosa* at HV for the sloped microtopography.

An increase in free stream velocity was detected inside and above the canopies. At LV and flat bed, velocity decreased within the bed when the water flowed from *C. prolifera* (upstream) to *C. nodosa* (downstream); however, such decrease was not close to the edge at HV. On the other hand, regardless the velocity level, the existence of microtopography (i.e. sloped level) resulted in a layer of very low velocity within the first 0.1 m from the leading edge in *C. nodosa* bed, which extended 0.5 m downstream. Within this layer, magnitude of velocity was clearly lower with microtopography than in the flat level. This effect was especially clear at HV.

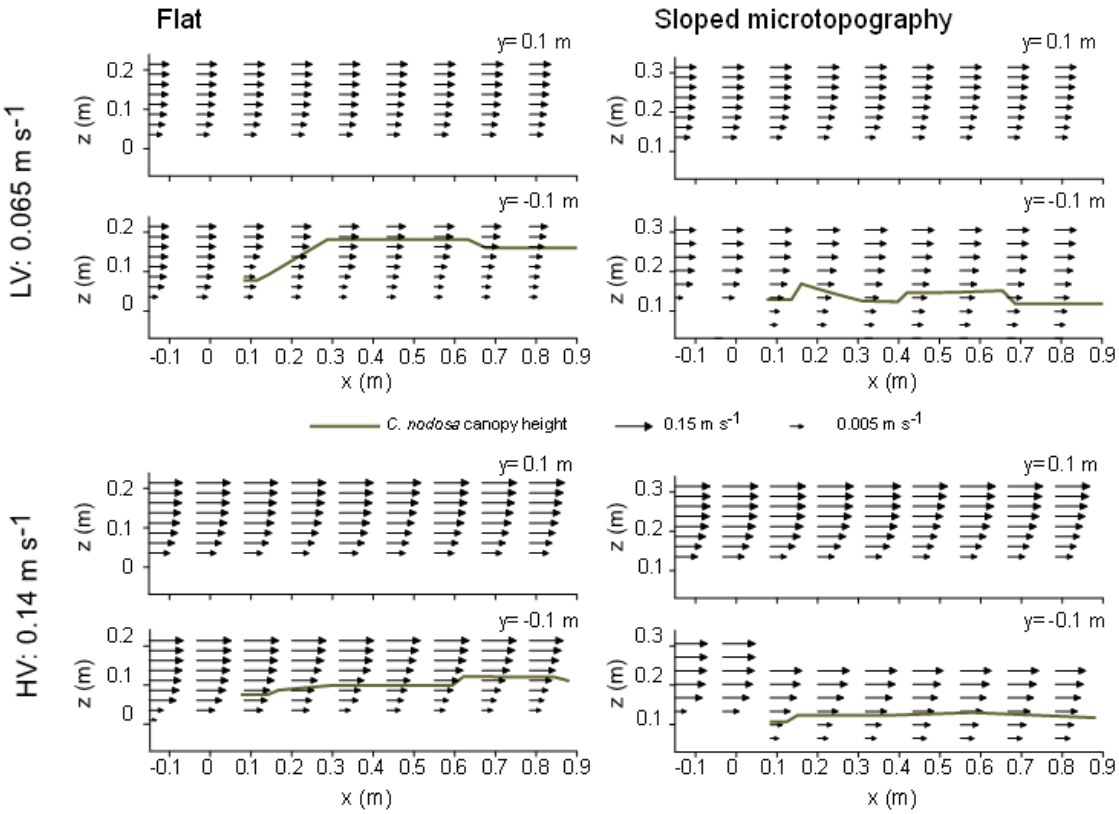

Figure 2. Vertical profiles of the u component of velocity (m s^{-1}) along the test section (x), at low velocity (LV=0.065 m s^{-1}) (up) and at high velocity (HV=0.14 m s^{-1}) (down), for flat (left) and sloped (right) microtopography. Graphs of *Caulerpa prolifera* bed correspond to y=0.1 m and the *Cymodocea nodosa* bed to y=-0.1 m. Size of vector plots is proportional to the u value. *Cymodocea nodosa* canopy height is indicated with green lines.

Volumetric flow rates and canopy height

Increases in free stream velocity resulted in a proportional increase on the total volumetric flow rate (Q). Differences on bed form and water column height associated to microtopography (see material and methods) produced Q values for the sloped treatment 17% higher than that for the flat one (Fig. 3).

The percentage of volumetric flow rate through the canopies (%Q_c) was mostly below 10%, in contrast with the range of percentage above canopies (%Q_{above}, 30-55%,

Fig 3). Differences in canopy height (h_c) between *C. nodosa* (0.175 and 0.08 m at LV and HV respectively) and *C. prolifera* (0.04 m, Fig. 4) seemed to be one of the main factors determining observed differences in $\%Q_c$. In fact, $\%Q_c$ within *C. nodosa* bed almost doubled (3.5-8%) the values within *C. prolifera* one (1.7-3.2 %) regardless the experimental treatment.

For flat bed, the $\%Q_{above}$ the *Cymodocea nodosa* canopy was lower (34 – 40 %) than that for the *C. prolifera* one (52 - 55%), indicating that flow was preferentially redirected above *C. prolifera* bed. However, such differences were not recorded for the sloped microtopography (c.a. $\%Q_{above}$ mean value 47% for both canopies, Fig. 3). Such result could be explained by the increased water column level at *C. nodosa* side, which resulted in enhanced $\%Q_{side}$ values. A reduction in $\%Q_c$ was observed for the sloped microtopography treatment. However, whereas in *Caulerpa prolifera* the decrease (from 3% to 1.5%) was unaffected by the velocity treatment, in *C. nodosa* this reduction was affected by velocity (from 8% to 4% at LV, and from 5.5% to 3.5% at HV), being the reduction observed at HV due to the more intense bending of leaves (Figs. 3 and 4).

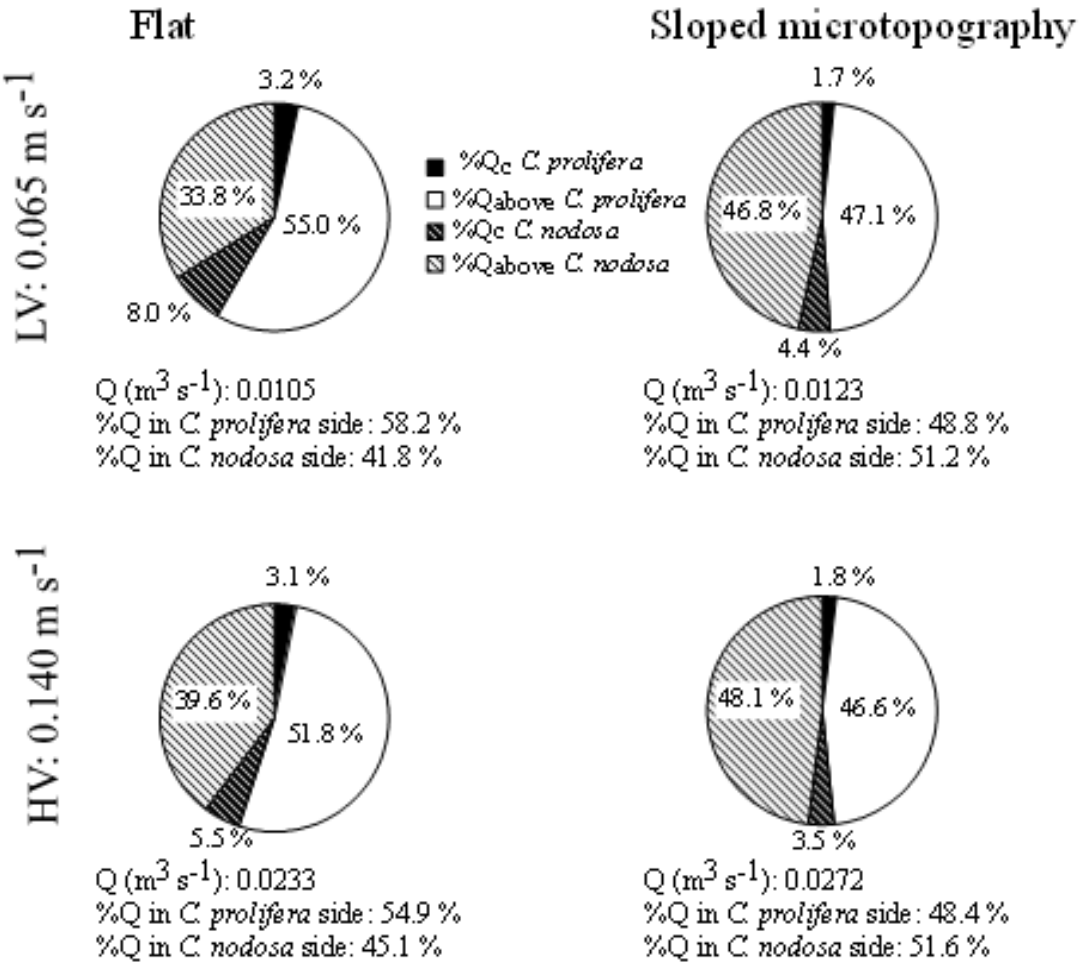

Figure 3. Distribution of the volumetric flow rate on the transition zone (TZ) for free stream velocity (high velocity, HV and low velocity, LV) and microtopography (flat and sloped). Data are expressed as percentages of total volumetric flow rate (Q) and they have been separated as percentage of Q crossing the canopies ($\%Q_c$), as well as the percentage of Q above those canopies ($\%Q_{above}$). The percentage of Q crossing each side (i.e. $\%Q_c + \%Q_{above}$) of the flume tank is also indicated below each graph. For all the cases, the $\%Q_c$ crossing the canopy of *C. prolifera* on the upstream section was 5%.

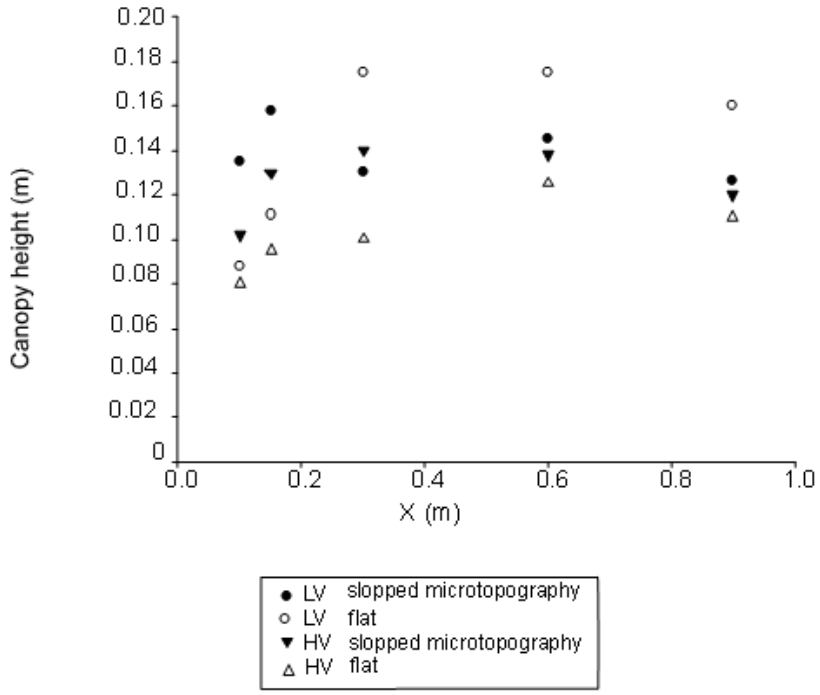

Figure 4. Canopy height of *Cymodocea nodosa* (m) along distance on the transition zone (TZ, x), at low velocity (LV=0.065 m s^{-1}, circles) and at high velocity (HV=0.14 m s^{-1}, triangles), for flat (white) and sloped (black) microtopography.

Bottom shear stress

Along the TZ, the τ values ranged between 0.005-0.080 Pa. The contour maps showed a high spatial variability on τ for every treatment, suggesting the existence of sedimentation gradients along two spatial directions (Fig. 5). The first gradient was in the cross-stream direction (y-axis direction), with a reduction on τ values from *Caulerpa prolifera* to *Cymodocea nodosa* areas (0.005-0.01 Pa). This gradient became particularly evident at HV (0.06 Pa difference in 0.2 m of distance). For the sloped microtopography, the physical separation of both beds required a separated interpolation of the τ values, explaining the discontinuities in the contour maps at the middle axis of

TZ. The second gradient was observed in the x-direction with decreasing τ values from *C. prolifera* (the upstream bed) to TZ at HV, regardless microtopography treatment.

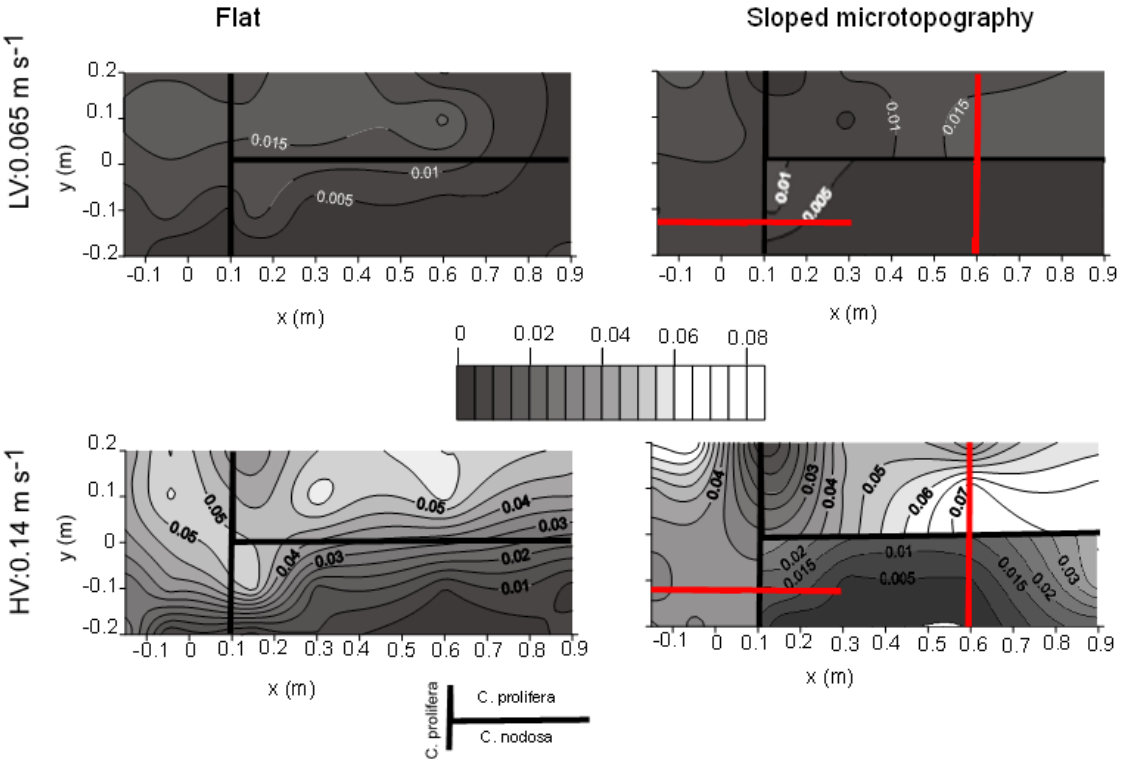

Figure 5. Contour maps of bottom shear stress (τ, Pa) at low velocity (LV=0.065 m s^{-1}) (up) and at high velocity (HV=0.14 m s^{-1}) (down), for flat (left) and sloped (right) microtopography. The cross-stream and downstream gradients used on figure 6 are also drawn (red lines).

A three-way ANOVA analysis (table II) revealed that the free stream velocity ($F=13.85$, $p<0.001$) and the species bed composition ($F=16.63$, $p<0.001$) had significant effects on τ along TZ. Although the spatial patterns of τ seemed to be affected by the microtopography (Fig. 5), the averaged τ values were unaffected ($F=2.68$, $p=0.107$). When the percentage of total variance explained by each factor was considered, free stream velocity accounted for 13% whereas the nested factor species bed composition

accounted for 31%. The error term explained 54% of variance, and it represented the spatial variability of τ due to cross-stream and downstream gradients.

Table II. Three-way ANOVA performed to test the significance (α=0.05) of free stream velocity, microtopography and species on bed shear stress (τ) (n=8).

Factor	**F value**	**% Sum of squares between treatments**	**p-value**
Free stream velocity	13.85	12.73%	<0.001
Microtopography	2.68	2.46%	0.11
Species (nested on microtopography)	16.63	30.57%	<0.001
Error	-	54.23%	-

The regions EROS, SUSP and SED were based on the comparison between the τ gradients and the threshold values τ_{cr} and τ_{sed} (Fig. 6). The two thresholds (τ_{cr} and τ_{sed}) define three regions when representing τ versus x-distance or y-distance: (1) the top region represents the τ -values to expect erosion or initiation of bottom sediment motion (EROS, $\tau \geq \tau_{cr}$) (2) the bottom region represents the τ -values to expect sedimentation (SED, $\tau \leq \tau_{sed}$), and (3) the medium region correspond to the τ -values that will generate suspended transport, where neither erosion or sedimentation are expected (SUSP, $\tau_{sed} < \tau < \tau_{cr}$).

No differences were observed between the cross-stream and the downstream gradients, exhibiting a peak of τ at the centre of the gradient and a decrease towards the edges. The observed τ range was within the limit between suspension and sedimentation processes, implying that the input of additional energy to the system (e.g. orbital flow) could counterbalance predictions achieved under unidirectional flow conditions. Data

revealed that, with exception of the fine-sand fraction associated to the *Caulerpa prolifera* bed, τ did not exhibited values associated to erosive processes (i.e. no data in EROS region). Thus, for the assayed conditions, sediment re-allocation is not expected to happen by direct sediment erosion from *C. prolifera* patch boundary. In the particular case of fine sand, the τ_{sed} threshold was higher than the τ_{cr} one, explaining the coexistence of the EROS+SED regions. The clay fraction was clearly the less favorable for sedimentation in *C. prolifera* bed, whereas silt and fine sand could settle under LV. At HV, most of the sediment transported through *C. prolifera* bed would have no favorable conditions to be deposited. Contrastingly, sediment in *Cymodocea nodosa* bed would potentially settle regardless velocity treatment or particle size. Therefore, a re-allocation of non-deposited sediment from *C. prolifera* bed to the *C. nodosa* one could occur at the TZ during HV events.

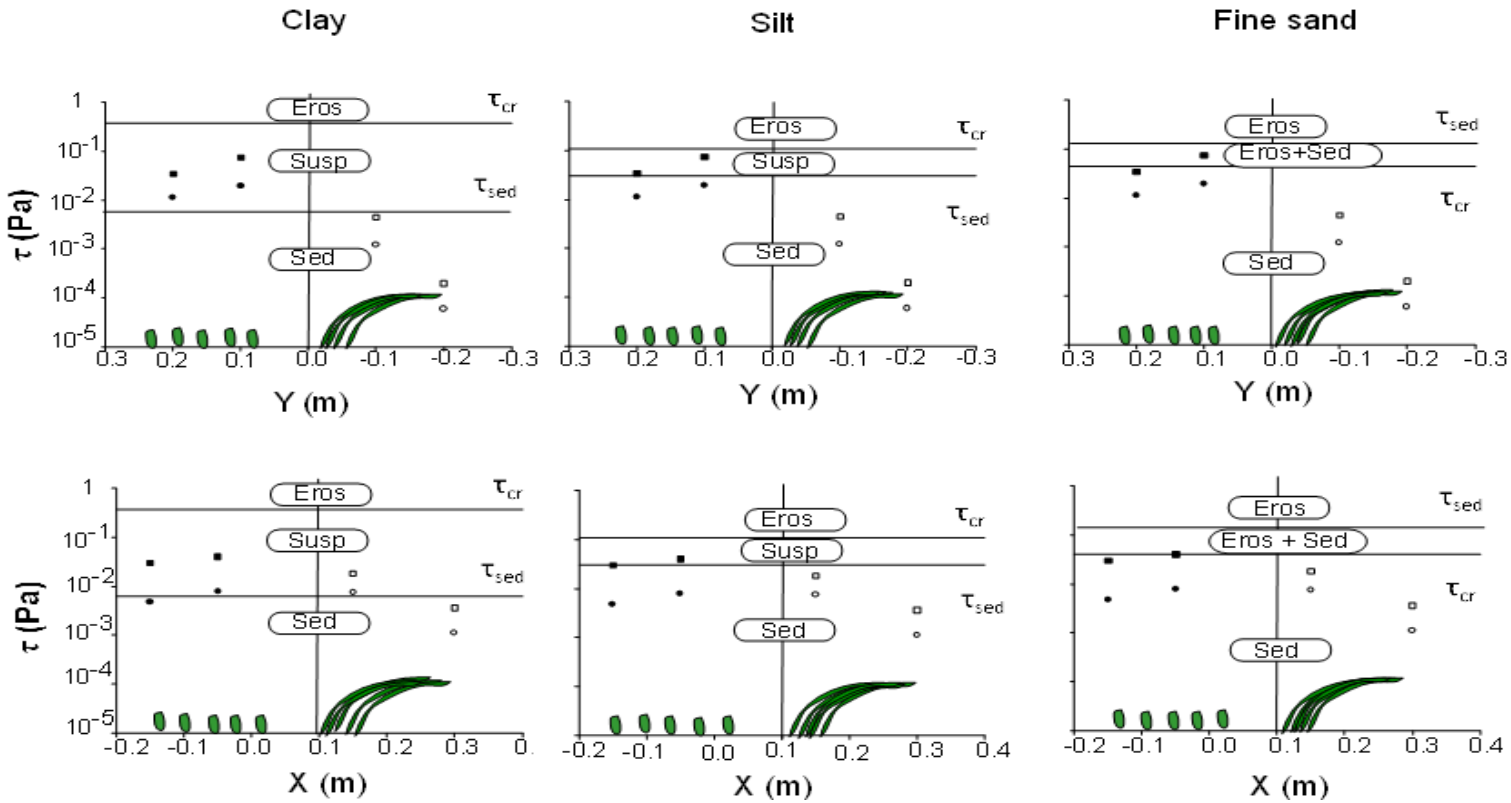

Figure 6. Cross-stream (up, Y=-0.2-0.2 m) and downstream (down, X=-0.15-0.3 m) gradients of bed shear stress (τ, Pa) in relation to the thresholds of erosion (τ_{cr}) and sedimentation (τ_{sed}) occurrence for model clay (d≈4 μm, ρ=2800 kg m^{-3}), silt (d≈44 μm, ρ=2800 kg m^{-3}) and fine-sand (d≈280 μm, ρ=2600 kg m^{-3}) particles. Gradients cover *Caulerpa prolifera* bed (black) and *Cymodocea nodosa* bed (white) for sloped microtopography, at low velocity (LV=0.065 m s^{-1}) (circles) and at high velocity (HV=0.14 m s^{-1}) (squares). Only graphs for sloped microtopography are shown since microtopography had no significant effects on τ.

TKE above canopies

Values of TKE above canopies ranged between 50 and 400 mm^2 s^{-2} although heterocedasticity of data did not allow test significant differences due to macrophyte species (Fig. 7). However, this type of differences was not expected since the error bars (95% confidence intervals) for both species overlapped for every treatment level. For each species, a two-way ANOVA (table III) was performed to check the effects of free stream velocity and microtopography. For *Caulerpa prolifera* and *Cymodocea nodosa* beds, both the free stream velocity (F=300.69; F=9.72; respectively, $p<0.001$) and the microtopography (F=64.74; F=12.2, respectively, $p<0.001$) had significant effects. The free stream velocity accounted for most of the total variance in *C. prolifera* bed (76% compared to 16% attributed to the microtopography), whereas microtopography explained 36% of the variance in *C. nodosa* bed (a 28% of the variance was attributed to the free stream velocity). No significant effects of the interaction between velocity and microtopography were detected.

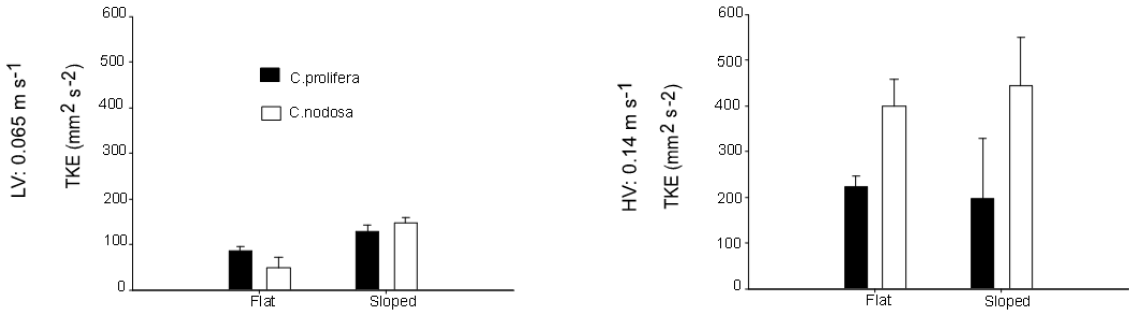

Figure 7. Graphic bars of turbulent kinetic energy (TKE, mm^2 s^{-2}) above canopies of *Caulerpa prolifera* (black) and *Cymodocea nodosa* (white) at low velocity (LV=0.065 m s^{-1}) (up) and at high velocity (HV=0.14 m s^{-1})(down) for flat and sloped microtopography. Error bars are 95% confidence intervals.

Table III. Two-way ANOVA performed to test the significance (α=0.05) of free stream velocity and microtopography on turbulent kinetic energy (TKE) above canopies (n=8).

(A) *Caulerpa prolifera* (n=8)

Factor	**F value**	**% Sum of squares between treatments**	**p-value**
Free stream velocity	300.69	76%	<0.001
Microtopography	64.75	16.4%	<0.001
Free stream velocity*Microtopography	2.39	-	0.13

(B) *Cymodocea nodosa* (n=8)

Factor	**F value**	**% Sum of squares between treatments**	**p-value**
Free stream velocity	9.72	28.29%	<0.001
Microtopography	12.20	35.50%	<0.001
Free stream velocity*Microtopography	0.02	-	0.85

DISCUSSION

Hydrodynamic-mediated processes at the transition zone

Our results show that, at the transition zone in between *C. nodosa* and *C. prolifera* (TZ), changes in free stream velocity have larger effects on turbulence (i.e. TKE and τ) than the existence of microtopography (tables II and III, Fig. 7), suggesting that the physical control of the turbulence at the TZ is more linked to short term processes (i.e. velocity changes associated to tides or wind) than to long term ones (i.e. changes in microtopography). The major control of the free stream velocity contrasts with previous reports on TZs from *Spartina maritima* to another intertidal species, where the elevation

of the *S. maritima* bed (considered a long term process as consequence of sediment accretion) seems the major factor in determining the exposition to hydrodynamic stress (Castellanos et al. 1994, Sanchez et al. 2001). As long as short term hydrodynamics drives the spatial interaction (i.e. by changes in turbulence levels), this implies a high temporal heterogeneity in natural disturbances determining the evolution of the TZ.

Within benthic macrophytes, an increase in free stream velocity usually promotes an increase on turbulence proportionally higher than the velocity augmentation (Morris et al. 2008, Hendriks et al. 2010). For homogeneous *Caulerpa prolifera* canopies, increases on free stream velocity from 0.05 m s^{-1} to 0.10 m s^{-1} may produce a 2-fold TKE raise (Hendriks et al. 2010), whereas for homogeneous *Cymodocea nodosa* canopies, a similar increase on free stream velocity (i.e. 0.05 m s^{-1} to 0.15 m s^{-1}) is able to produce a 10-fold TKE (Morris et al. 2008). Our data showed that along the TZ, the increase from LV to HV resulted in a 2.5-fold increase on the TKE above the canopy (i.e. turbulent mixing strength, Fig. 7). This effect likely enhances the sediment availability within the canopies by increasing inputs from the overlaying flow (Nepf et al. 2007, Hendriks et al. 2010). Nevertheless, the associated increase of bed shear stress and its effects on sedimentation probability depends on the τ_{sed} threshold (Zong and Nepf 2010).

From the assayed free stream velocity conditions and the sediment grain size threshold considered, the comparison of τ and τ_{sed} threshold showed that the hydrodynamic environment of *Cymodocea nodosa* favors the sediment deposition whereas in *Caulerpa prolifera* depends on the free stream velocity (Fig. 6). *Caulerpa prolifera* favors the deposition of silt and fine sand fractions at LV, whereas they should tend to remain on suspension at HV. At HV, the contrasting effects of *C. nodosa* and *C. prolifera* beds on bed shear stress suggest that the sediment that was not deposited on

the *C. prolifera* bed was susceptible of being re-allocated and deposited on adjacent *C. nodosa* areas. This mechanism would promote a depositional scenario along downstream and cross-stream *C. nodosa* patch edges, which could imply a key step favorable to the *C. prolifera* bed expansion (Stafford and Bell 2006).

The values of τ_{cr} (i.e. erosion threshold) revealed that the free stream velocity tested in this work was not high enough to generate risk of sediment erosion on *Caulerpa prolifera* sediment, excepting for the fine sand fraction. Previous works showed that seagrass beds did not increase the erosion threshold (τ_{cr}) in comparison to bare sediment under simulated unidirectional flow (e.g. *Thalassia* sp. and *Syringodium* sp., Heller 1987), or under *in situ* conditions (e.g. *C. nodosa* at Venice lagoon, Amos et al. 2004). Nevertheless, the values of τ_{cr} can be modified by (1) the existence of waves (Heller 1987) and (2) biotic factors that affect sediment cohesiveness, such as diatom-synthesized carbohydrates, bioturbation or coalescent organic matter (e.g. de Brouwer et al. 2000, Widdows and Brinsley 2002, Mecozzi and Pietrantonio 2006). At Cadiz Bay Natural Park, the bioturbator *Macoma* sp. inhabits *C. nodosa* meadows (Gonzalez-Ortiz 2009), whereas no bioturbators have been identified in *C. prolifera* beds (Rueda and Salas 2003). In addition, Sanchiz (1996) reported that *C. prolifera* sediment has 2–fold higher organic matter content than the *C. nodosa* one occurring at some locations of the Mediterranean Sea. These previous results on natural conditions suggest that biotic factors could decrease τ_{cr} values for *C. nodosa* canopies and increase them on *C. prolifera* ones. However, further *in situ* studies are necessary to fully understand the role of erosion on the TZ, and particularly because microtopographic pattern is modeled by long term and large-scale process (e.g. effects of benthic structures, Bouma et al. 2007).

Peralta et al. (2008) postulated that canopy volumetric flow rate (Q_c) was a good proxy of the sediment load transported through the canopy, and it depended on both canopy height and the mean velocity within the canopy. In the present work, Q_c at the TZ seemed to be more related to the canopy height than to the mean velocity within the canopy (Fig. 3 and 4), explaining the higher $\%Q_c$ within the *C. nodosa* canopy when compared with the *C. prolifera* one. This difference is also probably due to the higher permeability of *C. nodosa* canopies in comparison to *C. prolifera* ones, associated to a higher space in between shoots, supporting also the hypothesis on sediment reallocation on *C. nodosa* canopies adjacent to *C. prolifera*.

There are few studies dealing with the effects of the microtopography of vegetated bottoms on hydrodynamics (e.g. Carpenter and Williams 1993). These authors described *in situ* the existence of small depressions in the bed of turf algae communities with a vertical step ranging between 10^{-2} - 10^{-1} m. Such depressions increased the thickness of the boundary layer, generating a layer of low velocity. Our results showed that vertical depressions in *C. nodosa* canopies (i.e. 0.1 m step) had a similar effect. The outcome of microtopography on the velocity profile would favor the deposition of particles, also fostering the *C. prolifera* expansion. However, the sedimentation efficiency on the microtopographic depressions is also affected by the availability of sediment through canopies, which decreases with velocity reduction (i.e. $\%Q_c$ decreases with velocity). Therefore, the efficiency of sloped microtopography as sediment traps seems restricted to events of high sediment availability.

Consequences to studies about spatial interaction

The present study suggests that different hydrodynamic properties between *Cymodocea nodosa* and *Caulerpa prolifera* beds may define the rules for the space occupation process. We have focused on the microtopography as an important

component on TZs because (1) it may promote small-scale changes on hydrodynamics (Walter 1971, Carpenter and Williams 1993), and (2) changes on microtopography are mainly located at TZs between vegetation types (e.g. Marani et al. 2004).

A conceptual model of the proposed mechanism is shown in Fig. 8. The microtopography associated to TZs between *C. prolifera* and *C. nodosa* influences the near bed hydrodynamics (1) by reducing the velocity profile within the depressions observed for *C. nodosa* canopies, but also (2) by reducing the volumetric flow through canopies, thus modifying the canopy flow properties of *C. prolifera* and *C. nodosa* beds. If the reduced $\%Q_c$ is counterbalanced by a further sediment load, it would facilitate the sediment deposition within *C. nodosa* canopies. Hence, the effect of the sediment dynamics on the vegetated beds is not a permanent interaction but a relation subjected to the existence of events of high sediment availability. The species-specific response to sedimentary scenarios will determine the resulting spatial interactions and the competitive outcome. In addition, the sediment dynamic processes can shift the microtopographic pattern along the TZ, which in turn, the likely influence on hydrodynamics in a feed-back process.

The competitive characteristics of both species for space occupation are that *Caulerpa prolifera* clonal growth is fast on new bare areas (i.e. areas of recent sediment deposition, Stafford and Bell 2006), and that *Cymodocea nodosa* is sensitive to high sedimentation rates, being its growth limited with burial > 0.07 m (Marbà and Duarte 1994). In Cadiz Bay, the vertical step observed between *C. prolifera* and *C. nodosa* floor is within the range of 0.05 – 0.10 m, suggesting that positive sedimentation conditions would favor the spreading of *C. prolifera*.

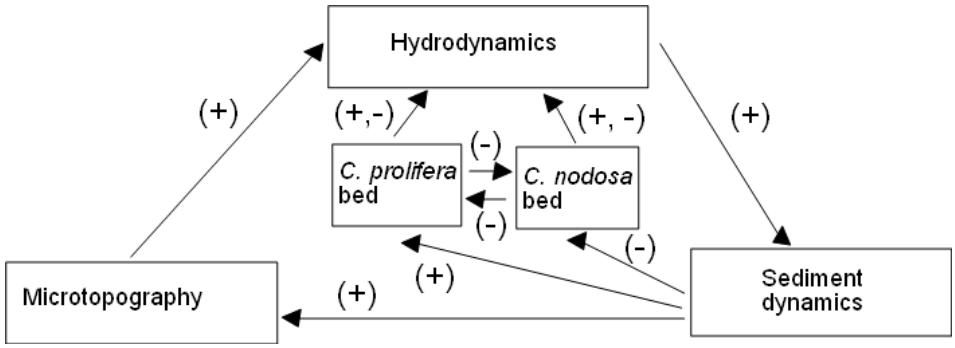

Figure 8. Conceptual model of the tested mechanism of microtopography due to macrophytes beds interacting with hydrodynamics.

Herben et al. (2000) defined the spatial competition in grassland communities as a feed-back mechanism where the presence of a plant species facilitates the occupation of the species already occupying the site. In our case, the spatial competitive process between *Caulerpa prolifera* and *Cymodocea nodosa* seems more close to an inhibitory mechanism where the conditions are hydrodynamically-mediated. The divergences on bed shear stress between both species are consequence of species-specific differences on both, bed velocity attenuation (Chen et al. 2007) and canopy drag coefficient (which depends on macrophyte density and leaf size, Nepf 1999, Chen et al. 2007). However, our results support that previous experiments with homogeneous non-overlapping canopies are not directly comparable to TZ conditions (e.g. Hendriks et al. 2010). Data showed a large spatial variability of τ along cross-stream and downstream TZ gradients not explained by experimental factors (ie. 54% out of total, table II), thus implying emergent thresholds when compared to homogeneous canopies. This fact highlights the importance of simulating patchiness conditions when hydrodynamic benthic transitions are analyzed, an approach that is rarely performed or discussed over literature (Fonseca and Koehl 2006).

ACKNOWLEDGEMENTS

This work was supported by the Spanish National Research Projects EVAMARIA (CTM2005-00395/MAR), IMACHYDRO (CTM2008-0012/MAR) and by the Andalusian Excellence Research Project FUNDIV P07-RNM-02516. First author is supported by a FPI grant of the Spanish Ministry of Science and Technology. First author specially like to thank Thijs for his valuable help collecting sediment.

REFERENCES

Achab M and Gutierrez-Mas JM (2005). Nature and distribution of the sand fraction components in the Cadiz Bay bottoms (SW-Spain). Rev Soc Geol Esp 18 (3-4):133-143.

Almasi M N, Hoskin CM, Reed JK and Milo J (1987). Effects of natural and artificial Thalassia on rates of sedimentation. J Sed Petrol 57: 901-906.

Alvarez O, Izquierdo A, Tejedor B, Mañanes R, Tejedor L. and Kagan BA (2000). The influence of sediment load on tidal dynamics, a case study: Cádiz Bay. Estuar Coast Shelf Sci 48:439-450.

Amos CL, Bergamasco A, Umgiesser G, Cappurci S, Cloutier D, DeNat L, Flindt M, Bonardi M and Cristante S (2004). The stability of tidal flats in Venice Lagoon- the results of in-situ measurements using two benthic, annular flumes. J Mar Sys 51:211-241.

Biron PM, Robson C, Lapointe MF and Gaskin SJ (2004). Comparing different methods of bed shear stress estimates in simple and complex flow fields. Earth Surf Process Landf 29(11): 1403-1415.

Benavente J, Peralta G, Lara M and Martinez-Ramos C (2008). Influencia de la vegetación en el desarrollo de la morfología de una laguna mareal. In: Tinoco JG, Paez MC, Puyana M, Amaya C, Carolina D (eds). Las ciencias y las tecnologías marinas al servicio del país. Proc 13th Nat Mar Sci and Tech Symp. San Andres Isla, Colombia.

Bouma TJ, De Vries MB, Low E, Peralta G**, Tánczos IC, van de Koppel J and Herman PMJ (2005)**. Trade-offs related to ecosystem-engineering: a case study on stiffness of emerging macrophytes. Ecology 86: 2187 - 2199.

Bouma TJ, van Duren LA, Temmerman S, Claverie T, Blanco-Garcia A, Ysebaert T and Herman PMJ (2007). Spatial flow and sedimentation patterns within patches of epibenthic structures: Combining field, flume and modelling experiments. Cont Shelf Res 27(8):1020-1045.

Carpenter RC and Williams SL (1993). Effects of algal turf canopy height and microscale substratum topography on profiles of flow speed in a coral forereef environment. Limnol Oceanogr 38(3): 687-694.

Castellanos EM, Figueroa ME and Davy AJ (1994). Nucleation and facilitation in saltmarsh succession: interactions between *Spartina marítima* and *Athrocnemum perenne*. J. Ecol 82:239-248.

de Brouwer JFC, Bjelic S, de Deckere EMGT and Stal LJ (2000). Interplay between biology and sedimentology in a mudflat (Biezelingse Ham, Westerschelde, The Netherlands). Cont Shelf Res 20:1159-1178.

Chen SN, Sanford LP, Koch EW, Shi F and North EW (2007). A nearshore model to investigate the effects of seagrass bed geometry on wave attenuation and suspended sediment transport. Estuaries Coasts 30(2): 296-310.

Fonseca MS and Fischer JS (1986). A comparison of canopy friction and sediment movement between four species of seagrass with reference to their ecology and restoration. Mar Ecol Prog Ser 29: 15-22.

Fonseca MS and Koehl MAR (2006). Flow in seagrass canopies: the influence of patch width. Est Coast Shelf Sci 67: 1-9.

Gacia E, Granata T and Duarte CM. (1999). An approach to the measurement of particle flux and sediment retention within seagrass (*Posidonia oceanica*) meadows. Aquat Bot 65: 255-268.

Gacia E, Duarte CM, Marba N, Terrados J, Keneddy H, Fortes MD and Tri NH (2003). Sediment deposition and production in SE-Asia seagrass meadows. Est Coast Shelf Sci 56:909-919.

Gonzalez-Ortiz V (2009). Las praderas de angiospermas marinas como islas de biodiversidad. MS thesis, University of Cadiz, Spain.

Gutierrez-Mas JM, Lopez-Galindo A and Lopez-Aguayo F (1997). Clay minerals in recent sediments of the continental shelf and the Bay of Cádiz (SW, Spain). Clay Minerals 32:507-515.

Gutierrez-Mas JM, Luna del Barco A, Parrado JM, Sanchez E, Fernandez-Palacios A and Ojeda J (2000). Variaciones de turbidez de las aguas de la bahía de Cádiz determinadas a partir del análisis de imágenes Landsat TM. Geogaceta 27, 79-82.

Heller DY (1987). Sediment transport through seagrass beds. Ms thesis, University of Virginia, 72 pp.

Hendriks IE, Bouma TJ, Morris EP and Duarte CM (2010). Effects of seagrass and algae of the *Caulerpa* family on hydrodynamics and particle trapping rates. Mar Biol 157(3): 473-481.

Herben T, During HJ and Law R (2000). Spatio-temporal patterns in grassland communities. In: The geometry of ecological interactions. Simplifying spatial complexity. Cambridge University Press, pp 58-59.

Hernandez I, Morris EP, Vergara JJ, De los Santos CB, Gonzalez-Ortiz V, Villazan B, Peralta G, Olive I, Brun FG, Garcia-Marin P, Lara M and Perez-Llorens JL (2010). Praderas de fanerógamas marinas en la Bahía de Cádiz: Conservación y gestión. In: Conama10.es/comunicaciones técnicas. Madrid, Spain.

Holmer M, Marbá N, Lamote M and Duarte CM (2009). Deterioration of sediment quality in seagrass meadows (*Posidonia oceanica*) invaded by macroalgae (*Caulerpa* sp.). Estuaries Coasts 32(3): 456-466.

Irving AD and Connell SD (2002). Interactive effects of sedimentation and microtopography on the abundance of subtidal turf-forming algae. Phycologia 41(5): 517-522.

Jonsson PR, van Duren LA, Amielh M, Asmus R, Aspden RJ, Daunys D, Friedrichs M, Friend PL, Olivier F, Pope N, Precht E, Sauriau PG and Schaaff E. (2006). Making water flow: a comparison of the hydrodynamic characteristics of 12 different benthic biological flumes. Aquat Ecol 40: 409-438.

Kagan BA, Alvarez O, Izquierdo A, Mañanes R, Tejedor B and Tejedor L (2003). Weak wind-wave/tide interaction over a moveable bottom: results of numerical experiments in Cadiz Bay. Cont Shelf Res 23(5):435-456.

Marbá N and Duarte CM (1994). Growth response of the seagrass *Cymodocea nodosa* to burial and erosion. Mar Ecol Prog Ser 107: 307-311.

Marani M, Lanzoni S, Silvestri S and Rinaldo A (2004). Tidal landforms, patterns of halophytic vegetation and the fate of the lagoon of Venice. J Mar Syst 51:191-210.

Mecozzi M and Pietrantonio E (2006). Carbohydrates proteins and lipids in fluvic and humic acids of sediments and its relationships with mucilaginous aggregates in the Italian seas. Mar Chem 101:27-39.

Meinesz A, Belsher T, Thibaut T, Antolic B, Mustapha KB, Boudouresque F, Chiaverini D, Cinelli F, Cottalorda J-M, Djellouli A and others (2001). The introduced green algae *Caulerpa taxifolia* continues to spread in the Mediterranean. Biol Invasions 3(2): 202-210.

Morris EP, Peralta G, Brun FG, van Duren L, Bouma TJ and Pérez-Lloréns JL (2008) Interaction between hydrodynamics and seagrass canopy structure: spatially explicit effects on ammonium uptake rates. Limnol Oceanogr 53: 1531–1539.

Morris EP, Peralta G, Benavente J, Freitas R, Rodrigues AM, Quintino V, Alvarez O, Valcarcel-Perez N, Vergara JJ, Hernández I and Pérez-Lloréns JL (2009). Caulerpa prolifera stable isotope ratios reveal anthropogenic nutrients within a tidal lagoon. Mar Ecol Prog Ser 390: 117 – 128.

Nepf HM (1999). Drag, turbulence and diffusion in flow through emergent vegetation. Water Resour Res 35: 479-489.

Nepf H, Ghisalberti M, White B and Murphy E (2007). Retention time and dispersion associated with submerged aquatic canopies. Water Resour Res 43, W04422.

Occhipinti-Ambrogi A and Savini D (2003). Biological invasions as a component of global change in stressed marine ecosystems. Mar Pollut Bull 46(5): 542-51.

Orth RJ, Carruthers TJB, Dennison WC, Duarte CM and others (2006). A global crisis for seagrass ecosystems. BioScience 56: 987–996.

Peralta G, van Duren LA, Morris EP and Bouma TJ (2008). Consequences of shoot density and stiffness for ecosystem engineering by benthic macrophytes in flow dominated areas: a hydrodynamic flume study. Mar Ecol Prog Ser 368: 103 – 115.

Piazzi L, Ceccherelli G and Cinelli F (2001). Threat to macroalgal diversity: effects of the introduced green alga *Caulerpa racemosa* in the Mediterranean. Mar Ecol Prog Ser 210: 149-159.

Piazzi L, Balata D, Ceccherelli G and Cinelli F (2005). Interactive effect of sedimentation and *Caulerpa racemosa* var. cylindracea invasion on macroalgal assemblages in the Mediterranean Sea. Estuar Coast Shelf Sci 64: 467-474.

Piazzi L, Balata D, Foresi L, Cristaudo C and Cinelli F (2007). Sediment as a constituent of Mediterranean benthic communities dominated by *Caulerpa racemosa* var. cylindracea. Sci Mar 71(1): 129-135.

Rueda JL and Salas C (2003). Seasonal variation of a molluscan assemblage living in a *Caulerpa prolifera* meadow within the inner Bay of Cadiz (SW Spain). Estuar Coast Shelf Sci 57:909-918.

Sanchez JM, San Leon DG and Izco J (2001). Primary colonisation of mudflat estuaries by *Spartina marítima* (Curtis) Fernald in northwest Spain: vegetation structure and sediment accretion. Aquat Bot 69:15-25.

Sanchiz C (1996). Bioacumulació de mercuri, cadmi, plom i zinc en les praderies de macròfits bentònics sobre substrat solt del litoral mediterrani ibéric. PhD thesis, University of Valencia, Spain.

Self RFL, Nowell ARM and Jumars PA (1989). Factors controlling critical shears for deposition and erosion of individual grains. Mar Geol 86:181-199.

Smith C and Walters LJ (1999). Fragmentation as a strategy for *Caulerpa* species: Fates of fragments and implications for management of an invasive weed. Mar Ecol 20(3-4): 307-319.

Stafford NB and Bell SS (2006). Space competition between seagrass and *Caulerpa prolifera* (Forsskaal) Lamouroux following simulated disturbances in Lassing Park, FL. J Exp Mar Biol Ecol 333(1): 49-57.

Soulsby RL (1983). The bottom boundary layer of shelf seas. In: Johns B (Ed.) Physical oceanography of Coastal and Shelf Sea. Elsevier Oceanography Series 35: 189-266.

Tweedley JR, Jackson EL and Attrill MJ (2008). *Zostera marina* seagrass beds enhance the attachment of the invasive alga *Sargassum muticum* in soft sediments. Mar Ecol Prog Ser 354: 305-309.

van Rijn LC (2007). Unified view of sediment transport by currents and waves. I: Initiation of motion, bed roughness and bed-load transport. J Hydraul Eng 133(6):649-667.

Vergara JJ, García-Sánchez MP, Olivé I, García-Marín P, Brun FG, Pérez-Lloréns JL and Hernández I (2012). Seasonal functioning and dynamics of *Caulerpa prolifera* meadows in shallow areas: An integrated approach in Cadiz Bay Natural Park. Est Coast Shelf S 112:255-264.

Walter HG (1971). Bedform mechanics. In: Hydraulics of sediment transport. Mc Graw Hill, 513 pp.

Widdows J and Brinsley M (2002). Impact of biotic and abiotic processes on sediment dynamics and the consequences to the structure and functioning of the intertidal zone. J Sea Res 48:143-156.

Wright JT and Davis AR (2006). Demographic feedback between clonal growth and fragmentation in an invasive seaweed. Ecology (USA) 87: 1744-1754.

Zong L and Nepf H (2010). Flow and deposition in and around a finite patch of vegetation. Geomorphology 116(3-4): 363-372.

CHAPTER 2:

Sedimentary effects of individual seagrass patches

Sedimentation patterns within an artificial *Cymodocea nodosa* patch: A flume tank study

M. Lara[1], E.W. Koch[2], G. Peralta[1], D. Booth[2], J. L. Perez-Llorens[1]

[1]Department of Biology, Faculty of Marine and Environmental Sciences, University of Cadiz, 11510 Puerto Real (Cadiz), Spain

[2]Horn Point Laboratory, University of Maryland, Centre for Environmental Science, Cambridge, MD 21613, USA

ABSTRACT

Seagrass patches may modify sediment dynamics by reducing current velocity and allowing a horizontal sediment transport trough their canopies. Such effect is not spatially homogeneous along the patch, and this fact is relevant for seagrass restoration success. However, few studies have been focused on sedimentation patterns within seagrass stands, specifically under tidal (i.e. non orbital) low flow conditions. To cope with this objective, we studied the effects of an artificial patch of the seagrass *Cymodocea nodosa* (1.8 m long) on the spatial sedimentation patterns. This study was performed in a flume tank under three relatively slow velocities usually recorded in Cadiz Bay under natural conditions (0.03, 0.065 and 0.13 m s^{-1}). Simultaneously to direct measurements on sedimentation rate, several variables have been also studied attempting to find a hydrodynamic proxy to explain such sedimentary effects. Hydrodynamic analysis included spatial gradients on velocity profiles, integrated velocity values above the canopy (u_{above}), and volumetric flow rate within the canopy (Q_c). Sedimentation rates were maxima close to the leading edge of the seagrass patch (ie. the principal patch edge oriented perpendicular to flow) and decreased exponentially downstream with distance. This decrease could be related to the corresponding increases on shear stress on top of the canopy. Data suggests that submersed vegetation patches have a horizontal spatial threshold (x_{edge}=0.4-0.6 m) that once surpassed sedimentation becomes minimum. Our results support the hypothesis that under the studied velocity range, sediment availability is limited, accounting Q_c for total patch sedimentation rate (S_{bed}), but this does not explain the spatial pattern, which seems inversely related to u_{above}.

INTRODUCTION

Seagrass species are widely considered as ecosystem engineers because its abilility in modifying the abiotic surroundings (Jones et al. 1997). These modifications also include the sedimentary environment (Koch 2001). In fact, seagrasses are able to (1) increase sediment accretion (Gacia et al. 1999, Gacia et al. 2003, Bos et al. 2007), (2) select grain size (Schubel 1973, Cabaço et al. 2010), (3) stabilize bottom substrate (Fonseca and Fischer 1986) and (4) prevent erosion (Thompson et al. 2004). Such effects are of prime importance for their own survival, because they modulate the physical environment to be close to their habitat requirements. For example, seagrass canopies attenuate turbidity by sediment trapping increasing light availability (van der Heide et al. 2007, de Boer 2007) and, potentially, the subsequent photosynthesis and growth.

The capacity of seagrasses to modify sedimentary dynamics has strong implications for restoration purposes, as stated by several authors (Fonseca and Fischer 1986, van Keulen et al. 2003, Cabaço et al. 2008; van Katwijk et al. 2009). The ability of seagrasses to stabilize and retain sediment particles (Fonseca and Fischer 1986, Gacia et al. 1999, de Boer 2007) has been related to their capacity to reduce water velocity (e.g. Fonseca et al. 1983, Almasi and Hoskin 1987, Hendriks et al. 2010), which depends directly on (1) shoot density (Peterson et al. 2004, Peralta et al. 2008) and (2) patch size (Fonseca et al. 1983). In fact, recent research with artificial vegetation suggests that patch size-flow scaling effects promotes divergent patterns on sediment deposition, because the longitudinal distance that current can penetrate is limited (Zong and Nepf 2011).

Despite sedimentary effects are quite relevant to seagrass ecology, their spatial explicit analysis is rarely performed. A submerged vegetation with patchy distribution

tend to develop physical gradients affecting burial and erosion processes as it has been described for saltmarshes (Bouma et al. 2007), vegetated channels (Zong and Nepf 2010) and lake vegetation (Pluntke and Kozersky 2003). From previous hydrodynamic studies, it is known that seagrass patches develop horizontal hydrodynamic gradients (Gambi et al. 1990, Morris et al. 2008) which imply that (1) the edge of a seagrass patch must be quite effective trapping sediment in comparison with its center (Fonseca et al. 1982) and that (2) sediment trapping capacity must increase directly with the volumetric flow through the canopy (Morris et al. 2008, Peralta et al. 2008). However, further investigation is required to demonstrate these hypotheses.

The biological and hydrodynamic conditions of Cadiz Bay, an Atlantic tidal lagoon of siliciclastic sediment, are excellent as a model of the effects of seagrasses on spatial patterns of sediment dynamics (Gutierrez-Mas et al. 1999). The inner water body is extensively populated by submersed vegetation (> 90%, Morris et al. 2009), being the patchy meadows of *Cymodocea nodosa* Ucria (Ascherson) one of the dominating at the tidal zone. Tidal velocities usually range from 0 to 0.08 m s^{-1} (e.g. Kagan et al. 2003) and sediment transport is controlled by unidirectional currents after wind-storm re-suspension events (Gutierrez-Mas et al. 2000). However, to elucidate the underlying processes on small-scale patches it is necessary to perform detailed hydrodynamic measurements and in such a case, laboratory experiments with model vegetation provide better conditions (Bouma et al. 2007). The use of mimic plants allows specifically modulating morphology, shoot density and stiffness on seagrass populations (e.g. Peralta et al. 2008).

The aims of this study are (1) to analyze spatial patterns of sedimentation rates along a gradient within a seagrass patch model, (2) to determine the spatial limit of leading edge effects on sedimentation, and (3) to relate hydrodynamic variables with

sedimentation rates within the patch. To achieve these objectives, we used an artificial canopy to determine experimentally the effects of (1) current velocity and (2) the distance from the leading edge, on sedimentation rates. The artificial canopy was constructed with flexible mimics that emulate *Cymodocea nodosa* shoots. Current velocity, grain size and sediment concentration were selected according to reference conditions in the inner Cadiz bay.

MATERIAL AND METHODS

Artificial seagrass canopy

The dimensions of the *Cymodocea nodosa* shoot mimics were chosen to emulate the annually averaged *C. nodosa* shoots growing in Cadiz bay (Fig. 1, Brun et al. 2006). Shoots were constructed on millar plastic with 4 flexible leaves (see figure 1A for mimic morphometry). The shortest leaf was at the core of the shoot. A sheath was simulated by wrapping the blades at the base with a piece of soft wood (Fig. 1A). Natural buoyancy of seagrass leaves was allowed by adding small floats of rubber to the leaf tips. These mimics were inserted in a 2 x 0.5 m PVC plate. A 540 shoots m^{-2} density was distributed in a regular pattern to study the hydraulic effects (Fig. 1B). The distance between shoots was 3 and 4 cm from lateral and downstream directions respectively. Lateral shoot arrangement was alternated between lines (see Fig. 1B and 1C).

Flume tank description and flow measurements

The flume tank was a 7.5 m straight and unidirectional model with 0.5 m water column (Fig. 2, Jonsson et al. (2006) for more details). Measurements were performed at low (LV, 0.03 m s^{-1}), medium (MV, 0.065 m s^{-1}) and high (HV, 0.13 m s^{-1}) free

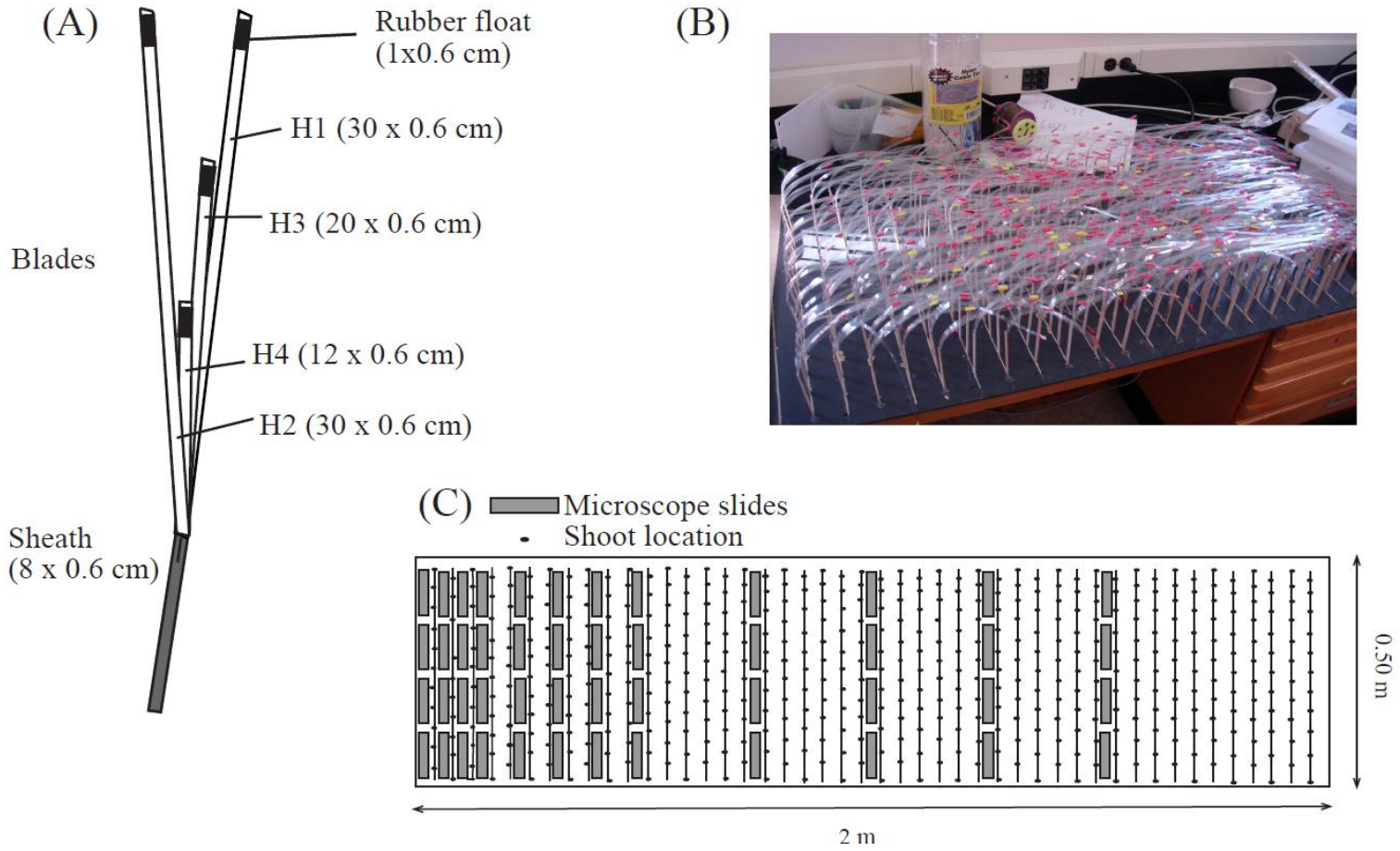

Figure 1. **The artificial canopy** (A) A mimic shoot (dimensions between brackets). (B) Picture of the artificial canopy. (C) Scheme on the microscope slide and artificial shoot distribution within the mimic *Cymodocea nodosa* canopy.

stream velocities. To develop a stable hydrodynamic regime prior to measurements, the flume tank was running for at least 10 min.

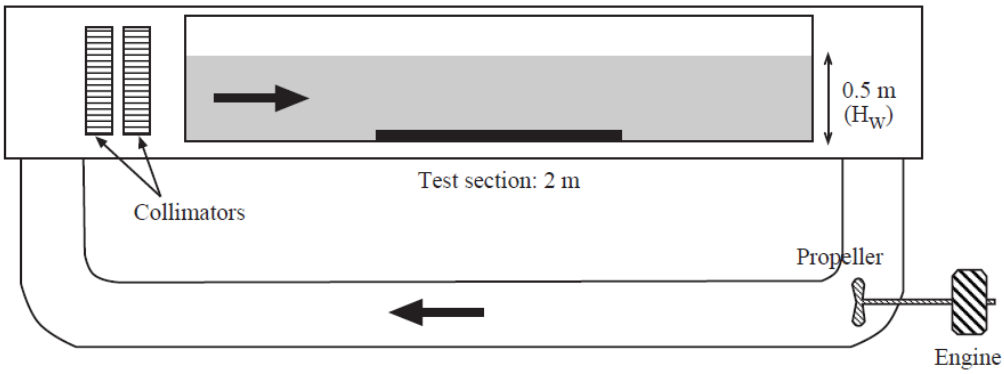

Figure 2. **Flume tank scheme**. H_W indicates the height of the water column. The arrows indicate the direction of the water flux.

Main velocity component (u) was measured with portable Aquadopp current meter (± 0.01 m s^{-1}). Vertical profiles of u were estimated by measuring at 0.06, 0.1, 0.2, 0.3, 0.4 and 0.5 m above the bottom floor. To measure at 0.06 m it was necessary to remove 3 shoots, generating a free-obstacle area of 96 cm^2.

At each free stream velocity, the hydrodynamic profiles were studied in a horizontal transect from 1 m upstream to 0.5 m behind the canopy. Considering 0 the leading edge of the canopy, the velocity profiles were studied at -1.00, 0.00, 0.04, 0.12, 0.28, 0.44, 0.92, 1.40, 2.00 and 2.30 m (the last two profiles were at 0.20 and 0.50 m out, behind the canopy). The measurements corresponding to each x-location were treated as independent vertical velocity profiles. Canopy height was recorded at each position.

Sedimentation rate

The sediment used during the experiments was a silt-clay novaculite 44 µm (AGSCO Corporation, New Jersey). This grain size is representative of the sediment type found at Cadiz Bay, where *Cymodocea nodosa* meadows thrive (Gutierrez-Mas et al. 1997). At every velocity, it was used a suspended solid concentration of 0.363 kg m^{-3}, being this value considered as representative of an extreme sediment transport event (i.e. two-fold higher than that found at inner Cadiz Bay, Muñoz Pérez and Sánchez Lamadrid 1994).

Sedimentation patterns were studied at LV, MV and HV free stream velocities, with two replicates per treatment. During each measurement, the sediment was added to the water column at 1 m upstream of the canopy leading edge. Sediment release was done at an intermediate depth and mixed gently with the water column to avoid floating particles above the water surface. Every experiment was run during 2 hours, time enough to detect any significant sedimentation. After every experiment, the flume tank was quickly emptied (<5 min).

To determine sedimentation rates, microscope slides were placed at pre-selected positions (Fig. 1C). The microscope slides (0.075 x 0.025 m) are thick enough to prevent any sediment accumulation due to horizontal floor sediment transport. Four parallel samples evenly distributed and separated by 4 cm were taken at 12 x-positions (i.e. 0.00, 0.04, 0.08, 0.12, 0.20, 0.28, 0.36, 0.44, 0.68, 0.92, 1.16 and 1.40 m) from the leading edge of the canopy. Microscope slides were carefully removed from the bed, dried (24-48 h, 60ºC) and weighted after each assay. From each sample, sedimentation rate was estimated by weight difference between after and before the experiment. To ensure that the bottom was free of deposited particles for the following runs, the bed without glass slides was cleaned and the flume was filled and emptied twice.

Variable estimations

As a hydrodynamic proxy to understand the sedimentary dynamics, we focus on the volumetric flow rate (Q). The volumetric flow rate through the canopy (Q_C) was calculated by vertically integrating the velocity profile on the canopy height (h_c) for the flume tank width (y_w) (eq.1, see Peralta et al. 2008 for further details). To reveal the underlying hydrodynamic processes involved in the sedimentation patterns, we compared edge and center conditions of the seagrass patch. Edge conditions were calculated as Q_c at 0.04 m from the leading edge, whereas center conditions were calculated at 0.92 m downstream the leading edge:

$$Q_C = \int_0^{y_W} \int_0^{h_C} u(z)\,dz\,dy = \sum_0^{h_C} Q_i \qquad \text{(eq. 1)}$$

where,

$$Q_i = y_W (z_i - z_{i-1}) u_{zi}$$

The sedimentation rate (S) was estimated as dry weight of settled sediment per unit area and unit time (g DW m^{-2} h^{-1}; eq. 2):

$$S = \frac{(W_2 - W_1)}{A_{plate} * (t_2 - t_1)} \qquad \text{(eq. 2)}$$

where:

S: sedimentation rate (g DW m^{-2} h^{-1})

W_2: microscope slide weight at the end of the experiment (g DW)

W_1: microscope slide weight at the beginning of the experiment (i.e. no sediment) (g DW)

A_{plate}: microscope slide surface (0.075 x 0.025 m^2)

t_2-t_1: experimental time (2 hours)

To integrate the sedimentation rate for the entire canopy (S_{bed}), and since the microscope slides were not equidistant, the S values were spatially weighted according to equation 3:

$$S_{bed} = \frac{\sum_{j=1}^{4}\sum_{i=1}^{12} S_{ij}(x_{i+1} - x_i)(y_{j+1} - y_j)}{A} \qquad \text{(eq. 3)}$$

where:

S_{bed}: weighted sedimentation rate for the entire canopy (g m^{-2} h^{-1})

S_{ij}: sedimentation rate at the microscope slide on position ij (g m^{-2} h^{-1}).

x_i: x position of the microscope slide on position ij (m)

y_j: y position of the microscope slide on position ij (m)

A: total area covered by the canopy (m^2).

To discriminate the sedimentation processes due to edge effects, the sedimentation rates were newly estimated assuming the canopy divided into two areas (i.e. edge and center; S_{edge} and S_{center}). The limit between these two areas was selected as the distance where the sedimentation rate value stabilizes as a function of x-distance, being the edge zone (x_{edge}) the area where sedimentation rate decreases with x (eq. 4) and the center zone (x_{center}) the area where sedimentation rate is constant with x (eq. 5).

$$S_{edge} = \frac{\sum_{j=1}^{4}\sum_{i=1}^{7} S_{ij} * (x_{i+1} - x_i) * (y_{j+1} - y_j)}{A_{edge}} \qquad \text{(eq. 4)}$$

$$S_{center} = \frac{\sum_{j=1}^{4}\sum_{i=8}^{12} S_{ij} * (x_{i+1} - x_i) * (y_{j+1} - y_j)}{A_{center}} \qquad \text{(eq. 5)}$$

where:

S_{edge}: sedimentation rate within the part of the canopy that is affected by edge effects ($g\ m^{-2}\ h^{-1}$)

S_{center}: sedimentation rate within the part of the canopy that is not affected by edge effects ($g\ m^{-2}\ h^{-1}$)

A_{edge}: area of the canopy affected by edge effects (m^2)

A_{center}: area of the canopy not affected by edge effects (m^2) ($A_{center}=A - A_{edge}$)

Statistics

To detect any relationships between sedimentation rate and distance to the canopy edge, exponential regressions were applied by minima square differences. Due to problems of heteroscedasticity, the existence of significant effects of free stream velocity on sedimentation rate was estimated using the non-parametric Friedman's test (Siegel, 1970). Finally, linear correlations were established between the average velocity above the canopy and the corresponding sedimentation rate. Significance level was always set at 0.05.

RESULTS

Canopy height

Canopy height (h_C) was maximum at LV (0.38 m) and minimum at HV (0.17 m) (Fig. 3A), and within every velocity treatment, h_C also increased with distance to the leading edge (i.e. downstream). Nevertheless, it can be observed that the effects on canopy height were not proportional to the free stream velocity increase (i.e. from LV to HV, h_C decreased 1.3 fold maximum vs. a maximum increase of 4.3 times for velocity).

Hydrodynamics

The presence of the seagrass canopies clearly affected the velocity profile showing this effect also a clear gradient along x distance (Fig. 3B). Close to the bottom floor, velocity ranged between 0.01 - 0.10 m s^{-1} depending on the velocity treatment. The effects of the seagrass patch was especially clear at the HV (Fig. 3B), decreasing by 20 - 50 % within the canopy, whereas at LV the velocity attenuation needed longer distances to be detected (i.e. 0.44 - 1.40 m within the canopy). In general, reduction velocity effects were negligible along x_{edge}. Flow was accelerated above the canopy, and increasing with distance from the leading edge. In relative terms, the magnitude of water acceleration was similar in all the treatments, increasing the velocity 1.2 - 2.5 fold as a function of x-position and canopy height. The highest velocity value (0.25 m s^{-1}) was observed on top of the canopy at HV.

The vertical profiles within the canopy showed typical sigmoidal shapes (Fig. 3B). The typical velocity increase on top of the canopy was enhanced by the distance to the leading edge (x-position) and by the free stream velocity (Fig. 4A). The volumetric flow rate through the canopy (Q_C) ranged between 0.007- 0.013 m^3 s^{-1} (Fig. 4B). For both, edge and the center of the patch, Q_C was maxima at MV. Nevertheless, at every

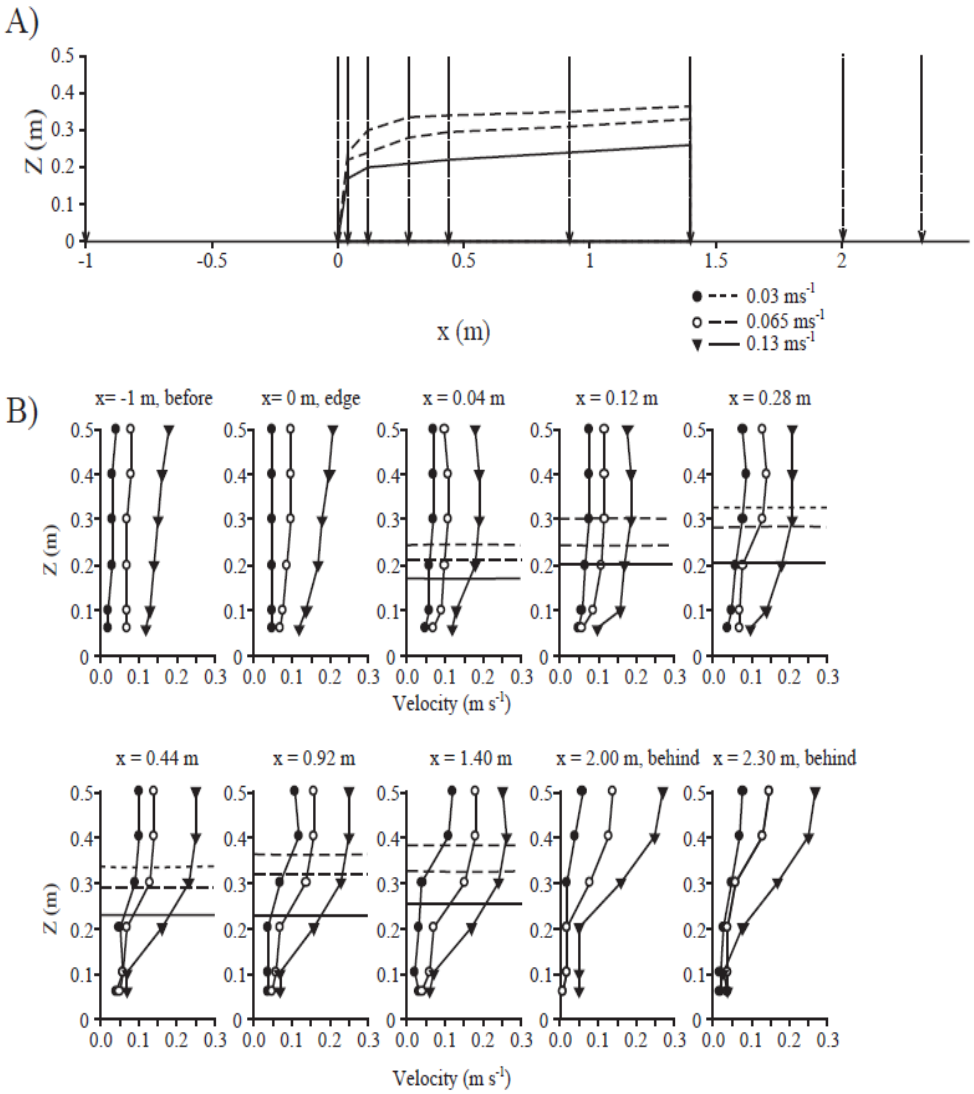

Figure 3. **(**A) Canopy height according to the velocity treatment. Vertical dashed arrows indicate the location where vertical velocity profiles were measured (x= -1.00, 0.00, 0.04, 0.12, 0.28, 0.44, 0.92, 1.40, 2.00 and 2.30 m). (B) Vertical velocity profiles at 0.03 m s^{-1}, 0.065 m s^{-1} and 0.13 m s^{-1}. Canopy height is also indicated within the corresponding graphs.

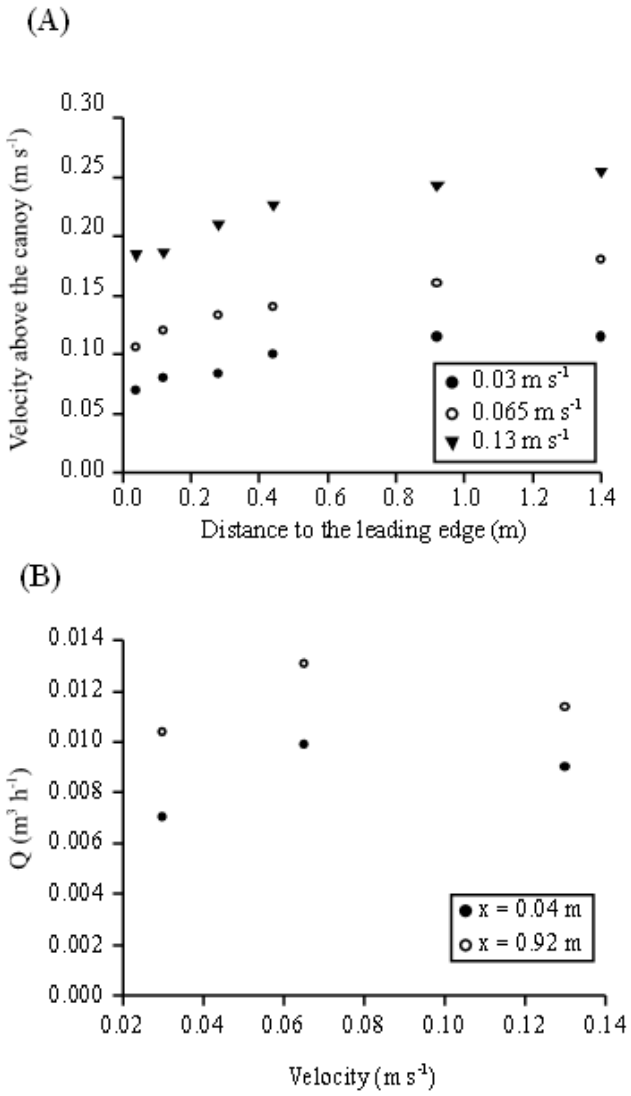

Figure 4. (A) Average velocity above the canopy (u_{above}, m s^{-1}) as a function of distance to the leading edge (0.03 m s^{-1} black circles, 0.065 m s^{-1} white circles, 0.13 m s^{-1} black triangles). (B) Volumetric flow rate through the canopy (Q_c, m^3 s^{-1}) as function of free stream velocity (x=0.04 m black circles, x=0.92 m white circles).

velocity treatment, Q_C was higher in the center that in the edge (Fig. 4B) probably due to increases on canopy height.

Spatial patterns on sedimentation rate

Velocity and distance to the leading edge had significant effects on the sedimentation rate within the canopy (Figures 5 and 6 respectively; non-parametric Friedman's test for velocity effects $\chi^2=18$; $p<0.001$). Maximum sedimentation rate was always found at the leading edge of the canopy. Furthermore, differences between edge and centre were clearly lower at LV than at MV or HV (Fig. 5). Accordingly, the integrated sedimentation rate (S_{bed}) was at LV half than those observed at MV or HV (Fig. 5). For every velocity treatment, the sedimentation rate exponentially decreased with increasing distance to the leading edge (Fig. 6, fitting parameters are indicated in the figure). However, this gradient clearly smoothed with decreasing velocities (i.e. the exponential slope decreased with free stream velocity, Fig 6A).

The main difference due to the velocity treatment was the x distance of edge effects (i.e. edge effect limit). The horizontal limit for edge effects (x_{edge}) was selected according to the distance where sedimentation rate reached the minimum asymptote. At MV and HV, the x_{edge} was estimated at 0.5-0.6 m from the leading edge (Fig. 6), while at LV it was at 0.4 m. Once discriminated edge and center zones, significant differences on sedimentation rates due to velocity were clearly attributable to the edge zones, with values higher at MV and HV than at LV (70-60 vs. 30 g m^{-2} h^{-1}, respectively). No significant differences were observed in center zones. In these areas, sedimentation rate was constant and around 20 g m^{-2} h^{-1}.

The average velocity above the canopy (u_{above}) was used as a proxy for shear stress. Accordingly, the negative linear correlations found between sedimentation rate

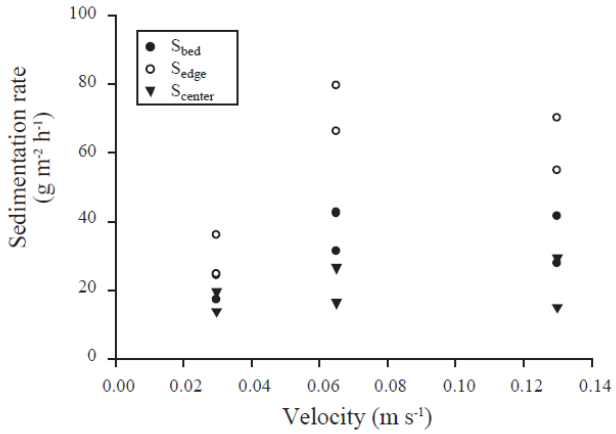

Figure 5. Sedimentation rate (g m^{-2} h^{-1}) as function of the free stream velocity. The values of sedimentation rate have been integrated for the entire patch (S_{bed}), the edges (S_{edge}) and the center zones (S_{center}).

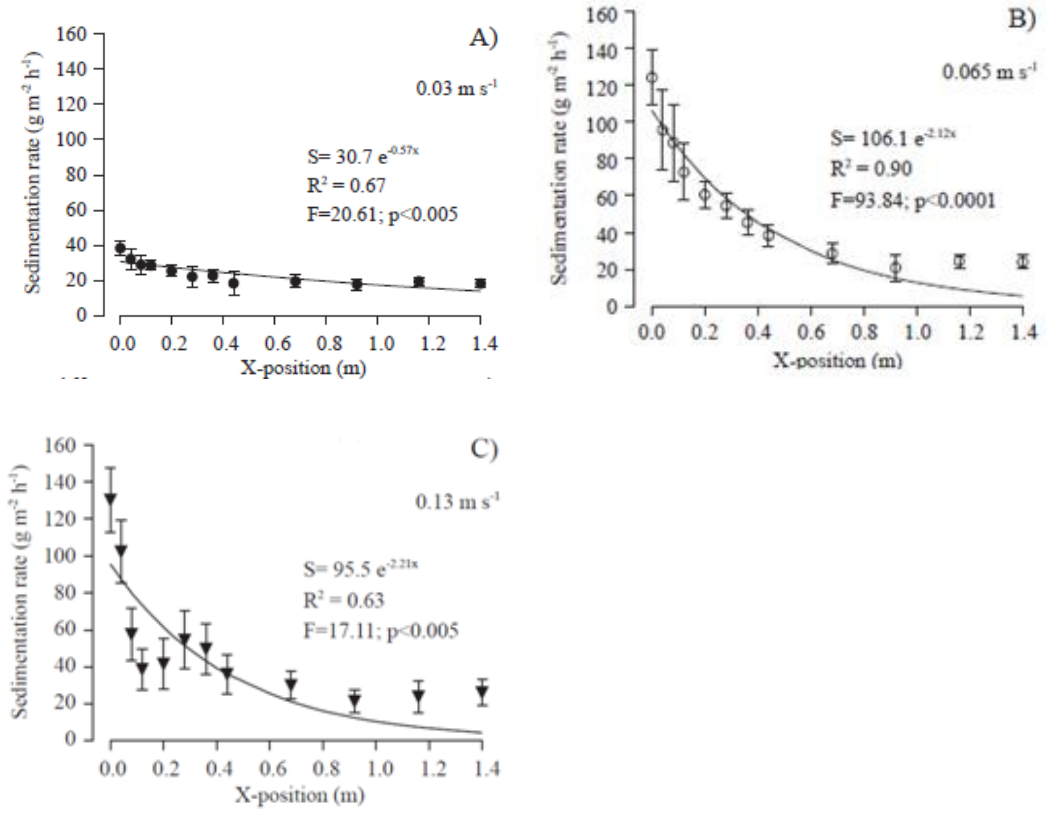

Figure 6. Sedimentation rate (g m^{-2} h^{-1}) as function of distance to the leading edge at (A) 0.03 m s^{-1}, (B) 0.065 m s^{-1} and (C) 0.13 m s^{-1}. Error bars represent 95% confidence intervals. Parameters of negative exponential adjust are also indicated.

and u_{above} (Fig. 7) suggest that the decrease on sedimentation rate when moving downstream from the leading edge can be due to the corresponding increase of shear stress on top of the canopy. The slope of this last correlation (Fig. 7) expresses the quantity of retained sediment by the canopy per unit of u_{above} reduction. Therefore, it could be used as a proxy for sediment trap efficiency, being such sediment trap efficiency highest at MV and lowest at LV.

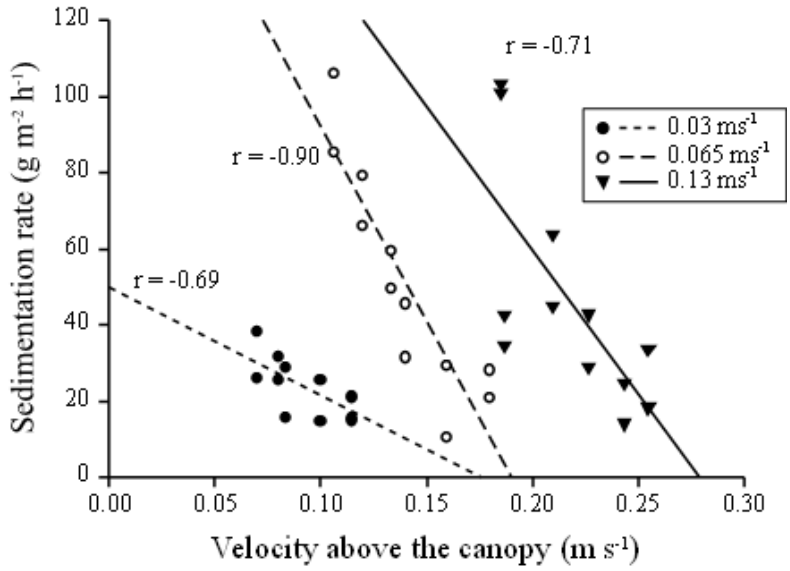

Figure 7. Sedimentation rate (g m^{-2} h^{-1}) versus average velocity above the canopy (u_{above}, m s^{-1}) at the corresponding x-position for the three velocity treatments. Linear correlations and corresponding correlation coefficient are represented.

DISCUSSION

Sedimentation within a seagrass patch depends on (1) an effective velocity reduction to favor sediment deposition (Almasi and Hoskin 1987, Hendriks et al. 2010) and (2) sufficient sediment availability, that in turns depends on suspended sediment

and enough volumetric water flow through the canopy (Q_c, Peralta et al. 2008). Present work demonstrates that both, velocity reduction and Q_c within *Cymodocea nodosa* mimic canopies vary within the free stream velocity range studied (i.e. 0.03 – 0.13 m s^{-1}). It has been previously demonstrated that the simultaneous effect of the free stream velocity on both variables strongly depends on the shoot stiffness, which determines the relative volume of the water column occupied by the canopy and, consequently, the water volume under reduced velocity (Peralta et al. 2008). Hence, previous works and our results support that the relationship between free stream velocity and sedimentation rate is not simple, and the understanding of the underlying mechanisms needs a deeper analysis.

Cymodocea nodosa populations allow a gentle volumetric flow through their shoots (Q_c) in comparison with other seagrass species like *Zostera noltii* (Morris et al. 2008) or *Posidonia oceanica* (Hendriks et al. 2010), being this property related to the high porous canopy architecture of *C. nodosa* stands compared to the others (Morris et al. 2008). The high Q_c suggests that velocity reduction is not very intense at the edge zone (x_{edge}), contrasting to previous studies on *Zostera marina* that described the edge as the most active flow reduction zone (e.g. Fonseca et al. 1982). In fact, the 20 – 50 % of velocity reduction described in our work is in agreement with the 60 - 80% described at 0.2 m s^{-1} for a 3.5 times higher density bed (i.e. 1800 shoots m^{-2}, Morris et al. 2008), but in our case, most of this reduction occurred downstream x_{edge}. Because differences on sedimentation rates were located mostly at x_{edge}, it could be inferred that the effect of velocity reduction on sedimentation rate is horizontally limited.

The observed Q_c trend (i.e. increase from LV to MV, but not from MV to HV, Fig. 4B) agrees with the sedimentation rate value at the edge, which is lower at LV when compared with either MV or HV, and similar between MV and HV. This pattern

is also consistent with the hypothesis that sediment availability should be higher at MV than at LV, highlighting the importance of a gentle horizontal sediment transport, as in previous seagrass sedimentation models (Chen et al. 2007). Accordingly, it can be concluded that, *C. nodosa* sedimentation rate mainly depends on Q_c, and, therefore, being constrained by sediment availability within the velocity range assayed.

The volumetric flow rate (Q_c) explains properly the effects of free stream velocity on the canopy sedimentation rate, but not its spatial patterns. Regardless the velocity treatment, sedimentation is significantly lower in the center of the patch (Fig. 6), despite Q_c is 1.3-fold higher in the center (0.011-0.013 m^3 s^{-1}) than in the edge (0.007-0.010 m^3 s^{-1}). To our knowledge, this pattern has not been previously described. However, literature on seagrass sediment dynamics is not abundant, and previous works clearly stated that the effects on sediment dynamics highly depend on canopy features. For instance, using dense mimics Bouma et al. (2007) demonstrated that stiff submersed vegetation edges are erosive zones. Pluntke and Kozersky (2003) did not find any significant spatial sedimentation pattern for natural lake vegetation. Zong and Nepf (2010) reported the existence of two regions within a vegetated channel: (1) a region close to the leading edge, where sedimentation rate increased due to the flow deceleration, and (2) a zone of fully developed flow where the sedimentation rate decreased downstream due to the depleting sediment availability. In any case, differences on stiffness and shoot density of canopies could account for all these divergences (Peralta et al. 2008).

In our case, sedimentation patterns could be related to the shear stress pattern above canopy. On one hand, shear stress is proportional to velocity (Fonseca and Fischer 1986) and above the canopy can avoid vertical sediment settlement (Jumars and Nowell 1984). On the other hand, the development of skimming flow induces water

acceleration on top of the canopy (Gambi et al. 1990), increasing this effect with distance to the leading edge (e.g. Morris et al. 2008 within a *Cymodocea nodosa* patch). We propose to use such acceleration effect as a proxy to estimate shear stress on top of the canopy. Therefore, we defined u_{above} as the averaged velocity on top of the canopy. Correlating sedimentation rate with u_{above} (Fig. 7), it can be observed that at HV, u_{above} explained the 80% of the spatial variability (see correlation coefficients) and 50% at MV and LV. Accordingly, our results suggest that the shear stress established at the canopy-water interface can be partly responsible for the sedimentation spatial pattern, and sedimentation was favored because of the reduced shear stress at the leading edge. This hypothesis is supported by Fonseca and Fisher (1986) work, where it was described an increase of shear stress and a decrease of sedimentation probability with distance to the leading edge for *Thalassia testudinum*, *Halodule wrightii* and *Zostera marina* stands. The consideration of u_{above} as a predictor of sedimentation rates at low range of free stream velocity is feasible because, in such a case, the sediment horizontal transport is limited downstream the canopy edge and vertical settlement from the above canopy region become important (Jumars and Nowell 1984). In the case of predominant high free stream velocities (i.e. velocity >0.20 m s^{-1}), velocity reduction is the process that controls sedimentation within canopy (Fonseca et al. 1982) and bottom shear stress would better explain sedimentation patterns (Zong and Nepf 2010).

A remarkable result from our work is the detection of a horizontal threshold behind sedimentation rate reached a minimum. The establishment of a horizontal limit for edge effects on sedimentation processes could be a key factor to improve success on seagrass restoration techniques. This finding could help to take decisions on minimum transplant size or on landscape design (e.g. homogenous vs. patchy transplant designs). At landscape scale, seagrass fragmentation should increase sedimentation capacity due

to the enhanced edge proportions. Consequently, although it is expected a high sedimentation belt around a homogeneous transplant design, patchy design may enhance burial risks because (1) their small patch size, and (2) their high perimeter/area ratio. At any case, it seems that the effects of *C. nodosa* would be a coadjutant in reducing the risk of patch burial, once reached a minimum size, by sediment accretion at the edges and sedimentation avoidance at the patch center.

Our results illustrate the role of *Cymodocea nodosa* on the sediment dynamics of low flow environments, as Cadiz Bay Natural Park (CBNP). At CBNP, tidal velocities are within our experimental range (0 - 0.08 m s^{-1}, Kagan et al. 2003, Lara et al. submitted), although sporadically East wind storms can increase temporally turbidity and relocate the transported sediment (Gutierrez-Mas et al. 1999, 2000). According to our results, velocity increases within 0.03 - 0.065 m s^{-1} range should intensify sedimentation probability precisely when sediment availability is enhanced after wind storm. Hence, our results contribute to explain how shoot density and patch size can improve seagrass resilience to wind storms, which generate sediment resuspension and physically stress to seagrass habitats (Kirkman and Kuo 1990, Preen et al. 1995). The main effect of shoots density and patch size is to buffer wind-induced hydrodynamic forces (van Keulen et al. 2003; Bos and van Katwijk 2007, van Katwijk et al. 2009), but also to reduce the chance of seagrass patch burial by concentrating the deposited sediment at the edge zones.

ACKNOWLEDGEMENTS

This work was supported by the Spanish National Research Project IMACHYDRO (CTM2008-0012/MAR) and by the Andalusian Excellence Research Project FUNDIV P07-RNM-2516. First author is supported by a FPI grant of the Spanish Ministry of Science and Technology.

REFERENCES

Almasi MN, Hoskin CM, Reed JK and Milo J (1987). Effects of natural and artificial Thalassia on rates of sedimentation. J Sediment Res 57(5):901-906.

Brun FG, Vergara JJ, Peralta G, Garcia-Sanchez MP, Hernández I and Pérez-Lloréns JL (2006). Clonal building, simple growth rules and phylloclimate as key steps to develop functional-structural seagrass models. Mar Ecol Prog Ser 323: 133 - 148.

Bouma TJ, van Duren LA, Temmerman S, Claverie T, Blanco-Garcia A, Ysebaert T and Herman PMJ (2007). Spatial flow and sedimentation patterns within patches of epibenthic structures: Combining field, flume and modelling experiments. Cont Shelf Res 27(8):1020-1045.

Bos AR and van Katwijk MM (2007). Planting density, hydrodynamic exposure and mussel beds affect survival of transplanted intertidal eelgrass. Mar Ecol Prog Ser 336:121-129.

Bos AR, Bouma TJ, de Kort GLJ and van Katwijk MM (2007). Ecosystem engineering by anual intertidal seagrass beds: Sediment accretion and modification. Estuar Coast Shelf S 74(1-2):344-348.

Cabaço S, Santos R and Duarte CM (2008). The impact of sediment burial and erosion on seagrasses: A review. Estuar Coast Shelf S 79(3):354-366.

Cabaço S, Ferreira O and Santos R (2010). Population dynamics of the seagrass *Cymodocea nodosa* in Ria Formosa lagoon following inlet artificial relocation. Estuar Coast Shelf S 87(4):510-516.

Chen SN, Sanford LP, Koch EW, Shi F and North EW (2007). A nearshore model to investigate the effects of seagrass bed geometry on wave attenuation and suspended sediment transport. Estuar Coast 30(2):296-310.

de Boer W (2007). Seagrass-sediment interactions, positive feedbacks and critical thresholds for occurrence: a review. Hydrobiologia 591:5-24.

Fonseca MS, Fisher JS, Zieman JC and Thayer GW (1982) Influence of the seagrass, *Zostera marina* L., on current flow. Estuar Coast Shelf S 15: 351-364.

Fonseca MS, Zieman JC, Thayer GW and Fisher JS (1983). The role of current velocity in structuring eelgrass (*Zostera marina* L.) meadows. Estuar Coast Shelf S 17:367-380.

Fonseca MS and Fischer JS (1986). A comparison of canopy friction and sediment movement between four species of seagrass with reference to their ecology and restoration. Mar Ecol Prog Ser 29:15-22.

Gacia E, Granata T and Duarte CM. (1999). An approach to the measurement of particle flux and sediment retention within seagrass (*Posidonia oceanica*) meadows. Aquat Bot 65: 255-268.

Gacia E, Duarte CM, Marbá N, Terrados J, Kennedy H, Fortes M D and Tri N H. (2003). Sediment deposition and production in SE-Asia seagrass meadows. Estuar Coast Shelf S 56 (5-6):909-919.

Gambi MC, Novell, ARM and Jumars PA (1990). Flume observations on flow dynamics in *Zostera marina* (eelgrass) beds. Mar Ecol Prog Ser 61:159-169.

Gutierrez-Mas JM, Lopez-Galindo A and Lopez-Aguayo F (1997). Clay minerals in recent sediments of the continental shelf and the Bay of Cadiz (SW Spain). Clay Miner 32:507-515.

Gutierrez-Mas JM, Sanchez-Bellon A, Achab M, Ruiz Segura J, Gonzalez Caballero JL, Parrado Roman JM and Lopez-Aguayo F (1999). Continental shelf zones influenced by the suspended matter flows coming from Cadiz Bay. Boletin Instituto Español de Oceanografía 15(1-4):145-152.

Gutierrez-Mas JM, Luna del Barco A, Parrado JM, Sanchez E, Fernandez-Palacios A and Ojeda J (2000). Cadiz Bay waters turbidity variations from Landsat TM images analysis. Geogaceta 27:79-82.

Hendriks IE, Bouma TJ, Morris EP and Duarte CM (2010). Effects of seagrass and algae of the *Caulerpa* family on hydrodynamics and particle trapping rates. Mar Biol 157(3):473-481.

Jones CG, Lawton JH and Shachak M (1997). Positive and negative effects of organisms as physical ecosystem engineers. Ecology 78:1946–1957.

Jonsson PR, van Duren LA, Amielh M, Asmus R, Aspden RJ, Daunys D, Friedrichs M, Friend PL, Olivier F, Pope N, Precht E, Sauriau PG and Schaaf E (2006). Making water flow: a

comparison of the hydrodynamic characteristics of 12 different benthic biological flumes. Aquat Ecol 40: 409-438.

Jumars PA and Nowell ARM (1984). Fluid and sediment dynamic effects on marine benthic community structure. Am Zool 24:45-55.

Kagan BA, Alvarez O, Izquierdo A, Mañanes R, Tejedor B and Tejedor L (2003). Weak wind-wave/tide interaction over a moveable bottom: results of numerical experiments in Cadiz Bay. Cont Shelf Res 23(5):435-456.

Kirkman H and Kuo J (1990). Pattern and process in southern Western Australian seagrasses. Aquat Bot 37:367-382.

Koch EW (2001). Beyond light: physical, geological and geochemical parameters as possible submersed aquatic vegetation habitat requirements. Estuaries 24: 1-17.

Morris EP, Peralta G, Brun FG, van Duren L, Bouma TJ and Pérez-Lloréns JL (2008). Interaction between hydrodynamics and seagrass canopy structure: spatially explicit effects on ammonium uptake rates. Limnol Oceanogr 53:1531–1539.

Morris E. P., Peralta G, Benavente J, Freitas R, Rodrigues AM, Quintino V, Alvarez O, Valcárcel-Pérez N, Vergara JJ, Hernández I and Pérez-Lloréns JL (2009). *Caulerpa prolifera* stable isotope ratios reveal anthropogenic nutrients within a tidal lagoon. Mar Ecol Prog Ser 390: 117–128.

Muñoz Pérez JL and Sánchez-Lamadrid A (1994). El medio físico y biológico en la Bahía de Cádiz: Saco interior. Informaciones técnicas, 28/94. pp 49-50, 54-58. Junta de Andalucía. Consejería de Agricultura y Pesca.

Peralta G, van Duren LA, Morris EP and Bouma TJ (2008). Consequences of shoot density and stiffness for ecosystem engineering by benthic macrophytes in flow dominated areas: a hydrodynamic flume study. Mar Ecol Prog Ser 368: 103 – 115.

Peterson CH, Luettich RA Jr, Micheli F and Skilleter GA (2004). Attenuation of water flow inside seagrass canopies of differing structure. Mar Ecol Prog Ser 268:81-92.

Pluntke T and Kozersky HP (2003). Particle trapping on the leaves and on the bottom in simulated submerged plant stands. Hydrobiologia 506-509:575-581.

Preen AR, Lee Long WJ and Coles RG (1995). Flood and cyclone related loss and partial recovery of more than 1000 km^2 of seagrass in Hervey Bay, Queensland, Australia. Aquat Bot 52:3–17.

Siegel S (1970). Non parametric statistics for the behavioral sciences. Mc Graw Hill, pp 195-203.

Schubel JR (1973). Some comments on seagrasses and sedimentary processes. Special report 33, reference 73-12. Chesapeake Bay Institute. The Johns Hopkins University.

Thompson CEL, Amos CL and Umgiesser, G (2004). A comparison between fluid shear stress reduction by halophytic plants in Venice Lagoon, Italy and Rustico Bay, Canada—analyses of in situ measurements. J Mar Syst 51: 293-308.

van der Heide T, van Nes EH, Geerling GW, Smolders AJP, Bouma TJ and van Katwijk MM (2007). Positive feedbacks in seagrass ecosystems: Implications for success in conservation and restoration. Ecosystems 10(8): 1311-1322.

van Katwijk MM, Bos AR, de Jonge VN, Hanssen LSAM, Hermus DCR and de Jong DJ (2009). Guidelines for seagrass restoration: Importance of habitat selection and donor population, spreading of risks and ecosystem engineering effects. Mar Pollut Bull 58:179-188.

van Keulen M, Paling EI and Walker CJ (2003). Effect of planting unit size and sediment stabilization on seagrass transplants in Western Australia. Restor Ecol 11: 50-55.

Zong L and Nepf H (2010). Flow and deposition in and around a finite patch of vegetation. Geomorphology 116(3-4): 363-372.

Zong L and Nepf H (2011). Spatial distribution of deposition within a patch of vegetation. Water Resour Res. 47, W03516.

CHAPTER 3:

Seagrass patches fragmentation, flow and solutes availability.

Effects of intertidal seagrass habitat fragmentation on turbulent diffusion and retention time of solutes

M. Lara[1*], G. Peralta[1], J.J. Alonso[2], E. P. Morris[1,3], V. González-Ortiz[1], J.J. Rueda-Márquez[1], and J. L. Pérez-Lloréns[1]

[1]Department of Biology, Faculty of Marine and Environmental Sciences, University of Cadiz, 11510 Puerto Real (Cadiz), Spain.

[2]Department of Applied Physics, Faculty of Marine and Environmental Sciences, University of Cadiz, 11510 Puerto Real (Cadiz), Spain.

[3]Department of Ecology and Coastal Management, ICMAN-CSIC, Campus de Puerto Real, 11510 Puerto Real (Cadiz), Spain.

Marine Pollution Bulletin (2012), 64:2471-2479

ABSTRACT

An in-depth knowledge of solutes advection and turbulent diffusion is crucial to estimate dispersion area and retention time (t_R) of pollutants within seagrass habitats. However, still it is little known the influence of seagrass habitat fragmentation on such mechanisms. A set of dye tracer experiments and acoustic Doppler velocimeter measurements (ADV) were conducted. Solute transport conditions were compared in between fragmented (FM) vs homogeneous (HM) intertidal meadows, and in vertical gradients (canopy vs overlaying flow). Results showed the highest horizontal diffusion coefficient (K_y, c.a. 10^{-3} m^2 s^{-1}) on FM and at the canopy-water column interface, whereas t_R (2.6-5.6 min) was not affected by fragmentation. These suggest that (1) FM are more vulnerable to pollution events in terms of dispersion area and (2) at low tide, advection rather than turbulent diffusion determines t_R. Furthermore, Taylor's theorem is revealed as a powerful tool to analyze vertical gradients on K_y within seagrass canopies.

INTRODUCTION

An accelerating decline in seagrass habitats has been observed worldwide in recent decades (Waycott et al. 2009). The main causes of these habitat losses are direct or indirect anthropogenic pressures that reduce water quality (Short and Willie-Echeverria 1996, Ralph et al. 2006 and references therein). Anthropogenic activities have augmented coastal nutrient and toxic compound loading, promoting eutrophication (Clavero et al. 1999, Cabaço et al. 2008), and direct toxic effects on seagrasses (Short and Willie-Echeverria 1996, Brun et al. 2002, Macinnis-Ng and Ralph 2003). These disturbances can be persistent over time, as regular wastewater discharges (e.g. Cabaço et al. 2008, Fernandes et al. 2009) or episodic, such as oil spills (Zieman et al. 1984, Dean et al. 1998).

Effective management of both temporal scales of disturbances needs models that can predict seagrass responses to decreasing water quality (Ralph et al. 2006). To provide forecasting, these models should account for both, the area affected by the discharges as well as the residence time of pollutants (Bricker et al. 1999), which requires an in-depth knowledge of solute transport mechanisms in coastal systems. Turbulent diffusion and advection are the main mechanisms for solute transport in coastal systems, and both depend on the local hydrodynamics. Turbulent diffusion (also mentioned in this work as dispersion) is the transport due to stochastic motions of fluid containing solute molecules, whereas advection is the transport due to the unidirectional displacement of a water volume (Csanady 1973, Alonso 2005). Seagrass canopies affect the local hydrodynamics (1) by reducing current velocity within the canopy (Worcester 1995, Koch and Gust 1999) and (2) by increasing turbulence at the top of the canopy (Worcester 1995, Morris et al. 2008). Hence, the effects of seagrass canopies on the

turbulent diffusion and advection of solutes play a decisive role on their response to nutrient loading or toxic pollution.

Solute dispersion within macrophyte canopies has been addressed in several studies with seaweeds (Escartín and Aubrey 1995), seagrasses (Ackerman and Okubo 1993, Worcester 1995, Ackerman 2002), saltmarshes (Serra et al. 2004, Lightbody and Nepf 2006, Zeng et al. 2011) and artificial structures (Nepf et al. 1997, Nepf 1999) revealing that (1) in a horizontal plane, the turbulent diffusion coefficient (K_y) comprises two components, a first one related to the turbulent mixing of flow and a second one due to the lateral movement of fluid at the scale of individual structures (i.e. mechanical diffusion) (Nepf 1999); (2) when compared with non-vegetated areas, submersed canopies decrease, or not affect, turbulent mixing and consequently affecting K_y values (Ackerman and Okubo 1993, Worcester 1995); and (3) mechanical diffusion contributes to higher K_y values than those predicted by turbulent mixing (Nepf 1999, Serra et al. 2004, Lightbody and Nepf 2006).

Despite numerous studies being focused on solute dispersion through macrophyte canopies, very few have explored it at *in situ* conditions (Worcester 1995, Ackerman 2002). *In situ* conditions differ from those of flume tank, or described by models, mainly in (1) landscape configuration (i.e. patchy or homogeneous) and (2) tidal dynamics. Seagrass habitats can occur either as homogeneous or fragmented meadows (e.g. Brun et al. 2003, Sleeman et al. 2005). This can create substantial variance in the velocity field leading to transient-storage or dead-zone dispersion (Nepf and Ghisalberti 2008), suggesting that spatial heterogeneity may represent an additional important component of longitudinal dispersion within natural systems.

As many seagrass species inhabit intertidal regions, changing canopy submergence depths also represent an important factor determining near-bed water renewal rates. During a tidal cycle maximum water velocities occur about midway between high and low water (Bouma et al. 2005). At low tide, especially in beds from shallow sites, the water flow is forced to pass through the seagrass canopy, potentially increasing within canopy water velocities and dead zone dispersion. However, in such a moment, tidal velocity (i.e. advection) is minimum or very low, supporting that solute renewal could also be affected by turbulent diffusion. Under these conditions, patch size may dictate the relative importance of longitudinal advection and turbulent mixing in the water renewal within the canopy (Nepf et al. 2007).

A way to estimate the water renewal rate is to calculate the retention time (t_R). The $t_{R,}$ usually referred as 'flushing time', quantifies the ratio between a tracer mass and its renewal (Orfila et al. 2005), and it can be read as the average time required to displace a solute molecule out of the canopy. Although some t_R values have been estimated for wetland and kelp canopies (Harvey et al. 2005, Nishihara et al. 2011), as far as we know this paper brings the first estimations of t_R within seagrass canopies.

The horizontal dispersion of solutes usually shows a vertical gradient (Ackerman and Okubo 1993). When the water column starts to exceed the canopy height, a layer of high velocity is developed above it to compensate the effects of the velocity reduction within it. Within a seagrass canopy, the water column develops a vertical velocity gradient (e.g. Fonseca and Koehl 2006, Morris et al. 2008), determining a vertical gradient on transport magnitude. For example, within a *Zostera marina* canopy (1 m height), the horizontal diffusion coefficient had been predicted to be 9-fold higher at 0.6 m than at 0.2 m above the bed floor (Ackerman and Okubo 1993).

The aim of this work is to evaluate the role of turbulent diffusion on solute transport within intertidal seagrass landscapes. To cope with this goal, we focus on three specific objectives: (1) to examine the effects of habitat fragmentation (i.e. patchy vs homogeneous meadows) on the horizontal turbulent diffusion coefficient (K_y) and on the advection velocity (U), (2) to estimate the relative importance of turbulent diffusion compared to advection for determining canopy retentions time (t_R), and (3) to examine differences on turbulent diffusion and advection between the overlaying water column and the flow within the canopy. An *in situ* dye tracer technique was applied to address the first two objectives (Worcester 1995), whereas to determine objective 3, K_y was estimated according to Taylor's theorem for a stationary turbulent environment (Csanady 1973, Kundu 1990, Alonso 2005).

MATERIAL AND METHODS

Study site and experimental conditions

The study site was located in Cadiz Bay Natural Park (SW Spain, 36º 28'09''N-6º15'07''W). Cadiz bay has two basins, a shallow basin (inner bay) with 3 m (MLW) depth, and a deep basin (outer bay) with 12 m (MLW) depth (Rueda and Salas, 2003). Field measurements were conducted in the Southwestern corner of the inner bay, in the intertidal zone (> 0.4 m MLW). Two seagrass species thrive in the intertidal zone, *Zostera noltii* Hornem. (from high to mid intertidal elevations) and *Cymodocea nodosa* Ucria (Ascherson) (from mid intertidal to shallow subtidal locations). Experiments were carried out in monospecific stands of *Zostera noltii*.

According to the fragmentation degree, *Z. noltii* populations were classified in fragmented and homogeneous meadows (FM and HM, respectively). To quantify the

degree of patch fragmentation, a meadow fragmentation index (Y) was calculated, where Y is a factor proportional to the probability that the perimeter of a fragmented object would be intercepted, and it is estimated by simulating several random transects across such perimeter (Matern 1964) (eq. 1):

$$Y = \frac{\pi}{2}\frac{n}{M} \qquad \text{(eq. 1)}$$

where n is the number of intercepts with patch edges and M is the total length of the sampling transects. *Zostera noltii* patches with Y values around 3.7 where considered as fragmented meadows (FM), whereas homogeneous cases (HM) exhibited Y values below 0.1 (t-test paired samples: 12.48, p=0.006).

The dye tracer experiments were performed in summer when *Zostera noltii* shoot density is maximum (Brun et al. 2003), at 1-50 min after low spring tides (10/06, 12/06 and 27/07 in 2009; spring tides with 2.19, 1.89 and 2.30 m range, respectively). To analyze vertical gradients of flow during the flooding phase (90 min after low tide), 3D velocity measurements with high spatial and time resolutions were carried out over a homogeneous meadow (25/06/2009, 3 m tidal range, see section "Vertical gradients" below).

As the elevation of the FM and HM habitats was slightly different (≈ 20-40 cm), the onset of flooding was delayed between FM and HM locations every sampling day. To minimize the effects associated to differences in flooding time, tidal flow intensity was checked to be similar between the studied locations. To do so, temporal changes in water level were measured with an accuracy of ± 0.25 cm. Tidal flow intensity was estimated as the water level increase rate calculated as the linear slope of water level vs time. Tidal flow intensity did not show significant differences between FM ($0.8*10^{-4}$ m s^{-1}) and HM ($1*10^{-4}$ m s^{-1}) sites (t-test paired samples: -1.39, p>0.05). Hence, the

existence of significant differences in Y but not on tidal flow intensity implies that hydrodynamic differences between sites can be mainly attributed to habitat fragmentation rather than differences in tidal conditions.

Solute transport

The horizontal coefficient of turbulent diffusion (K_y) within *Zostera noltii* canopies was estimated using a dye-tracking technique developed by oceanographers, modified by Worcester (1995) for vegetated landscapes and standardized by Koch and Verduin (2001) for seagrasses. This consists in the instantaneous release of dye blobs into the water column and taking photographs at timed intervals. Advection was then estimated as the displacement rate of the centroid of the dye, while turbulent diffusion is estimated as the spread rate of the dye.

To apply this technique, a 3D reference system was constructed using graduated PVC poles (1.8 x 3.6 m, Fig. 1). The reference system was oriented parallel to the main tidal flow direction (N-S direction, Lara et al., submitted), allowing vertical and horizontal spatial transformation of the photographs. The dye was a dilution of fluorescein (MERCK, 3 g l^{-1}) prepared with seawater collected *in situ* and at the same time of experimental set up to avoid buoyancy effects (Koch and Verduin 2001). At the beginning of the experiment, the fluorescein solution was released upstream of the leading edge of the patch perpendicular to the main flow.

Digital photographs were taken using a platform located 2 – 3 m away from the dye release point. The position of the camera (1.8 m above bottom) was fixed during the experiments and the angle between the camera and the ground was measured (ɵ, 70-80º). The photographs were captured at 10-30 s time intervals resulting in 20 to 40 images per experiment.

Image and tracer data analysis

Prior to spatial analysis, the photographs were transformed to a planner plane using the *trans-camera view* function for MATLAB (developed by Nobuhito Mori, 2009). This function requires the input of three angles: (1) α or half-view angle (34º), depending on the focal distance; (2) ɵ* or camera elevation angle (35-40º), which was chosen as half ɵ to reduce the loss of the field of view due to transformation; and (3) ϕ or horizontal camera angle from x axis on (x, y) plain (0º).

Transformed images were analysed with the software ImageJ (http://rsb.info.nih.gov/ij, National Institute of Health, USA). The position of the centroid at time t_i ($x_0(t_i)$, $y_0(t_i)$) was estimated on the transformed photographs.

Advection velocity (U, m s^{-1}) at time t_i was calculated as displacement of the centroid over time (i.e. between successive photographs) by:

$$U(t_i) = \frac{\sqrt{(x_0(t_i) - x_0(t_{i+1}))^2 + (y_0(t_i) - y_0(t_{i+1}))^2}}{(t_{i+1} - t_i)} \qquad \text{(eq. 2)}$$

Turbulent kinetic energy (TKE, m^2 s^{-2}) and turbulent intensity (TI) were both estimated from U:

$$TKE = \frac{1}{2}\overline{U'^2} \qquad \text{(eq. 3)}$$

$$TI = \frac{\sqrt{TKE}}{\bar{U}} \qquad \text{(eq. 4)}$$

where U' is the fluctuation from the time-averaged velocity ($\bar{U}$). TI is used as an indicator of the turbulent component on K_y (Nepf 1999, Alonso 2005).

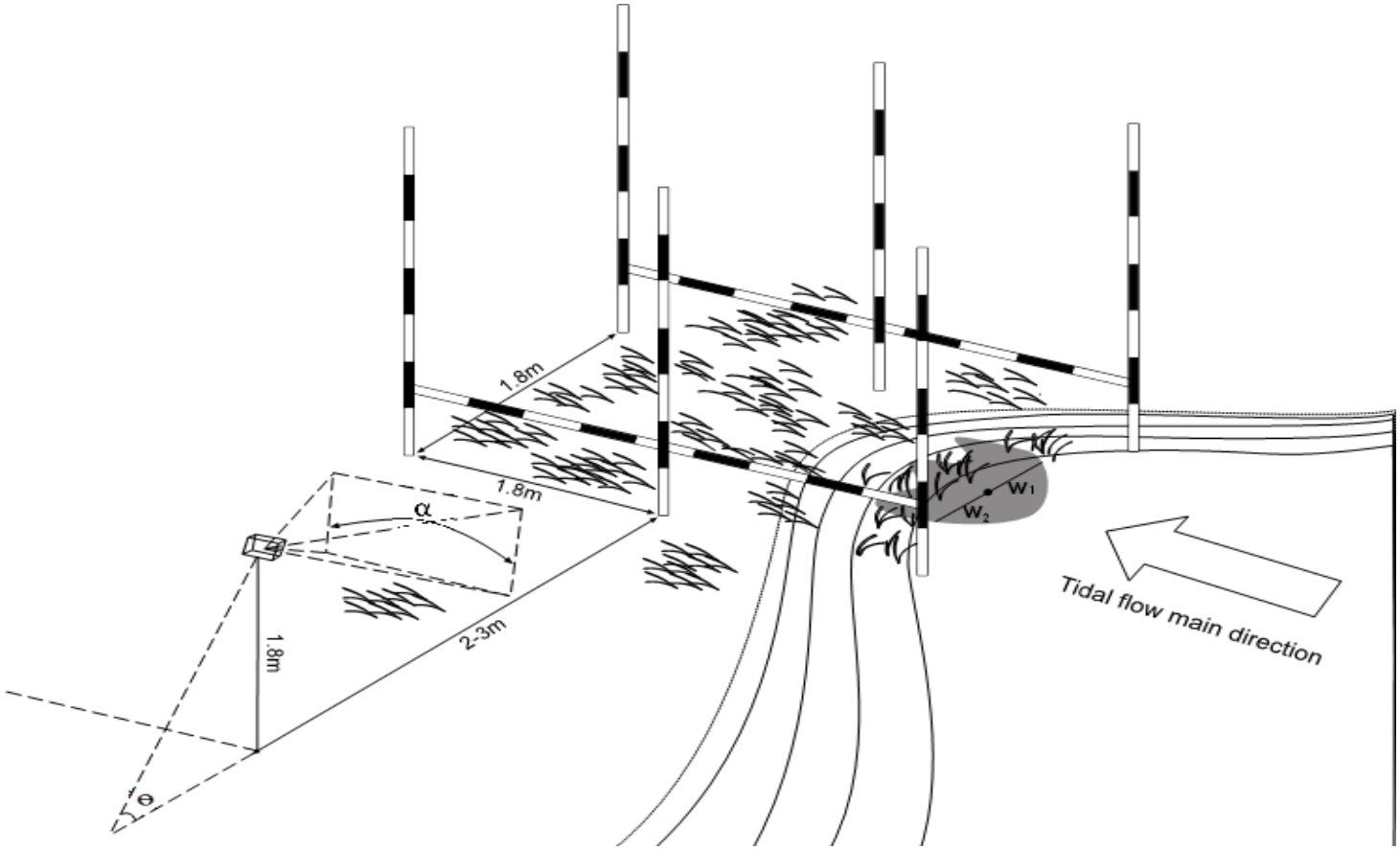

Figure 1. Scheme of dye tracer experiment within fragmented patches of *Zostera noltii* at the inner bay of Cadiz. Camera elevation (θ) and half view (α) angles are indicated.

Turbulent diffusion coefficient (K_y, $m^2\ s^{-1}$) has to be estimated as the increase rate of the variance of dye mass distribution $\left(\frac{d\sigma_w{}^2}{dt}\right)$, what can be simplified as the increase rate of the dye blob radius square ($w^2(t_i)$) (Fig. 2A; Worcester 1995, Alonso 2005).

$$K_y = \frac{1}{2}\frac{d\sigma_w{}^2}{dt} \approx \frac{1}{2}\frac{dw^2(t_i)}{dt} \qquad \text{(eq. 5)}$$

To calculate K_y, (1) only measurements occurring during the lineal increase of w^2 with time were considered (i.e. measurements in between 100 - 400 s for FM and in between 100 - 550 s for HM) and (2) only the perpendicular direction to flow was selected because turbulent diffusion and advection effects cannot be separated in main flow direction. For delimiting flow direction, the centroid was projected in a horizontal plane (x, y), with the flow direction determined by adjusting a linear regression to the positions with time ($x_0(t_i)$, $y_0(t_i)$). The dye blob radius was estimated on perpendicular directions to flow as the averaged distance between the centroid ($x_0(t_i)$, $y_0(t_i)$) and the two extremes of the dye blob, ($x_1(t_i)$, $y_1(t_i)$) and ($x_2(t_i)$, $y_2(t_i)$):

$$\overline{w^2}(t_i) = \frac{((x_1(t_i) - x_0(t_i))^2 + (y_1(t_i) - y_0(t_i))^2) + ((x_2(t_i) - x_0(t_i))^2 + (y_2(t_i) - y_0(t_i))^2)}{2} \qquad \text{(eq. 6)}$$

Solute retention time (t_R, s) was defined as the average time required to displace a solute molecule out of the canopy (Orfila et al. 2005). Values of t_R were estimated using the decay rate in dye concentration. Since the only dye input was the initial release, the dye concentration can be assumed to follow a first order exponential decay (Orfila et al. 2005), allowing t_R estimations as the inverse of the first order turn-over coefficient (C) (Fig. 2B). Relative dye concentration was estimated using the intensity of the blue channel (B_i) of the photographs, which is proportional to the relative dilution of dye (i.e. proportional to the seawater colour intensity). The values of the pixel were averaged

over a 0.9 x 0.9 m^2 section of the reference area, sited on the leading edge of the canopy. Because the RGB channels of photos are non-linear and dependent on view conditions (Stone 2003), the original values of the pixels (p, 0-255) were transformed to a linear colour scale and normalized by the range of the blue intensity on the photographs:

$$B_i = \left(\frac{p}{255} \right)^{\gamma} \quad \text{(eq. 7)}$$

$$\frac{B_i - B_o}{B_{\max} - B_o} = 1 - e^{-Ct} \quad \text{(eq. 8)}$$

$$t_R = \frac{1}{C} \quad \text{(eq. 9)}$$

where p is the original value of pixel, γ is the power coefficient for transforming colour scale (typically γ=2.2; Stone 2003), B_{max} is the blue intensity of seawater without dye and B_o is the initial blue intensity corresponding to the minimum dilution effect.

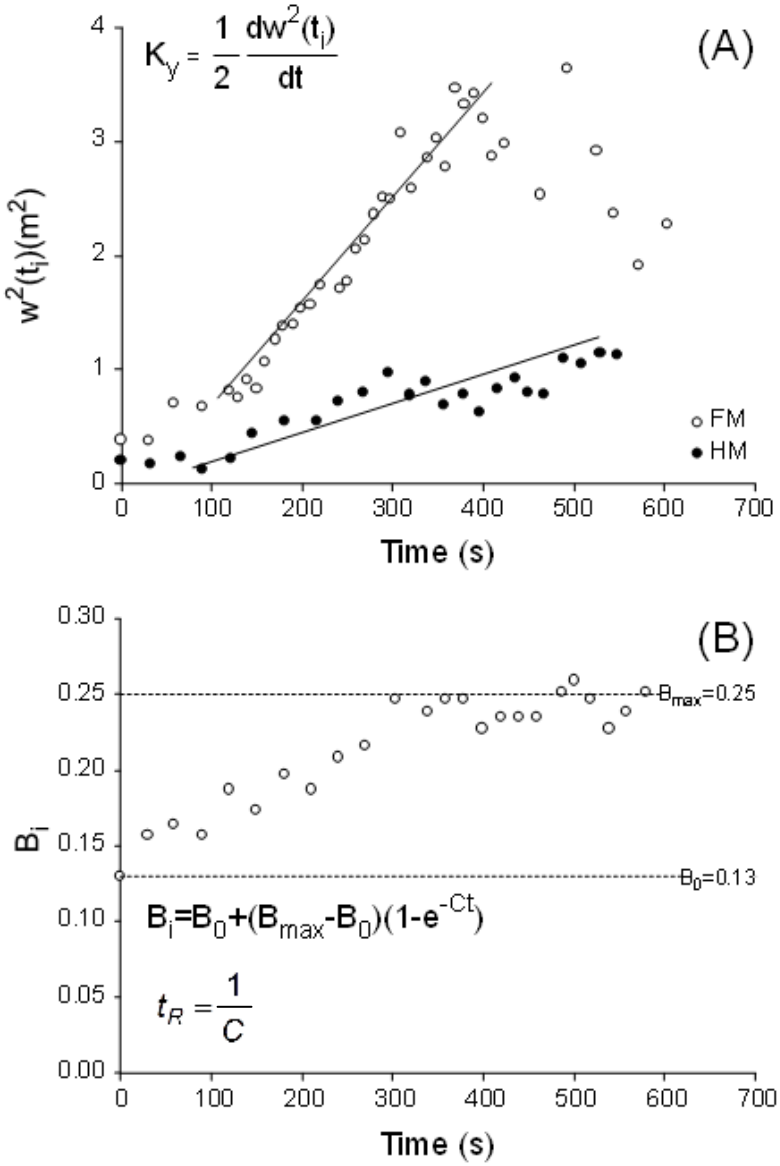

Figure 2. (A) Dye blob width temporal change (w^2, m^2) during the day 12-06-09. (B) Temporal changes on blue intensity (B_i) according to pictures taken on day 27-07-09. Solute retention time (t_R) on *Zostera noltii* patch edges it is estimated as the inverse of the first order turnover coefficient (C) of B_i decay with time.

The Sherwood number (S_h) is a dimensionless number that represents the ratio of convective to diffusive mass transport. In our case, S_h was used to estimate the relative importance of turbulent diffusion versus advection for solute transport. S_h represents the ratio of time required by a particle to move by advection transport in comparison to the time it required to move the same distance by diffusion (Purcell 1977):

$$Sh = \frac{LU}{K_y} \qquad \text{(eq. 10)}$$

where L is a characteristic linear dimension (transport length of the solute). In this study, L was set by the reference system size (approx. 4 m).

Significant differences between FM and HM were assessed using t tests of paired samples for all of the described variables. However, for descriptive purposes, Table I shows mean values and standard deviation.

Vertical gradients of advection and diffusion

Instantaneous velocities were recorded with an acoustic Doppler velocimeter (ADV, Nortek) at three different heights above the bottom floor: (1) inside the canopy (IN, z: 0.075 m), (2) just at the top of the canopy (i.e. at the canopy - water column interface; TOP, z: 0.15 m) and (3) above the canopy (ABOVE, z: 0.25 m). At the end of the velocity measurements, three biomass samples (0.1 x 0.1 m^2) were collected to estimate shoot density± SD (5000±1127 shoots m^{-2}). For each sample, 9 shoots were selected to estimate shoot length ± SD (0.17±0.06 m).

The x-axis was orientated towards the main tidal current direction (clockwise notation, 130º SW and 85º SE). Every sampling point was measured during 180 s at 32 Hz. Data with beam correlations below 70% were filtered (Morris et al. 2008), remaining between 4700 and 5670 data per time series. Once filtered, the horizontal components of the velocity (m s^{-1}) were analysed according to:

$$\mathrm{u} = \bar{u} + u' \qquad \text{(eq. 11)}$$

$$\mathrm{v} = \bar{v} + v' \qquad \text{(eq. 12)}$$

where u and v are the instantaneous velocity components, $\bar{u}$ and $\bar{v}$ are the time-averaged components, and u' and v' are the fluctuation terms. Furthermore, a horizontal module of velocity (U) was also estimated as:

$$U = \sqrt{u^2 + v^2} \qquad \text{(eq. 13)}$$

To calculate the turbulent diffusion coefficient (K_y), Taylor's theorem for stationary turbulent environment was applied. The variance of the blob width of a solute displacing stochastically ($\sigma_y^2(t)$) can be predicted from the autocorrelation function of fluid particle velocity (R (τ), Kundu 1990). In this case, R (τ) was estimated with time-series of the fluctuating term v':

$$\sigma_y^2(t) = 2\overline{v'^2}\int_0^t (t-\tau)R(\tau)d\tau \qquad \text{(eq. 14)}$$

where $\overline{v'^2}$ is the quadratic average of v' and τ is the time lag.

To avoid undesirable effects associated with the presence of periodic components embedded in the velocity, equation 14 was corrected as (Csanady 1973, Alonso 2005):

$$\sigma_y^2(t) = 2\overline{v'^2}\left|-\int_0^t \tau R(\tau)d\tau\right| \qquad \text{(eq. 15)}$$

Finally, K_y was calculated as half value of the slope of the linear part of $\sigma_y^2(t)$ (see eq. 5 above).

RESULTS

Turbulent diffusion and retention time

The dye blob radius (w^2) followed a saturation trend for both FM and HM, although the saturation level for HM led to a different scale (Fig. 2 A). Values of K_y were around 10^{-3} m^2 s^{-1} for both spatial configuration (Table I and Fig. 3A). Although small, K_y differences were significant showing higher values for FM than for HM (Table I).

Under the experimental conditions, patch configuration did not significantly affect to U, TI, S_h or t_R. (Table I). After pooling both FM and HM data no correlation between TI and K_y was found (data not shown, r=-0.4, P=0.22), suggesting that such relationship is specific for each patch configuration. The S_h values were on the range of 10^2 (Fig. 3C), revealing that solute transport was clearly controlled by advection rather than by turbulent diffusion. S_h values for HM were highly dispersed explaining the lack of significant differences with FM (Fig. 3C; Table I). The high variability of t_R (i.e. a coefficient of variation ≈ 51%, Table I), suggests a high sensitivity to temporal changes in transport conditions.

Table I. Mean values (±SD) of turbulent diffusion coefficient (K_y, m^2 s^{-1}), turbulent intensity (TI), horizontal module of velocity (U, m s^{-1}), retention time (t_R, s) and Sherwood number (S_h) within fragmented (FM) and homogeneous (HM) patches of *Zostera noltii*. Last column shows the paired samples t-test when comparing FM and HM. The p-values are indicated in between brackets.

Variable	FM (SD)	HM (SD)	Paired samples t-test
K_y	$4.58x10^{-3}$ ($2.77x10^{-3}$)	$1.32x10^{-3}$ ($1.08x10^{-3}$)	2.99 (*0.048)
TI	1.93 (0.26)	2.45 (0.28)	-2.39 (0.07)
U	0.028 (0.015)	0.031(0.006)	-0.30 (0.40)
t_R	336 (171)	157 (81)	1.46 (0.14)
S_h	32.70 (21.59)	148.57 (115.33)	-2.12 (0.08)

Vertical gradients

The study of a *Zostera noltii* homogeneous meadow when submerged under a 0.5 m of water column revealed a clear stratification of advection (represented by U, Fig. 4). The vertical pattern showed a layer of minimum advection at the canopy-water column interface (TOP, 0.01 m s^{-1}), acting as the interface of two layers of contrasting velocity: (1) a low velocity layer inside the canopy (IN, U = 0.017 m s^{-1}) and (2) a high velocity layer above the canopy (ABOVE, U = 0.035 - 0.044 m s^{-1}). Moreover, U values were homogeneous inside the canopy, but showed a vertical gradient above it, increasing magnitude with distance from the canopy (Fig. 4).

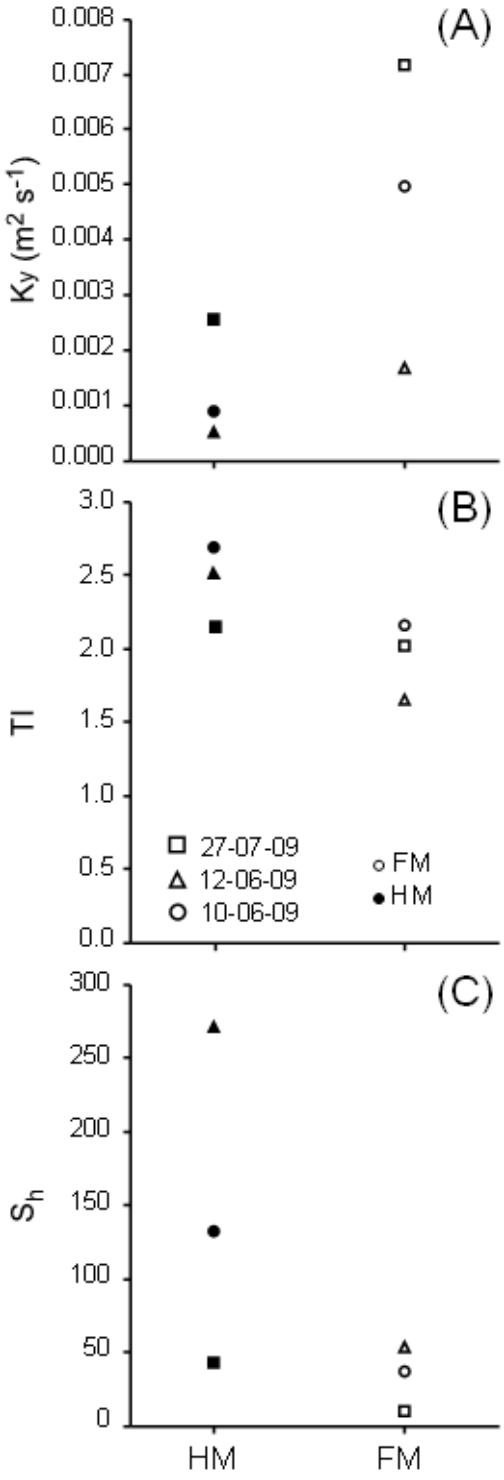

Figure 3. (A) Horizontal turbulent diffusion coefficient (K_y, m^2 s^{-1}) and (B) turbulence intensity (TI) and Sherwood number (S_h) estimated for fragmented (FM) and homogeneous (HM) meadows of *Zostera noltii*.

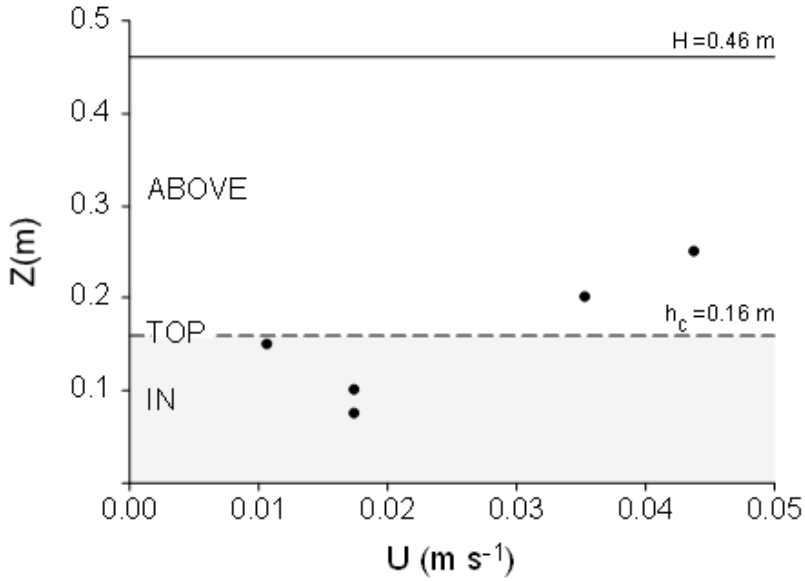

Figure 4. Horizontal velocity (U, m s^{-1}) measured for different vertical positions (z, m) above, on top and inside (IN) of a homogeneous *Zostera noltii* canopy. Canopy (h_c=0.16 m) and water column height (H=0.46 m) are indicated.

Turbulent diffusion transport also showed a vertical gradient when estimated from ADV measurements (Fig. 5). K_y was maximum at top of the canopy (TOP $2.25*10^{-3}$ m^2 s^{-1}) and minimum within it (IN $1.9*10^{-5}$ m^2 s^{-1}). The vertical gradient on K_y suggests a momentum transfer by friction from the water column (ABOVE) to the canopy (IN).

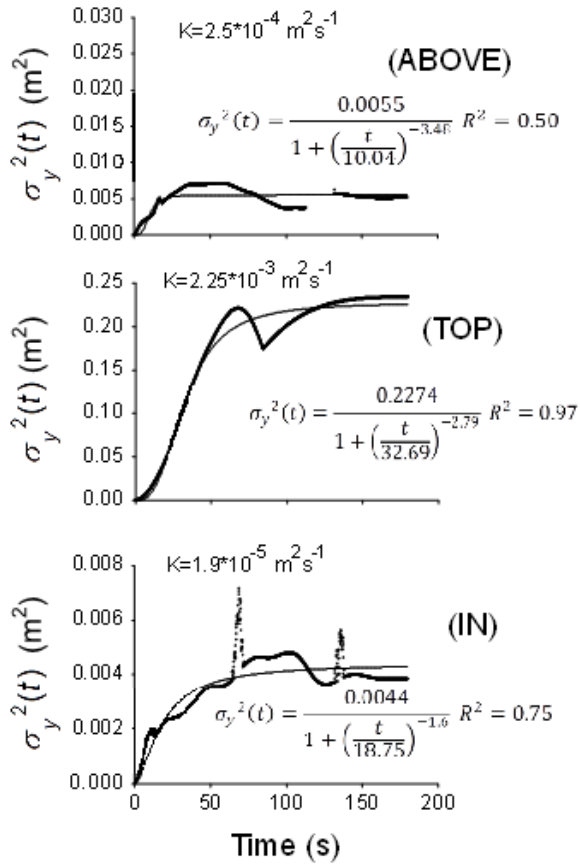

Figure 5. Calculated variance (σ_y^2, m^2) and turbulent diffusion coefficient (K_y, m^2 s^{-1}) from the v' component of velocity by applying Taylor's theorem. Estimations were made for different vertical positions: (1) Inside the canopy (IN), (2) on the interface canopy - water column (TOP) and (3) above the canopy at the free water column (ABOVE), at 0.075, 0.15 and 0.25 m above the bed floor respectively. σ_y^2 versus time was adjusted to a sigmoidal function. Specific sigmoidal equations and corresponding r^2 are indicated.

DISCUSSION

Turbulent diffusion and advection

Dye tracer *in situ* experiments have demonstrated that during the onset of the tidal flooding, habitat fragmentation increases turbulent diffusion within *Zostera noltii* canopies. Although K_y cannot be considered as an intrinsic population parameter (Okubo et al. 2001), and therefore a quantitative relationship between Y and K_y cannot

be estimated, our results demonstrate that habitat fragmentation affects K_y. In a previous field experiment for dye dispersion within *Zostera marina* canopies (also at low current conditions, U <0.05 m s^{-1}), Worcester (1995) described similar K_y values to our estimations (i.e. 10^{-3} m^2 s^{-1}) but without finding differences in the turbulent mixing between vegetated and bare areas, even when Ackerman and Okubo (1993) predicted that *Z. marina* canopies reduce turbulent mixing (75% lower). In our case, (1) shoot density was 25 times higher than in Worcester experiment (5000 vs 200 shoots m^{-2}, respectively), (2) TI values were similar for FM and HM and lower than in Worcester experiment, and (3) a lack of correlation between K_y and TI, suggesting that the mechanical component of the diffusion played a more important role than in previous works. As the influence of the mechanical component is proportional to the density of arrays or elements (i.e. shoot density, Nepf 1999, Serra et al. 2004), the effect of the spatial habitat structure is enhanced when compared to experimental conditions developed by Worcester (1995).

As a consequence of fragmentation effects on turbulent diffusion, the same volume of transported solute during the same time in both types of meadows (i.e. FM and HM) would generate a larger blob area in fragmented sites. Hence, it is expected that fragmentation would favor habitat vulnerability to episodic pollution, since fragmentation increases the area reached by the pollutant. Forecasting dispersion of pollutants within intertidal seagrass habitats requires the combination of knowledge on local hydrodynamics and on landscape configuration, highlighting the need of additional tools as aerial photography or remote sensing (Clark 1993, Pasqualini et al. 1999).

Habitat fragmentation did not affect advection patterns (i.e. no significant differences in U), suggesting that the tidal flow intensity is what determines the local

velocity independently on the seagrass landscape characteristics. Fonseca and Bell (1998) demonstrated *in situ* that high water velocity (0.1 - 0.4 m s^{-1}) can determine the seagrass landscape configuration (i.e. size, shape and pattern of seagrass patches). The effects of seagrasses on velocity patterns have only been demonstrated at scale of canopy (Peterson et al. 2004, Fonseca and Koehl 2006, Morris et al. 2008) although physical models evidenced such modification at the scale of landscape (Luhar et al. 2008). For *Zostera noltii* meadows thriving in Cadiz bay a tide-controled advection would be more favourable than an habitat structure-control advection, since tides allow the water turn-over of this shallow system in 0.5 – 1 day (table II), diluting efficiently the polluters. Nevertheless, further research during different tidal phases is needed to fully understand the effects of seagrass landscape on transport processes.

Despite the relative contribution of turbulent diffusion to canopy solutes renewal should be relatively high when current velocity is minimum or low, our results show that the advection dominates the renewal of solutes at the scale of canopy (S_h around 100). For a canopy with a height (H) 25-fold times shorter than its length (L) as our case (L = 4 m and H = 0.16 m), advection would dominate the solute renewal (Nepf et al. 2007). Morris et al. (2008) also demonstrated in a flume tank that advection controls the renewal of nutrients in *Zostera noltii* canopies. However, processes occurring within a seagrass canopy have many characteristic lengths (Koch et al. 2006). For example, within emergent canopies as our case, stem-scale type is the dominating turbulence process (i.e. 10^3-10^4 µm, Nepf et al. 1997). Therefore, the K_y values here found are also valid for processes at the scale of leaves (e.g. those affecting the pollutant partition along leaf area). The values of K_y and U with L=10^{-3} - 10^{-2} m generate a range of S_h between 0.1 and 1, so solute transport at the scale of leaf area will be dominated by diffusion rather than by advection. It would determine which epiphytes species

colonizing seagrass leaves are most exposed to pollution, because epiphyte community composition changes vertically along leaf (Reyes et al. 1998).

Retention time of solutes

Since under our experimental conditions, advection seems to control solute renewal within seagrass canopies and U was not affected by landscape configuration, retention time (t_R) was also unaffected by landscape configuration. For long-lasting pollutants, like some heavy metals (Prange and Dennison 2000), the t_R can be decisive to determine the local toxic dosage because the fast flushing away of the pollutant may reduce the exposition. Although our results suggest that t_R is independent of landscape configuration, extrapolation to the entire landscape still has to be done carefully, since this study is specifically focused on the leading edge and these areas are relatively permeable to flow, being the velocity on the leading edge higher than downstream the canopy (Peterson et al. 2004, Morris et al. 2008).

Several studies have previously estimated t_R within macrophyte canopies by different techniques (Table II). Whereas previous works directly measured tracer concentration (ie. sodium bromide or fluorescein), the present study used an indirect method by analyzing color intensity on photographs of the spatial and temporal dye evolution. Color intensity conversion to relative dye concentration has been successfully applied in previous works on flow in soils (Persson 2005), coastal diffusion (Bezerra et al. 1998) and artificial canopies (Ghisalberti and Nepf 2006). Such conversion allows a complete record of dilution effects without sophisticated artifacts obstructing dye transport.

In our case, the color intensity fits well and significantly to a theoretical exponential decay ($P<0.0001$, $R^2>0.70$), supporting that this variable is a good indicator to describe dye dilution on time. Our t_R estimations are within the range of previous

data (Table II). The high t_R values on wetland (i.e. 53 min) and *Posidonia oceanica* habitats (i.e. 14.5 – 30 days), when compared with *Zostera noltii* ones (2.6 – 3.6 min), can be consequence of the spatial scale tested (11 m^3 for wetland and $7.9*10^6$ m^3 for *P. oceanica* versus 0.14 m^3 for *Z. noltii*). In fact, when t_R is estimated at the inner Cadiz Bay spatial scale, the value increases to 0.5 - 1 day (table II). On the contrary, despite of a large spatial scale tested (i.e. 6 m^3), kelp canopies generate small t_R (i.e. 0.93 min, Orfila et al. 2005, table II). This can be explained by the dominance of waves, since kelp canopies thrive in exposed coastal environments and orbital flow opens up the canopies, increasing the vertical mixing in comparison to the unidirectional flow (Koch et al. 2006).

To detect physical limitation on nutrient uptake, the t_R values are compared with the corresponding theoretical time required for nutrient uptake (t_{Up}, table II). If t_R has larger values than t_{Up}, then physical limitation on nutrient uptake is expected (Kregting et al. 2011). The t_{Up} was estimated using averaged values of *Zostera noltii* leaf biomass, assuming that both ammonium and phosphate follows first order uptake kinetics (Pérez-Lloréns and Niell 1995, Alexandre et al. 2010). This assumption is reasonable for Cadiz

Table II. Retention time values (t_R) for macrophyte canopies at different spatial scale, under different conditions. Volume scale (m^3) is indicated. For comparison, theoretical nutrient uptake time values (t_{Up}) for *Zostera noltii* canopies are also included.

Retention time (t_R)					
t_R	Canopy type / System	Volume scale (m^3)	Tracer / Method of estimation	Conditions	Reference
2.61-5.6 min	Patch edges of *Zostera noltii* (Inner Cadiz Bay)	0.14	Fluorescein	Spring tides	Present study
14.5-30 day	Port of Cabrera, inhabiting *Posidonia oceanica* meadows	7.9×10^6	Simulated neutrally buoyant particles	Sea breeze- driven mixing. Summer stratification	Orfila et al. (2005)
0.5-1 day	Inner Cadiz Bay, inhabiting *Zostera noltii* meadows	8.5×10^7	Inflow/outflow rate	Average tidal flow	Benavente et al. (2011)
0.93 min	Kelp canopy of *Sargassum fusiforme*	6	Fluorescein	High wave energy	Nishihara et al. (2011)
53 min	Canopy of *Eleocharis* sp.+ *Utricularia* sp. (wetlands)	11	Sodium bromide	Unidirectional flow	Harvey et al. (2005)

Uptake time (t_{Up})				
t_{Up} (min)	Solute	Concentration range (µM)	AB (g DW m^{-2})	References
36.8	NH_4^+	0.5-3	277	Alexandre et al. (2010)
10	PO_4^{3-}	0.1-0.7		Pérez-Llorens and Niell (1995)

AB: Average of measured aboveground biomass

Bay since ammonium and phosphate concentrations are usually low ($[NH_4^+]$≈0.5-3 µM and $[PO_4^{3-}]$ ≈ 0.1-0.7 µM, De los Santos et al., unpublished data). In our case, t_{Up} for ammonium (36.8 min) and phosphate (10 min) were higher than t_R within *Z. noltii* patch edges (2.6 – 5.6 min), suggesting that nutrient uptake is not physically limited by solutes renewal at the leading edge of these patches. This statement is supported by Morris et al. (2008), who demonstrated in a flume tank that seagrass leading edges are active uptake zones.

Vertical gradients

When water column exceeded 2.8 times the canopy height, advection and turbulent diffusion patterns within *Zostera noltii* canopies were vertically stratified on three layers (i.e. ABOVE, TOP and IN). The increase of velocity above the canopy is a process frequently described when water column exceeded more than two times the canopy height (H/h > 2, Fonseca and Koehl 2006, Morris et al. 2008, Peralta et al. 2008). The canopy-water column interface (TOP) was the most active zone for turbulent diffusion (i.e. K_y coefficient was 100-fold higher than inside canopy). This is explained by turbulent momentum dissipation from the ABOVE layer (Ackerman 2002, Nepf and Ghisalberti 2008). Delay on saturation of mass distribution variance at the canopy-water column interface (TOP, Fig. 5) suggested that large-scale eddies were contributing to the vertical mixing between ABOVE and IN layers (Nepf and Ghisalberti 2008).

Hence, solute transport will be maximum when the source is located close to canopy- water column interface (TOP), but it will be limited when the source is inside the canopy, as the pattern described for seagrass pollen dispersion (Ackerman 2002). According to the vertical gradient, there are two layers with clear differences on solute

transport: (1) water column above the canopy, and (2) within the canopy. The transport above the canopy is rapid and dependent on current velocity, whereas within the canopy, solute transport is slow and local. The slow transport layer affects to solutes resuspended from the sediment (e.g. heavy metals and nutrients, Ralph et al. 2006). For cases where the source is within the slow transport layer, the dispersion of solute to the scale of the entire meadow needs to be mediated by previous vertical transport to TOP (or ABOVE) layer. This vertical transport is feasible by vertical secondary flows (Nepf and Koch 1999), and can be favored by benthic biological structures (Friedrichs et al. 2009).

CONCLUSIONS

In summary, this study provides central keys to forecast pollutant transport within an intertidal seagrass landscape. Under emergent conditions, habitat fragmentation increases horizontal diffusion coefficient, indicating that fragmentation may enhance seagrass vulnerability to pollution because a larger area of habitat will be affected. However, advection dominates solute transport at the patch spatial scale, being this type of transport not affected by fragmentation. As a consequence, solute retention times were similar in fragmented and homogeneous meadows, being both habitats susceptible of exposition to pollutants during the same time. When water column exceeded 2.8 times the canopy height, flow was stratified in three layers, distinguishing two contrasting regions for solute transport: rapid transport above the canopy, slow transport inside the canopy, and a canopy – water column interface where turbulent diffusion coefficient is maxima.

ACKNOWLEDGEMENTS

This work was supported by the Spanish National Research Projects EVAMARIA (CTM2005-00395/MAR), IMACHYDRO (CTM2008-0012/MAR) and by the Andalusian Excellence Research Project FUNDIV P07-RNM-2516. First author is supported by a FPI grant of the Spanish Ministry of Science and Technology.

REFERENCES

Ackerman JD and Okubo A (1993). Reduced mixing in a marine macrophyte canopy. Funct Ecol 7(3): 305-309.

Ackerman JD (2002). Diffusivity in a marine macrophyte canopy: Implications for submarine pollination and dispersal. Am J Bot 89(7): 1119-1127.

Alexandre A, Silva J and Santos R (2010). Inorganic nitrogen uptake and related enzymatic activity in the seagrass *Zostera noltii*. Mar Ecol 31:539-545.

Alonso JJ (2005). Oceanografía ambiental: Física de la difusión turbulenta en el océano, first ed. Editorial Tébar, Madrid (Spain).

Benavente J, Del Río L, Plomaritis T and Gracia J (2011). Características físicas de la marea en la Bahía de Cádiz. El caso de las grandes mareas de marzo de 2011. In: Consejería de Medio Ambiente, Junta de Andalucía (eds.). El Parque Natural Bahía de Cádiz, donde las mareas funden tierra y mar, pp 95-101.

Bezerra MO, Diez M, Medeiros C, Rodríguez A, Bahia E, Sanchez-Arcilla A and Redondo JM (1998). Study on the Influence of Wave on Coastal Diffusion Using Image Analysis. Appl Sci Res 59:191-204.

Bricker SB, Clement CG, Pirhalla DE, Orlando SP and Farrow DRG (1999). National Estuarine Eutrophication Assessment: Effects of Nutrient Enrichment in the Nation's Estuaries. NOAA, National Ocean Service, Special Projects Office and the National Centers for Coastal Ocean Science. Silver Spring, MD.

Brun FG, Hernández I, Vergara JJ, Peralta G and Pérez-Lloréns JL (2002). Assessing the toxicity of ammonium pulses to the survival and growth of *Zostera noltii*. Mar Ecol Prog Ser 225: 177–187.

Brun FG, Pérez-Lloréns JL, Hernández I and Vergara JJ (2003). Patch distribution and within-patch dynamics of the seagrass *Zostera noltii* Hornem in Los Toruños Salt-Marsh, Cádiz Bay, Natural Park, Spain. Bot Mar 46:513-524.

Bouma TJ, De Vries MB, Low E, Kusters L, Herman PMJ, Tanczos IC, Temmerman S, Hesselink A, Meire P and van Regenmortel S (2005). Flow hydrodynamics on a mudflat and in salt marsh vegetation: identifying general relationships for habitat characterizations. Hydrobiologia 540: 259-274.

Cabaço S, Machás R, Vieria V and Santos R (2008). Impacts of urban wastewater discharge on seagrass meadows (*Zostera noltii*). Est Coast Shelf S 78:1-13.

Clark CD (1993). Satellite remote sensing of marine pollution. Int J Remote Sens 14(16):2985-3004.

Clavero V, Izquierdo JJ, Palomo L, Fernández JA and Niell FX (1999). Water management and climate changes increases the phosphorus accumulation in the small shallow estuary of the Palmones river (southern Spain). Sci Total Environ 228(2-3): 193-202.

Csanady GT (1973). Turbulence diffusion in the environment. D. Reidel Publishing Company, Dordrecht (Holland).

Dean TA, Stekoll MS, Jewett SC, Smith RO and Hose JE (1998). Eelgrass (Zostera marina L.) in PrinceWilliam Sound, Alaska: Effects of the Exxon Valdez oil spill. Mar Pollut Bull 36: 201–210.

Escartín J and Aubrey DG (1995). Flow structure and dispersion within algal mats. Est Coast Shelf S 40:451-472.

Fernandes M, Bryars S, Mount G and Miller D (2009). Seagrasses as a sink for wastewater nitrogen: The case of the Adelaide metropolitan coast. Mar Pollut Bull 58:290-311.

Fonseca MS and Bell SS (1998). Influence of physical setting on seagrass landscapes near Beaufort, North Carolina, USA. Mar Ecol Prog Ser 171:109-121.

Fonseca MS and Koehl MAR (2006). Flow in seagrass canopies: the influence of patch width. Est Coast Shelf S 67:1-9.

Friedrichs M, Leipe T, Peine F and Graf G (2009). Impact of macrozoobenthic structures on near-bed sediment fluxes. J Marine Syst 75 (3-4):336-347.

Ghisalberti M and Nepf H (2006). Mass transport in vegetated shear flow. Environ Fluid Mech 5(6):527-551.

Harvey JW, Saiers JE and Newlin JT (2005). Solute transport and storage mechanisms in wetlands of the Everglades, south Florida. Water Resour Res 41, W05009.

Kregting LT, Stevens CL, Cornelisen CD, Pilditch AP and Hurd CL (2011). Effects of a small-bladed macroalgal canopy on benthic boundary layer dynamics: Implications for nutrient transport. Aquat Biol 14:41-56.

Koch EW and Gust G (1999). Water flow in tide- and wave-dominated beds of the seagrass *Thalasia testudinum*. Mar Ecol Prog Ser 184:63-72.

Koch EW and Verduin JJ (2001). Measurements of Physical Parameters in Seagrass Habitats. In: Short, F.T. and Coles, R.G. Global Seagrass Research Methods. Elsevier Science B.V., pp.325-344.

Koch EW, Ackerman J, van Keulen M and Verduin J (2006). Fluid Dynamics in Seagrass Ecology: from Molecules to Ecosystems. In: Larkum, A.W.D., R.J. Orth and C.M. Duarte (eds), Seagrasses: Biology, Ecology and Conservation. Springer Verlag, pp 193-225.

Kundu PK (1990). Fluid Mechanics, first ed. Academic Press, San Diego (California).

Lightbody A and Nepf H (2006). Prediction of velocity profiles and longitudinal dispersion in emergent salt marsh vegetation. Limnol Oceanogr 51(1):218-228.

Luhar M, Rominger J and Nepf H (2008). Interaction between flow, transport and vegetation spatial structure. Environ Fluid Mech 8:423-439.

Matern B (1964). A method for estimating the total length of roads by means of a line survey. Stud For Suec 185:68-70.

Morris EP, Peralta G, Brun FG, van Duren L, Bouma TJ. and Perez-Llorens JL (2008). Interaction between hydrodynamics and seagrass canopy structure: spatially explicit effects on ammonium uptake rates. Limnol Oceanogr 53: 1531–1539.

Nepf H, Sullivan J and Zavistoski R (1997). A model for diffusion within emergent vegetation. Limn Oceanogr 42(8):85-95.

Nepf H (1999). Drag, turbulence, and diffusion in flow through emergent vegetation. Water Resour Res 35(2):479-489.

Nepf H and Koch EW (1999). Vertical secondary flows in submersed plant-like arrays. Limnol Oceanogr 44(4):1072-1080.

Nepf H, Ghisalberti M, White B and Murphy E (2007). Retention time and dispersion associated with submerged aquatic canopies. Water Resour Res 43, W04422.

Nepf H and Ghisalberti M (2008). Flow and transport in channels with submerged vegetation. Acta Geophys 56 (3):753-777.

Nishihara GN, Terada R and Shimabukuro H (2011). Effects of wave energy on the residence times of a fluorescent tracer in the canopy of the intertidal marine macroalgae, *Sargassum fusiforme* (Phaeophyceae). Phycol Res 59:24-33.

Okubo A, Ackerman JD and Swaney DP (2001). Pasive Diffusion in Ecosystems. In: Okubo A. and Levin S.A. (eds). Diffusion and Ecological Problems. Modern Perspectives. Springer-Verlag, New York, pp 31-105.

Orfila A, Jordi A, Basterretxea G, Vizoso G, Marbà N, Duarte CM, Werner FE and Tintoré J (2005). Residence time and *Posidonia oceanica* in Cabrera Archipielago National Park, Spain. Cont Shelf Res 25:1339-1352.

Pasqualini V, Pergent-Martini C and Pergent G (1999). Environmental impact identification along the Corsican coast (Mediterranean Sea) using image processing. Aquat Bot 65:311–320.

Peralta G, van Duren LA, Morris EP and Bouma TJ (2008). Consequences of shoot density and stiffness for ecosystem engineering by benthic macrophytes in flow dominated areas: a hydrodynamic flume study. Mar Ecol Prog Ser 368:103 – 115.

Pérez-Lloréns JL and Niell FX (1995). Short-term phosphate uptake kinetics in *Zostera noltii* Hornem: a comparison between excised leaves and sediment-rooted plants. Hydrobiologia 297(1):17-27.

Persson M (2005). Accurate dye tracer concentration estimations using image analysis. J Soil Sci Soc Am 69:967-975.

Peterson CH, Luettich RA Jr, Micheli F and Skilleter GA (2004). Attenuation of water flow inside seagrass canopies of differing structure. Mar Ecol Prog Ser 268:81-92.

Prange JA and Dennison WC (2000). Physiological responses of five seagrasses species to trace metals. Mar Pollut Bull 41(7-12):327-336.

Purcell EM (1977). Life at low Reynolds number. Am J Physics 45: 3-11.

Ralph JP, Tomasko D, Moore K, Seddon S and Maccinis-Ng CMO (2006). Human impacts on seagrasses: Eutrophication, sedimentation, and contamination. In: Larkum, A. W. D. et al. (Eds.), Seagrasses: Biology, Ecology and Conservation. Springer, Netherlands, pp. 567–593.

Reyes J, Sanson M and Alfonso-Carrillo J (1998). Distribution of the epiphytes along the leaves of *Cymodocea nodosa* in the Canary Islands. Bot Mar 41:543-551.

Rueda JL and Salas C (2003). Seasonal variation of a molluscan assemblage living in a *Caulerpa prolifera* meadow within the inner Bay of Cadiz (SW Spain). Estuar Coast Shelf Sci 57:909-918.

Serra T, Harindra JSF and Rodríguez RV (2004). Effects of emergent vegetation on lateral diffusion in wetlands. Water Res 38:139-147.

Short FT and Wyllie-Echeverria S (1996). Natural and human induced disturbance of seagrasses. Environ Conserv 23:17–27.

Sleeman JC, Kendrich GA, Boggs GS and Hegge BJ (2005). Measuring fragmentation on seagrass landscapes: which indices are most appropriate for detecting change? Mar Freshwater Res 56(6):851-864.

Stone M (2003). Field Guide to Digital Color. A. K. Peters. Natick, MA (USA).

Waycott M, Duarte CM, Carruthers TJB, Orth R.J., Dennison WC, Olyarnik S, Calladine A, Fourqurean JW, Heck K Jr, Hughes AR, Kendrick GA, Kenworthy WJ, Short FT and Williams SL (2009). Accelerating loss of seagrasses across the globe threatens coastal ecosystems. PNAS 106(30):12377-12381.

Worcester SE (1995). Effects of eelgrass beds on advection and turbulent mixing in low current and low shoot density environments. Mar Ecol Prog Ser 126:223-232.

Zeng L, Chen GQ, Tang HS and Wu Z (2011). Environmental dispersion in wetland flow. Commun Nonlinear Sci 16(1):206-215.

Zieman JC, Orth R, Phillips RC, Thayer G and Thorhaug A (1984). The effects of oil on seagrass ecosystems. In: Cairns, J. and Buikema, A.L. (eds), Restoration of Habitats Impacted by Oil Spills, Butterworth, Boston, pp. 37–64.

DISCUSSION

1. Hidrodinámica y paisaje vegetal bentónico

La interacción entre la vegetación bentónica y la hidrodinámica es un aspecto clave para el funcionamiento de este tipo de comunidades, así como para todos los procesos ecológicos determinados o condicionados por el flujo de la corriente, tales como la deposición de partículas, la estabilidad del sustrato, o la renovación e incorporación de nutrientes (Koch 2001, Thomas and Cornelissen 2003, Bouma et al. 2007, Gruber and Kemp 2010).

A nivel de paisaje, la retroalimentación entre dichos procesos, el desarrollo de los doseles y los efectos hidrodinámicos asociados pueden modular la estructura espacial de las manchas de vegetación en un mecanismo auto-organizativo (van der Heide et al. 2010). Así, se ha demostrado una relación muy estrecha entre el espectro de tamaños de mancha y el régimen hidrodinámico dominante, de manera que un elevado flujo de corriente (i.e. >0.25 m s^{-1}) restringe su grado de agregación (Fonseca and Bell 1998). Esta limitación está determinada fundamentalmente por la constricción erosiva ejercida en la periferia de las manchas a través de pasillos desnudos de alta turbulencia (Fonseca and Koehl 2006), la cual (1) impide el asentamiento de nuevos haces (van der Heide 2010), y (2) promueve diferencias de relieve que favorecen la propia erosión lateral (Fonseca et al. 1982).

Los resultados obtenidos en la presente Tesis Doctoral apuntan, sin embargo, a que en las praderas de *Zostera noltii* del saco interno de la bahía de Cádiz no impera tal mecanismo, al ser una especie estabilizadora del sedimento incluso con bajas densidades de haces (Peralta et al. 2008). El flujo mareal en doseles de esta especie durante periodos de marea viva (1) presentó velocidades inferiores en magnitud a los umbrales estimados por Bouma et al. (2009 a) para la generación de micro-depresiones

(i.e. 0.03 versus 0.3 m s^{-1}), pero además (2) no hubo diferencias significativas entre los valores registrados en praderas continuas y en praderas dispersas o fragmentadas. A este hecho hay que unirle el que no se detectara limitación hidráulica de recursos en las zonas de borde, factor decisivo para la expansión clonal de las manchas porque en los haces apicales (mayoritarios en la periferia, Brun et al. 2003) la demanda de nutrientes es comparativamente superior a la de otro tipo de haces (Marbá et al. 2002). La presión marisquera, junto con la dinámica natural de crecimiento centrífugo y colonización rizomática son, por tanto, las principales causas modeladoras del paisaje de manchas de *Z. noltii* (Brun et al. 2003, Cabaço et al. 2005). Sin embargo, en las praderas intermareales del saco externo de la bahía de Cádiz el flujo de marea es mucho más intenso (e.g. 0.05-0.3 m s^{-1}, Brun et al. 2009, incluso 1 m s^{-1} en canales de marea, González et al. 2010), y parece existir una correlación entre la distribución espacial de las manchas y la presencia de pequeños montículos de sedimento (Peralta et al. investigación en curso).

A su vez, los principales atributos del paisaje vegetal bentónico, tales como el tamaño de las manchas (i.e. altura y extensión horizontal, Fonseca et al. 1983, Fonseca and Fischer 1986), el grado de fragmentación (Folkard 2005, Luhar et al. 2008), la microtopografía (Fonseca et al. 1983, Carpenter and Williams 1993) o las transiciones entre praderas de macrófitos con propiedades físicas claramente distintas (e.g. morfometría, demografía y flexibilidad) pueden incidir directamente en los patrones locales de velocidad y turbulencia. Uno de los efectos más notables del tamaño de las manchas es el que tiene sobre el re-direccionamiento y aceleración del flujo por encima del dosel, proceso que suele recibir menos atención en la bibliografía que la atenuación interior de la corriente (e.g. Granata et al. 2001, Peterson et al. 2004, Laccie and Willie-Echeverria 2011). Este proceso incrementa el estrés de fricción en la columna de agua

(Fonseca et al. 1982) y en consecuencia, tal y como se describe en el capítulo 2, puede resultar un impedimento a la deposición de partículas, favoreciendo que las máximas tasas se localicen en las zonas de borde. Trabajando en tanque de flujo con una pradera artificial de *Cymodocea nodosa* (0.03 y 0.065 m s^{-1}), los valores de aceleración de la corriente muestran claramente un incremento inicial y posterior asíntota con el tamaño de la mancha (Fig.1), a la vez que un aumento con su altura relativa, la cual se reduce debido al doblamiento de los haces (Fig. 1, y capítulo 2 Fig. 3A).

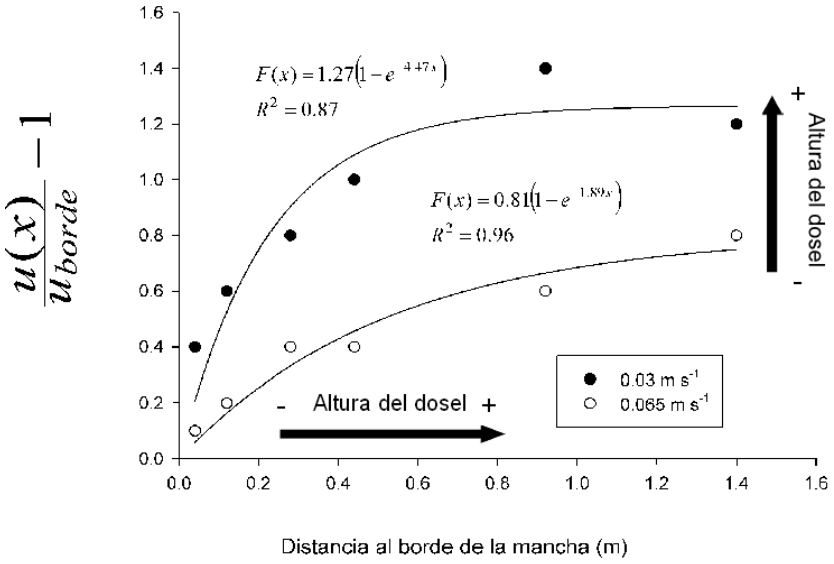

Figura 1. Aceleración del flujo por encima de una mancha artificial de *Cymodocea nodosa* como función de (1) la distancia horizontal al borde (corriente abajo) y (2) la velocidad libre (0.03 versus 0.065 m s^{-1}). Las velocidades están medidas en tanque de flujo, a 40 cm del fondo, tal y como se describe en el capítulo 2. Nótese la asociación positiva de la aceleración con la altura relativa del dosel, la cual puede reducirse tanto con el aumento de la velocidad libre como con la cercanía al borde de la mancha.

La estabilización de la aceleración de la corriente por encima del dosel a partir de un tamaño de la mancha puede explicarse indirectamente a partir de la combinación de los modelos actuales de reducción interior del flujo y la ley de continuidad, los cuales (1) también deducen un comportamiento exponencial negativo de la velocidad (Fig. 1), y (2) permiten predecir tamaños críticos de mancha para la estabilización de la corriente

(Abdelrhaman 2003, Peterson et al. 2004). El tamaño crítico de mancha oscila empíricamente entre 10 y 50 veces la altura del dosel (Granata et al. 2001, Hendriks et al. 2010), aunque hasta la fecha no existe ninguna recopilación de datos de campo que pueda corroborar una regla general. Además, las diferencias interespecíficas en biomecánica (Fonseca et al. 2007, De los Santos 2011), demografía y morfometría (Morris et al. 2008, Hendriks et al. 2010) dificultan *a priori* esa labor.

Los valores de aceleración del flujo obtenidos *in situ* para *Cymodocea nodosa* (capítulo 1), normalizados por la distancia horizontal de medida, a pesar de ser inferiores que los obtenidos en tanque de flujo, resultaron ser incluso más elevados que en el caso de otras especies tales como *Posidonia oceanica* o *Zostera novazelandica* (Fig. 2). El meta-análisis junto con medidas *in situ* de diversos estudios (Granata et al. 2001, Peterson et al. 2004, Bryan et al. 2007, Heiss et al. 2010) muestra una correlación positiva del factor de aceleración con la altura de la mancha en proporción a la profundidad (Fig. 2a). Sin embargo, no se observa correlación significativa con la densidad de haces (Fig. 2b), a pesar de que la distribución vertical de la luz induce a que la densidad de las praderas disminuya con la profundidad (Duarte 1991, Pergent et al. 1995). Este resultado preliminar sugiere que, a lo largo de una zonación costera completa, los factores de hábitat (profundidad y condiciones de marea) podrían ser más determinantes sobre los gradientes horizontales de velocidad en las manchas que su propia permeabilidad. Además, para praderas 10 veces menores que la profundidad de la columna de agua apenas se registra aceleración del flujo (Fig. 2a), estableciéndose en cambio un régimen hidrodinámico donde predomina el intercambio turbulento vertical (Nepf and Vivoni 2000). Dicho umbral de tamaño discrimina, por tanto, entre dos situaciones hidrodinámicas particulares del bentos de la región mediterránea (Short et

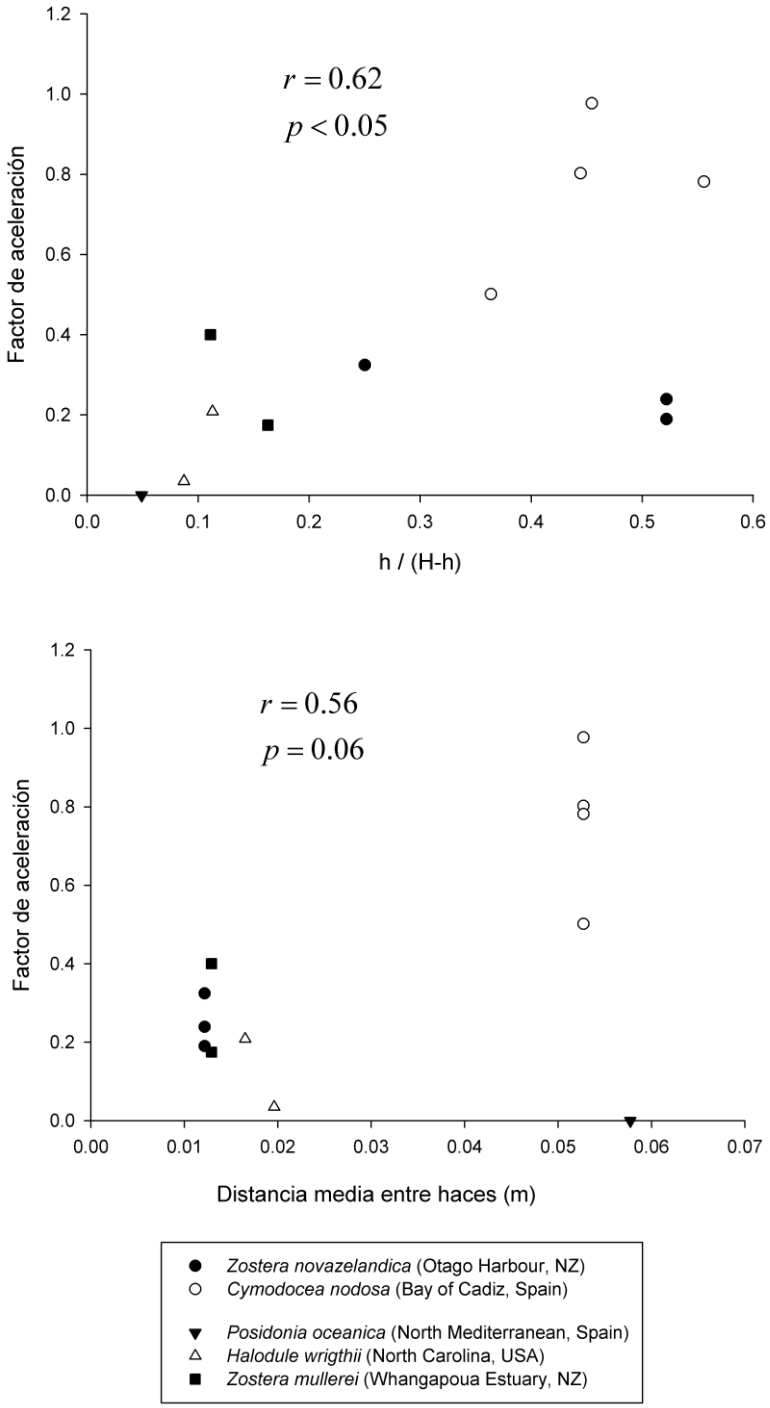

Figura 2. Aceleración del flujo por encima de praderas naturales de angiospermas marinas de diversa naturaleza bajo diferentes ambientes hidrodinámicos. Dicha aceleración se ha estudiado en función de (a) la altura de la mancha en proporción a la profundidad y (b) la separación media entre haces. Los valores están normalizados por la distancia horizontal al borde de la mancha**.** h: altura del dosel; H: profundidad. Se incluyen los datos obtenidos en el saco interno de la bahía de Cádiz para la pradera submareal de *Cymodocea nodosa*.

al. 2007). Por un lado, el paisaje de manchas de un sistema somero de control mareal (e.g. saco interno de la bahía de Cádiz), de alta heterogeneidad espacial; por otro lado,

un sistema profundo con bajas oscilaciones en el nivel del mar (e.g. rodales de *Posidonia oceanica*, Granata et al. 2001), y controlado por turbulencias de mayor escala que se disipan con la conectividad entre las manchas (Folkard 2005).

La microtopografía es otro factor de hábitat cuya repercusión sobre los patrones hidrodinámicos locales se ha demostrado en la presente Tesis Doctoral (capítulo 1). Este atributo del paisaje no sólo entraña pequeñas diferencias en el factor profundidad (e.g. Fonseca et al. 1983), sino que al estar asociado al desarrollo de praderas de contrastadas propiedades físicas (e.g. Hendriks et al. 2010), sus efectos van ligados al de las transiciones bentónicas. La simulación en tanque de flujo de una transición entre *Caulerpa prolifera* y *Cymodocea nodosa* reveló que un resalte de unos 10 cm en la frontera de estas dos especies promueve (1) la mezcla turbulenta y (2) una reducción de la velocidad de fondo, pero al mismo tiempo (3) disminuye la capacidad de transporte sedimentario en la sección de *C. nodosa*. Esta contraposición de efectos evidencia que la microtopografía bentónica no puede considerarse un agente físico simple (capítulo 1), sino condicionado jerárquicamente (*sensu* Hilborn and Stearns 1982) a la intensidad de la corriente y la disponibilidad de sedimento en suspensión. En consecuencia, este atributo implica una perturbación con un tiempo de recurrencia inferior al de su propia génesis (i.e. días frente a años), al contrario de lo que ocurre en los paisajes terrestres o de marisma, donde es la microtopografía (evolución lenta) la que condiciona perturbaciones inmediatas como el drenaje edáfico (Mc Grath et al. 2012) o el grado de de inundación (Castellanos et al. 1994, Sanchez et al. 2001).

2. Los macrófitos marinos como ingenieros de ecosistema en la bahía de Cádiz: perspectivas de futuro.

La modificación del entorno abiótico por parte de ingenieros de ecosistema de vida sumergida está, directa e indirectamente, mediada por procesos hidrodinámicos (e.g. Koch 2001, Bouma et al. 2005, Gruber and Kemp 2010). En consecuencia, todas las relaciones estudiadas a nivel de dosel y de paisaje bentónico en el presente trabajo suponen un avance importante hacia la comprensión de los mecanismos de ingeniería de los macrófitos marinos de la bahía de Cádiz.

Hasta la fecha se ha demostrado un efecto positivo de las praderas de *Zostera noltii* sobre la estabilidad del sustrato (Peralta et al. 2008), así como sobre las tasas de filtración de la comunidad faunística asociada, presumiblemente debido a una mayor retención hidráulica de recursos (Brun et al. 2009). Esta última hipótesis se ha visto reforzada recientemente con datos experimentales de deposición de partículas (Wilkie et al. 2012) o de marcaje isotópico (Lebreton et al. 2012). Dado que los tiempos de retención en praderas de *Z. noltii* están controlados por la intensidad de la corriente, mientras que la difusividad turbulenta se ve afectada también por su estructura de manchas (capítulo 3), se hace necesaria la formulación de un modelo espacialmente explícito, que incluya tanto la variabilidad temporal en el flujo de marea como la distribución de las praderas. La predicción de campos de velocidad a mayor escala (Alvarez et al. 1999) o el cartografiado de los hábitats bentónicos del saco interno (Freitas et al. 2008) constituyen esfuerzos previos a la consecución de este objetivo.

En las praderas de *Cymodocea nodosa*, además de facilitarse la disponibilidad de alimento para la fauna bentónica (Brun et al. 2009), se ha comprobado experimentalmente su capacidad de atrapar sedimento (Hendriks et al. 2010), así como

de promover la migración de dunas sumergidas (Marbá and Duarte 1995), transformaciones físicas del hábitat que repercuten necesariamente en la distribución, abundancia y composición de la materia y el flujo de energía del ecosistema (Jones and Gutierrez 2007). Tanto los patrones hidrodinámicos obtenidos *in situ* (capítulo 1), como los ensayos sedimentarios en tanque de flujo (capítulo 2) sugieren que para una arquitectura de dosel de *C. nodosa* característica en praderas submareales del saco interno de la bahía de Cádiz, el efecto borde favorece la sedimentación hasta una distancia crítica de 0.4-0.6 metros. Este valor de referencia resulta de utilidad para futuros diseños muestrales, en donde se intenten discernir diferencias estructurales y de asimilación ligadas a los procesos de ingeniería de ecosistema.

Cabe destacar que la capacidad de deposición de *Cymodocea nodosa* se mantiene incluso con niveles de velocidad extremos para las condiciones del saco interno de la bahía (i.e. 0.13 m s^{-1}), cuando se compara con niveles de una marea viva típica (i.e. 0.065 m s^{-1}, capítulo 2). Por otro lado, en la transición simulada de *Caulerpa prolifera-Cymodocea nodosa*, un flujo unidireccional con los mismos niveles de velocidad no generaba por sí solo un estrés de fondo de alcance erosivo (capítulo 1). Sin embargo, las medidas *in situ* de la turbidez en el interior de los doseles registran fenómenos de resuspensión del sedimento, durante eventos extremos generados por el viento de levante (García-San Miguel 2010). Este hecho evidencia, (1) la coexistencia de procesos erosivos junto con la idea de una pradera "trampa" de sedimento (Koch 1999), pero sobre todo (2) el desconocimiento del papel que ejerce el flujo orbital (oleaje) en la dinámica sedimentaria de los fondos vegetados de la bahía, a pesar de que los eventos de oleaje representan sólo un pequeño porcentaje de todo el año meteorológico. La experimentación con tratamiento de olas ha demostrado que la componente orbital de la corriente representa una fuente de estrés hidrodinámico añadido a la componente

unidireccional (Heller 1987, Fonseca and Cahalan 1992, Luhar et al. 2010), lo que lleva a considerarla cada vez más como un factor influyente en el desarrollo y el potencial ingeniero de los macrófitos bentónicos (e.g. La Nafie et al. 2012). La escasez actual de este tipo de estudios impide reconocer a la capa límite bentónica como una estructura disipable por perturbaciones puntuales (Thomas and Cornelissen 2003), pero sobre todo el efecto de la calidad (no sólo intensidad) de dichas perturbaciones energéticas sobre las comunidades de macrófitos marinos (Infantes et al. 2009).

CONCLUSIONS

CONCLUSIONS

1. The velocity range recorded at the seagrass distribution area in the inner body of Cadiz bay (0.01-0.08 m s^{-1}) is low compared to other seagrass habitats and compared to mechanical stress thresholds (>0.25 m s^{-1}). Accordingly, the diffusive boundary layer must be thicker than in other seagrass habitats and, therefore, diffusive-limited conditions must dominate in absence of storms.

2. Under natural conditions, the re-direction and acceleration of the current above *Cymodocea nodosa* canopy was not as intense as that observed in previous flume tank experiments. Furthermore, a cross data comparison with other seagrass species from different hydrodynamic environments revealed that the acceleration on top of *C. nodosa* (Cadiz bay) were high compared to other natural systems and that this phenomena was more affected by depth submergence and tidal conditions (habitat factors) than by canopy permeability.

3. The use of an artificial *Cymodocea nodosa* patch in a flume tank showed that the sedimentation pattern followed a negative exponential trend, with maximum sedimentation rate at the leading edge. This pattern was independent of the experimental free stream velocity. The rise in velocity increased the global sediment deposition rate, probably as consequence of the increase on volumetric flow rate through the canopy, and therefore, due to the increase of sediment load susceptible of being deposited.

4. In an *in situ* transition between adjacent populations of *Caulerpa prolifera* and *Cymodocea nodosa*, the TKE showed a relative maximum in C. nodosa at 0.7 m far

from the leading edge, whereas the resources transfer seems homogenous along the spatial gradient. This suggests that physical control of ecological processes on the edge area is more complex than expected from flume tank experiments.

5. By simulating a *Caulerpa prolifera-Cymodocea nodosa* transition in a flume tank, it was observed that, under a reasonable velocity range from Cadiz bay (i.e. 0.065 and 0.14 m s^{-1}), bottom shear stress levels under unidirectional flow were not enough to promote erosion, whereas sedimentation probability was higher in *C. nodosa* bed than in *C. prolifera* one.

6. Under natural conditions, fragmentation of intertidal *Zostera noltii* meadows increased horizontal turbulent diffusivity of solutes at low tide. However, retention time of solutes (i.e. water renewal rate) was not affected by landscape fragmentation because of the dominance of advection over turbulent diffusion as transport mechanism.

7. Present work highlights the importance of spatial heterogeneities (i.e. microtopography, patchiness and fragmentation) when studying the interaction of marine macrophytes with hydrodynamics. Particularly, the role of microtopography as an effect and a factor of ecosystem engineer dynamics is subjected to the existence of high flow events.

CONCLUSIONES

1. El rango de velocidad estimado en las áreas de distribución de las angiospermas marinas en el saco interno de la bahía de Cádiz (0.01-0.08 m s^{-1}) fue bajo en comparación con otros hábitats de angiospermas marinas y con los umbrales de estrés mecánico (>0.25 m s^{-1}). Consecuentemente, la capa límite difusiva alrededor de las hojas de estos macrófitos debe ser más gruesa que en otros hábitats y, por lo tanto, las condiciones de limitación física prevalecen en ausencia de tormentas.

2. En condiciones naturales, los fenómenos de re-direccionamiento y aceleración de la corriente por encima de *Cymodocea nodosa* no resultaron ser tan intensos como se han observado previamente en tanque de flujo. No obstante, un meta-análisis de datos obtenidos *in situ* en praderas de otras especies reveló que los valores de aceleración encontrados en las praderas de *C. nodosa* de la bahía de Cádiz fueron altos comparado con otros hábitats naturales y que dicho fenómeno estaba más afectado por la profundidad y las condiciones de marea (factores de hábitat) que por la permeabilidad del dosel.

3. El uso de una mancha artificial de *Cymodocea nodosa* en tanque de flujo mostró que el patrón espacial de sedimentación seguía una tendencia exponencial negativa, con tasas máximas localizadas en el borde de la mancha. Este patrón fue independiente de la velocidad libre empleada. El incremento de velocidad aumentó la tasa de sedimentación global probablemente como consecuencia de un aumento del flujo volumétrico a través del dosel, y por tanto, del aporte de sedimento susceptible de ser depositado.

4. En una transición natural entre poblaciones adyacentes de *Caulerpa prolifera* y *Cymodocea nodosa*, la turbulencia (TKE) presentó un máximo relativo en *C. nodosa* a 0.7 m de la zona de borde mientras que la transferencia de recursos no pareció mostrar variabilidad espacial a lo largo del gradiente. Esto sugiere que el control físico de los procesos ecológicos en la zona borde de praderas bentónicas es más compleja de lo previsto a partir de experimentos en tanques de flujo.

5. Simulando en tanque de flujo una transición *Caulerpa prolifera-Cymodocea nodosa* con un rango de velocidades razonable para la bahía de Cádiz (0.065 y 0.14 m s^{-1}), los valores de estrés de fondo bajo flujo unidireccional no fueron suficientes para generar niveles de erosión potencial, mientras que la probabilidad de sedimentación fue mayor en *C. nodosa* que en *C. prolifera*.

6. Bajo condiciones naturales, la fragmentación de las praderas intermareales de *Zostera noltii* aumentó la difusividad turbulenta horizontal en bajamar. Sin embargo, el tiempo de retención de los solutos (es decir, la renovación hidráulica) no se vio afectada por la fragmentación del paisaje debido a que la advección domina sobre la difusión turbulenta como mecanismo de transporte de los solutos.

7. La presente memoria muestra la importancia de las heterogeneidades espaciales (microtopografía, mosaico de manchas y fragmentación) en el estudio de la interacción de los macrófitos marinos con la hidrodinámica. En particular, el papel de la microtopografía como causa y a la vez efecto de la interacción espacial de los

ingenieros de ecosistema está supeditada a la existencia de eventos de elevado flujo hidrodinámico.

A brief fluid dynamics glossary for ecologists

Bottom shear stress (τ): Strain caused by near bottom turbulence over a parallel direction of flow. It is widely accepted as a hydrodynamic proxy of sediment bed stability (Thompson et al. 2004, Peralta et al. 2008, Hendriks et al. 2008). It is expressed as N m^{-2} (SI units).

Boundary layer: An unstirred layer of water close to the bottom or to a solid surface where a vertical gradient of minimum velocities extends away. By convention, its thickness is the distance where the average velocity is 99% of the average mainstream velocity (Denny 1988). It may range from μm (leaves, small sessile organisms) to m (benthic boundary layers).

Bulk velocity (U): Depth averaged velocity from the bottom to a characteristic water column height (Thomas et al. 2000). It is used as a representative flow velocity.

Drag forces: Resistance to motion through a fluid. When considering the resistance over flexible or rigid canopies, drag can be divided into two types: profile or form drag, which is due to the low pressure behind a plant due to flow separation (perpendicular to flow), and skin or friction drag, which results from viscous shear as a fluid moves over plants (parallel and often negligible).

Flushing time: A bulk or integrative parameter that describes the general exchange characteristics of a waterbody without identifying the underlying physical processes (Monsen et al. 2002). It is estimated as the ratio of the mass of a scalar in a reservoir to the rate of renewal of the scalar.

Free-stream velocity: Current velocity close to water column height and not affected by the benthic boundary layer effects.

Friction velocity (u*): A characteristic turbulence parameter which measures the magnitude and correlation of fluctuations in velocity near a solid (i.e. bottom) or a porous substrate (Denny 1988). It is expressed as m s^{-1} (SI units).

Momentum transfer: Transport of movement from gradients of horizontal velocity between adjacent planes of flow.

Monami: Spread of wavelike oscillations caused by instabilities that generate large coherent vortices at the interface between the canopy and the overlaying water column, where the velocity profiles display an inflection point (Ackerman and Okubo 1993).

Skimming flow: Flow water re-direction over the top of a submersed canopy which implies the trapping of the layer of water within it (Koch et al. 2006).

Turbulent kinetic energy (TKE): Mean (usually three-dimensional) kinetic energy per unit of mass associated with eddy activity. It is usually expressed as m^2 s^{-2} (SI units).

Volumetric flow rate (Q): Unit of water volume crossing a section perpendicular to current direction per unit of time (Peralta et al. 2008). It is expressed as m^3 s^{-1} (SI units).

BIBLIOGRAPHY

Abdelrhman (2003). Effect of eelgrass *Zostera marina* canopies on flow and transport. Mar Ecol Prog Ser 248:67-83.

Achab M and Gutierrez-Mas JM (2005). Nature and distribution of the sand fraction components in the Cadiz Bay bottoms (SW-Spain). Rev Soc Geol Esp 18 (3-4):133-143.

Ackerman JD and Okubo A (1993). Reduced mixing in a marine macrophyte canopy. Funct Ecol 7(3): 305-309.

Ackerman JD (1997 a). Submarine Pollination in the Marine Angiosperm *Zostera marina* (Zosteraceae): I. The Influence of Floral Morphology on Fluid Flow. Am J Bot 84(8):1099-1109.

Ackerman JD (1997 b). Submarine Pollination in the Marine Angiosperm *Zostera marina* (Zosteraceae): II. Pollen Transport in Flow Fields and Capture by Stigmas. Am J Bot 84(8):1110-1119.

Ackerman JD (2002). Diffusivity in a marine macrophyte canopy: Implications for submarine pollination and dispersal. Am J Bot 89(7): 1119-1127.

Allen BJ and Williams SL (2003). Native eelgrass *Zostera marina* controls growth and reproduction of an invasive mussel through food limitation. Mar Ecol Prog Ser 254:57-67.

Álvarez O, Izquierdo A, Tejedor B, Mañanes R, Tejedor L and Kagan BA (1999). The Influence of Sediment Load on Tidal Dynamics, a Case Study: Cádiz Bay. Est Coast Shelf S 48:439-450.

Arber A (1920). Water plants, a study of aquatic angiosperms. Cambridge University Press, Cambridge.

Beer S and Waisel Y (1982). Effects of light and pressure on photosynthesis in two seagrasses. Aquat Bot 13:331-337.

Benavente J, Peralta G, Lara M and Martínez-Ramos C (2008). Influencia de la vegetación en el desarrollo de la morfología de una laguna mareal. In: Tinoco JG, Paez MC, Puyana M, Amaya C, Carolina D (eds). Las ciencias y las tecnologías marinas al servicio del país. Proc 13th Nat Mar Sci and Tech Symp. San Andres Isla, Colombia.

Benavente J, Del Río L, Plomaritis T and Gracia J (2011). Características físicas de la marea en la Bahía de Cádiz. El caso de las grandes mareas de marzo de 2011. In: Consejería de Medio Ambiente, Junta de Andalucía (eds.). El Parque Natural Bahía de Cádiz, donde las mareas funden tierra y mar, pp 95-101.

Bell SS, Robbins BD and Jensen SL (1999). Gap dynamics in a seagrass landscape. Ecosystems 2(6):493-504.

Bouma TJ, De Vries MB, Low E, Peralta G, Tánczos IC, van de Koppel J and Herman PMJ (2005). Trade-offs related to ecosystem engineering: A case study on stifness of emerging macrophytes. Ecology 86:2187-2199.

Bouma TJ, van Duren LA, Temmerman S, Claverie T, Blanco-Garcia A, Ysebaert T and Herman PMJ (2007). Spatial flow and sedimentation patterns within patches of epibenthic structures: Combining field, flume and modelling experiments. Cont Shelf Res 27(8):1020-1045.

Bouma TJ, Friedrichs M, Klaassen P, van Wesenbeeck BK, Brun FG, Temmerman S, van Katwijk MM, Graf G and Herman PMJ (2009 a). Effects of shoots stiffness, shoot size and current velocity on scouring sediment from around seedlings and propagules. Mar Ecol Prog Ser 388:293-297.

Bouma TJ, Olenin S, Reise K and Ysebaert T (2009 b). Ecosystem engineering and biodiversity in coastal sediments: posing hypothesis. Helgol Mar Res 63:95–106.

Bos AR, Bouma TJ, de Kort GLJ and van Katwijk MM (2007). Ecosystem engineering by anual intertidal seagrass beds: Sediment accretion and modification. Estuar Coast Shelf S 74(1-2):344-348.

Brun FG, Pérez-Lloréns JL, Hernández I and Vergara JJ (2003). Patch distribution and within-patch dynamics of the seagrass *Zostera noltii* Hornem in Los Toruños Salt-Marsh, Cádiz Bay, Natural Park, Spain. Bot Mar 46:513-524.

Brun FG, Vergara JJ, Peralta G, Garcia-Sanchez MP, Hernández I and Pérez-Lloréns JL (2006). Clonal building, simple growth rules and phylloclimate as key steps to develop functional-structural seagrass models. Mar Ecol Prog Ser 323: 133 - 148.

Brun FG, van Zetten E, Cacabelos E and Bouma TJ (2009). Role of two contrasting ecosystem engineers (*Zostera noltii* and *Cymodocea nodosa*) on the food intake rate of *Cerastoderma edule*. Helgoland Mar Res 63 (1): 19-25.

Bryan KR, Tay HW, Pilditch CA, Lundquist CJ and Hunts HL (2007). The effects of Seagrass (*Zostera muelleri*) on Bounary-layer Hydrodynamics in Whangapoua Estuary, New Zeland. J Coast Res, Special issue 50:668-672.

Cabaço S, Alexandre A and Santos R (2005). Population-level effects of clam harvesting on the seagrass *Zostera noltii*. Mar Ecol Prog Ser 298:123-129.

Carpenter RC and Williams SL (1993). Effects of algal turf canopy height and microscale substratum topography on profiles of flow speed in a coral forereef environment. Limnol Oceanogr 38(3): 687-694.

Castellanos EM, Figueroa ME and Davy AJ (1994). Nucleation and facilitation in saltmarsh succession: interactions between *Spartina marítima* and *Athrocnemum perenne*. J Ecol 82:239-248.

Cornelisen CD and Thomas FIM (2006). Water flow enhances ammonium and nitrate uptake in a seagrass community. Mar Ecol Prog Ser 312:1-13.

Cunha AH, Santos RP, Gaspar AP and Bairros MF (2005). Seagrass landscape-scale changes in response to disturbance created by the dynamics of barrier-islands: A case of study from Ria Formosa (Southern Portugal). Est Coast Shelf S 64(4):636-644.

De los Santos CB, Brun FG, Bouma TJ, Vergara JJ and Pérez-Lloréns JL (2010). Acclimation of seagrass *Zostera noltii* to co-occurring hydrodynamics and light stresses. Mar Ecol Prog Ser 398:127-135.

De los Santos CB (2011). Mechanical stress in segrasses: Morphological, biomechanical and structural composition responses. PhD thesis, University of Cadiz, 150 pp.

den Hartog C (1970). The Sea-Grasses of the World. North-Holland publishing Company, Amsterdam.

Denny MW (1988). Benthic Boundary Layers. In: Biology and the Mechanics of the Wave-Swept Environment. Princeton University Press, New Jersey, pp 117-132.

Duarte CM (1991). Seagrass depth limits. Aquat Bot 40(4):363-377.

Enríquez S and Rodríguez-Roman A (2006). Effect of water flow on the photosynthesis of three marine macrophytes from a fringing-reef lagoon. Mar Ecol Prog Ser 323:119-132.

Folkard AM (2005). Hydrodynamics of model *Posidonia oceanica* patches in shallow water. Limnol Oceanogr 50(5):1592-1600.

Fonseca MS, Fisher JS, Zieman JC and Thayer GW (1982). Influence of the seagrass, *Zostera marina* L., on current flow. Est Coast Shelf S 15: 351-364.

Fonseca MS, Zieman JC, Thayer GW and Fisher JS (1983). The Role of Current Velocity in Structuring Eelgrass (*Zostera marina* L.) Meadows. Est Coast Shelf S 17:367-380.

Fonseca MS and Fischer JS (1986). A comparison of canopy friction and sediment movement between four species of seagrass with reference to their ecology and restoration. Mar Ecol Prog Ser 29: 15-22.

Fonseca MS and Kenworthy WJ (1987). Effects of current on photosynthesis and distribution of seagrasses. Aquat Bot 27: 59-78.

Fonseca MS and Cahalan JA (1992). A preliminary evaluation of wave attenuation by four species of seagrasses. Est Coast Shelf S 35(6):565-576.

Fonseca MS (1996). The role of seagrasses in nearshore sedimentary processes: a review. In: Nordstrom KF and Roman CT (eds). Estuarine Shores: Evolution, Environments and Human Alterations, pp 263-280.

Fonseca MS and Bell SS (1998). Influence of physical setting on seagrass landscapes near Beaufort, North Carolina, USA. Mar Ecol Prog Ser 171:109-121.

Fonseca MS and Koehl MAR (2006). Flow in seagrass canopies: the influence of patch width. Est Coast Shelf S 67: 1-9.

Fonseca MS, Koehl MAR and Koop BS (2007). Biomechanical factors contributing to self-organization in seagrass landscapes. J Exp Mar Biol Ecol 340:227-246.

Freitas R, Rodrigues AM, Morris EP, Perez-Llorens JL and Quintino V (2008). Single-beam acoustic ground discrimination of shallow water habitats: 50 kHz or 200 kHz frequency survey? Est Coast Shelf S 78(4): 613-622.

Gacia E, Granata T and Duarte CM (1999). An approach to the measurement of particle flux and sediment retention within seagrass (*Posidonia oceanica*) meadows. Aquat Bot 65: 255-268.

Gambi MC, Novell ARM and Jumars PA (1990). Flume observations on flow dynamics in *Zostera marina* (eelgrass) beds. Mar Ecol Prog Ser 61:159-169.

García-San Miguel C (2010). Efecto del viento en el coeficiente de atenuación de la luz en el agua para el saco interno de la Bahía de Cádiz. Ms thesis, University of Cadiz, 31 pp.

Ghisalberti M and Nepf H (2002). Mixing layers and coherent structures in vegetated aquatic flow. J Geophys Res C 107 (C2):1-11.

Granata TC, Serra T, Colomer J, Casamitjana X, Duarte CM and Gacia E (2001). Flow and particle distribution in a nearshore seagrass meadow before and after a storm. Mar Ecol Prog Ser 218:95-106.

Grizzle RE, Short FT, Newell CR, Hoven H and Kindblom L (1996). Hydrodynamically induced synchronous waving of seagrasses: `monami´and its possible effects on larval mussel settlement. J Exp Mar Biol Ecol 206(1-2):165-177.

González CJ, Álvarez O, Reyes J and Acevedo A (2010). Two-dimensional modeling of hydrodynamics and sediment transport in the San Pedro tidal creek (Cadiz Bay): Morphodynamical implications. Cienc Mar 36(4):393-412.

Gruber RK and Kemp WM (2010). Feedback effects in a coastal canopy-forming submersed plant bed. Limnol Oceanogr 55(6):2285-2298.

Gutierrez-Mas JM, Lopez-Galindo A and Lopez-Aguayo F (1997). Clay minerals in recent sediments of the continental shelf and the Bay of Cadiz (SW Spain). Clay Miner 32:507-515.

Gutierrez-Mas JM, Luna del Barco A, Parrado JM, Sanchez E, Fernandez-Palacios A and Ojeda J (2000). Cadiz Bay waters turbidity variations from Landsat TM images analysis. Geogaceta 27:79-82.

Hansen JCR and Reidenbach MA (2012). Wave and tidally driven flows in eelgrass beds and their effect on sediment suspension. Mar Ecol Prog Ser 448:271-287.

Heiss WM, Smith AM and Probert PK (2010). Influence of the small intertidal seagrass *Zostera novazelandica* on linear water flow and sediment texture. New Zeal J Mar Fresh 34(4):689-694.

Heller DY (1987). Sediment transport through seagrass beds. Ms thesis, University of Virginia, 72 pp.

Hendriks IE, Sintes T, Bouma TJ and Duarte CM (2008). Experimental assessment and modeling evaluation of the effects of the seagrass *Posidonia oceanica* on flow and particle trapping. Mar Ecol Prog Ser 356: 163-173.

Hendriks IE, Bouma TJ, Morris EP and Duarte CM (2010). Effects of seagrass and algae of the *Caulerpa* family on hydrodynamics and particle trapping rates. Mar Biol 157(3): 473-481.

Hilborn R and Stearns SC (1982). On inference in ecology and evolutionary biology: the problem of multiple causes. Acta Biotheor 31: 145-164.

Huettel and Gust (1992). Impact of bioroughness on interfacial solute exchange in permeable sediments. Mar Ecol Prog Ser 89:253-267.

Infantes E, Terrados J, Orfila A, Cañellas B and Álvarez-Ellacuria A (2009). Wave energy and the upper depth limit distribution of *Posidonia oceanica*. Bot Mar 52(5):419-427.

Jones CG, Lawton JH and Shachak M (1997). Positive and negative effects of organisms as physical ecosystem engineers. Ecology 78:1946–1957.

Jones CG and Gutierrez JL (2007). On the purpose, meaning, and usage of the physical ecosystem engineering concept. In: Cuddington K, Byers JE, Wilson WG and Hastings A (eds). Ecosystems engineers: Plants to protists. Academic Press, USA.

Kagan BA, Alvarez O, Izquierdo A, Mañanes R, Tejedor B and Tejedor L (2003). Weak wind-wave/tide interaction over a moveable bottom: results of numerical experiments in Cadiz Bay. Cont Shelf Res 23(5):435-456.

Kemp WM, Boynton WR et al. (2005). Eutrophication of Chesapeake Bay: historical trends and ecological interactions. Mar Ecol Prog Ser 303:1-29.

Koch EW (1994). Hydrodynamics, diffusion-boundary layers and photosynthesis of the seagrasses *Thalassia testudinum* and *Cymodocea nodosa*. Mar Biol 118: 767-776.

Koch EW and Gust G (1999). Water flow in tide- and wave-dominated beds of the seagrass *Thalasia testudinum*. Mar Ecol Prog Ser 184:63-72.

Koch EW (1999a). Preliminary evidence on the interdependent effect of currents and porewater geochemistry on *Thalassia testudinum* seedlings. Aquat Bot 63(2):95-102.

Koch EW (1999b). Sediment resuspension in a shallow *Thalassia testudinum* banks ex König bed. Aquat Bot 65(1-4):269-280.

Koch EW (2001). Beyond light: physical, geological and geochemical parameters as possible submersed aquatic vegetation habitat requirements. Estuaries 24: 1-17.

Koch EW, Ackerman J, van Keulen M and Verduin J (2006). Fluid Dynamics in Seagrass Ecology: from Molecules to Ecosystems. In: Larkum AWD, Orth RJ and Duarte CM (eds), Seagrasses: Biology, Ecology and Conservation. Springer Verlag, pp 193-225.

Lacy JR and Willie-Echeverria S (2011). The influence of current speed and vegetation density on flow structure in two macrotidal eelgrass canopies. Limnol Oceanogr-F&E 1:38-55.

La Nafie Y, De los Santos CB, Brun FG, van Katwijk MM and Bouma TJ (2012). Waves and high nutrient loads jointly decreases survival and separately affect morphological and biomechanical properties in the seagrass *Zostera noltii*. Limnol Oceanogr 57(6):1664-1672.

Lebreton B, Richard P, Galois R, Radenac G, Brahmia A, Colli G, Grouazel M, André C, Grillou G and Blanchard GF (2012). Food sources used by sediment meiofauna in an intertidal *Zostera noltii* seagrass bed: a seasonal stable isotope study. Mar Biol 159(7):1537-1550.

Lobo FJ, Hernández-Molina FJ, Somoza L, Rodero J, Maldonado A and Barnolas A (2000). Patterns of bottom current flow deduced from dune asymmetries over the Gulf of Cadiz shelf (sothwest Spain). Mar Geol 164(3-4):91-117.

Luhar M, Coutu S, Infantes E, Fox S and Nepf H (2010). Wave-induced velocities inside a model seagrass bed. J Geophys Res 115 C 12005.

Macreadie PI, Hindell JS, Keough MJ, Jenkins GP and Connolly RM (2010). Resource distribution influences positive edge effects in a seagrass fish. Ecology 91:2013-2021.

Malta E, Ferreira DG, Vergara JJ and Pérez-Lloréns JL (2005). Nitrogen load and irradiance affect morphology, photosynthesis and growth of *Caulerpa prolifera* (Bryopsidales: Chlorophyta). Mar Ecol Prog Ser 298:101-124.

Maltese A, Cox E, Folkard A, Ciraolo G, La Loggia G and Lombardo G (2007). Laboratory measurements of flow and turbulence in discontinuous distributions of ligulate seagrass. J Hydraul Eng 133(7):750-760.

Marbá N and Duarte CM (1995). Coupling of seagrass (*Cymodocea nodosa*) patch dynamics to subaqueous dune migration. J Ecol 83:381-389.

Marbá N, Hemminga MA, Mateo MA, Duarte CM, Mass YEM, Terrados J and Gacia E (2002). Carbon and nitrogen translocation between seagrass ramets. Mar Ecol Prog Ser 226:287-300.

Mc Grath GS, Paik K and Hinz C (2012). Microtopography alters self-organized vegetation patterns in water limited ecosystems. J Geophys Res 117 G 03021.

Mc Kone KL (2009). Light available to the seagrass *Zostera marina* when exposed to currents and waves. Ms thesis, University of Maryland, 193 pp.

Merrel KC (1996). The effect of flow and mixing on *Vallisneria* and its associated community in experimental mesocosms. Ms thesis, University of Maryland, 83 pp.

Moore KA (2004). Influence of seagrasses on water quality in shallow regions of the lower Chesapeake Bay. J Coast Res, Special issue 45:162-178.

Morris EP, Peralta G, Brun FG, van Duren L, Bouma TJ and Perez-Llorens JL (2008). Interaction between hydrodynamics and seagrass canopy structure: spatially explicit effects on ammonium uptake rates. Limnol Oceanogr 53:1531–1539.

Morris EP, Peralta G, Benavente J, Freitas R, Rodrigues AM, Quintino V, Alvarez O, Valcarcel-Pérez N, Vergara JJ, Hernández I and Pérez-Lloréns JL (2009). *Caulerpa prolifera* stable isotope ratios reveal anthropogenic nutrients within a tidal lagoon. Mar Ecol Prog Ser 390: 117 – 128.

Nepf H and Koch EW (1999). Vertical secondary flows in submersed plants-like arrays. Limnol Oceanogr 44(4):1072-1080.

Nepf H and Vivoni ER (2000). Flow structure in depth limited, vegetated flow. J Geophys Res 105 (C12):28547-28557.

Nepf H, White B, Lightbody A and Ghisalberti M (2007). Transport in aquatic canopies. In: Gayev YA and Hunt JCR (eds). Flow and Transport Processes with Complex Obstructions, pp 221-250.

Nepf H and Ghisalberti M (2008). Flow and transport in channels with submerged vegetation. Acta Geophys 56 (3):753-777.

Neumeier U and Ciavola P (2004). Flow Resistance and Associated Sedimentary Processes in a *Spartina maritima* Salt Marsh. J Coast Res 20(2):435-447.

Nowell ARM and Jumars PA (1984). Flow environments of aquatic benthos. Annu Rev Ecol Systematics 15:303-328.

Paling EI, van Keulen M, Wheleer KD, Phillips J and Dyhrberg R (2003). Influence of spacing on Mechanically Transplanted Seagrass Survival in a High Wave Energy Regime. Restor Ecol 11(1):56-61.

Peralta G, Brun FG, Hernández I, Vergara JJ and Pérez-Lloréns JL (2005). Morphometric variations as acclimation mechanisms in *Zostera noltii* beds. Est Coast Shelf S 64:347-356.

Peralta G, Brun FG, Pérez-Lloréns JL and Bouma TJ (2006). Direct effect of current velocity on the growth, morphometry and architecture of seagrasses: a case study on *Zostera noltii*. Mar Ecol Prog Ser 327:135-142.

Peralta G, van Duren LA, Morris EP and Bouma TJ (2008). Consequences of shoot density and stiffness for ecosystem engineering by benthic macrophytes in flow dominated areas: a hydrodynamic flume study. Mar Ecol Prog Ser 368: 103 – 115.

Pérez-Lloréns JL and Niell FX (1993). Seasonal dynamics of biomass and nutrient content in the intertidal seagrass *Zostera noltii* Hornem from Palmones River estuary, Spain. Aquat Bot 46(1):49-66.

Pergent G, Pergent-Martini C and Boudouresque CF (1995). Utilisation de l'herbier à *Posidonia oceanica* comme indicateur biologique de la qualité du milieu littoral en Méditerraneé: Etat des connaissances. Mésogée 54: 3–29.

Peterson CH, Luettich RA Jr, Micheli F and Skilleter GA (2004). Attenuation of water flow inside seagrass canopies of differing structure. Mar Ecol Prog Ser 268:81-92.

Robbins BD and Bell (2000). Dynamics of a subtidal seagrass landscape: Seasonal and annual change in relation to water depth. Ecology 81(5):1193-1205.

Rueda JL and Salas C (2003). Seasonal variation of a molluscan assemblage living in a *Caulerpa prolifera* meadow within the inner Bay of Cadiz (SW Spain). Estuar Coast Shelf Sci 57:909-918.

Sanchez JM, San Leon DG and Izco J (2001). Primary colonisation of mudflat estuaries by *Spartina marítima* (Curtis) Fernald in northwest Spain: vegetation structure and sediment accretion. Aquat Bot 69:15-25.

Scoffin TP (1970). The trapping and binding of subtidal carbonate sediments by marine vegetation in Bimini Lagoon, Bahamas. J Sed Petrol 40(1):249-273.

Shanz A and Asmus H (2003). Impact of hydrodynamics on development and morphology of intertidal seagrasses in the Wadden Sea. Mar Ecol Prog Ser 261:123-134.

Short F, Carruthers T, Dennison W and Waycott M (2007). Global seagrass distribution and diversity: a bioregional model. J Exp Mar Biol Ecol 350(1-2):3-20.

Sleeman JC, Kendrich GA, Boggs GS and Hegge BJ (2005). Measuring fragmentation on seagrass landscapes: which indices are most appropriate for detecting change? Mar Freshwater Res 56(6):851-864.

Thomas FIM, Cornelisen CD and Zande JM (2000). Effects of water velocity and canopy morphology on ammonium uptake by seagrass communities. Ecology 81(10):2704-2713.

Thomas FIM and Cornelisen CD (2003). Ammonium uptake by seagrass communities: effects of oscillatory versus unidirectional flow. Mar Ecol Prog Ser 247:51-57.

Thompson CEL, Amos CL and Umgiesser G (2004). A comparison between fluid shear stress reduction by halophytic plants in Venice Lagoon, Italy and Rustico Bay, Canada—analyses of in situ measurements. J Mar Syst 51: 293-308.

Twilley RR, Kemp WM, Staver KW, Stevenson JC and Boynton WR (1985). Nutrient enrichment of estuarine submersed vascular plant-communities. Algal growth and effects on production of plants and associated communities. Mar Ecol Prog Ser 23(2):179-191.

van der Heide T, van Nes EH, Geerling GW, Smolders AJP, Bouma TJ and van Katwijk MM (2007). Positive feedbacks in seagrass ecosystems: Implications for success in conservation and restoration. Ecosystems 10(8): 1311-1322.

van der Heide T, Bouma TJ, van Nes EH, van de Koppel J, Scheffer M, Roelofs JGM, van Katwijk MM and Smolders AJP (2010). Spatial self-organized patterning in seagrasses along a depth gradient of an intertidal ecosystem. Ecology 91(2):362-369.

van Katwijk MM and Hermus DCR (2000). Effects of water dynamics on *Zostera marina*: transplantation experiments in the intertidal Dutch Wadden Sea. Mar Ecol Prog Ser 208:107-118.

van Keulen M and Borowitzka MA (2002). Comparison of water velocity profiles through morphologically dissimilar seagrasses measured with a simple and inexpensive current meter. B Mar Sci 71:1257-1267.

Vergara JJ, García-Sánchez MP, Olivé I, García-Marín P, Brun FG, Pérez-Lloréns JL and Hernández I (2012). Seasonal functioning and dynamics of *Caulerpa prolifera* meadows in shallow areas: An integrated approach in Cadiz Bay Natural Park. Est Coast Shelf S 112:255-264.

Ward LG, Kemp WM and Boynton WR (1984). The influence of waves and seagrass communities on suspended particles in an estuarine embayment. Mar Geol 59(1-4):85-103.

Wilkie L, O´Hare MT, Davidson I, Dudley B and Paterson DM (2012). Particle trapping and retention by *Zostera noltii*: A flume and field study. Aquat Bot 102:15-22.

Worcester SE (1995). Effects of eelgrass beds on advection and turbulent mixing in low current and low shoot density environments. Mar Ecol Prog Ser 126:223-232.